JAERI-Tech
96-048

CONCEPTUAL DESIGN OF SEPARATED FIRST WALL AND TESTING OF SMALL SIZE MOCK-UPS

November 1996

Koichi KOIZUMI, Masataka NAKAHIRA
Masanao SHIBUI*, Hideyuki TAKATSU
and Eisuke TADA

日本原子力研究所
Japan Atomic Energy Research Institute

本レポートは，日本原子力研究所が不定期に公刊している研究報告書です。
入手の問合わせは，日本原子力研究所研究情報部研究情報課（〒319-11 茨城県那珂郡東海村）あて，お申し越しください。なお，このほかに財団法人原子力弘済会資料センター（〒319-11 茨城県那珂郡東海村日本原子力研究所内）で複写による実費頒布をおこなっております。

This report is issued irregularly.
Inquiries about availability of the reports should be addressed to Research Information Division, Department of Intellectual Resources, Japan Atomic Energy Research Institute, Tokai-mura, Naka-gun, Ibaraki-ken 319-11, Japan.

編集兼発行　日本原子力研究所
印　　刷　日立高速印刷株式会社

Conceptual Design of Separated First Wall and Testing of Small Size Mock-ups

Koichi KOIZUMI, Masataka NAKAHIRA [-], Masanao SHIBUI [*]
Hideyuki TAKATSU [+] and Eisuke TADA [+]

Department of ITER Project
Naka Fusion Research Establishment
Japan Atomic Energy Research Institute
Naka-machi, Naka-gun, Ibaraki-ken

(Received October 18 , 1996)

Design studies and R&D activities on the separate first wall for tokamak fusion experimental reactors have been progressed. The first wall is expected to be exposed to severe damages because of high heat and particle loads and it requires easy replacement in case of failure. In order to satisfy the requirement of assembly and maintenance, the first wall mechanically separated and separately cooled from a massive blanket module has been proposed as a promising concept with a number of advantageous features, such as easy handling during assembly/disassembly due to light weight (~350kg), short shut-down-time for maintenance operation, minimized amount of radwaste and so on.

A fail-safe sturucture, which is consistent with in-service-inspection, has been realized by employing a reliable double-walled thin shell structure sandwiching metal mesh. A quilting structure of austenitic stainless steel (SS316) cooled by low pressure (2 MPa), low temperature (100 -150 ℃) water is employed to accommodate high surface heat flux of more than 0.3 MW/m^2 and nuclear heating together with large electromagnetic loads up to 2 MPa.

This report describes the outlines of the structural design of the separated first wall, cooling and manifolds, mechanical connection to blanket structure, fabrication procedure, results of thermo-mechanical analyses and related R&D activities.

Keywords: Fusion Experimental Reactor, ITER, Separated First Wall, Double Wall

---

[+] Department of Fusion Eugineering Research

[*] Toshiba Corp.

分離第一壁の概念設計及び小型モックアップ試験

日本原子力研究所那珂研究所
小泉　興一・中平　昌隆[+]・渋井　正直[*]
高津　英幸[+]・多田　栄介[+]

（1996年10月18日受理）

トカマク型核融合実験炉における分離第一壁の設計検討及び研究開発が進められている。第一壁は，高熱負荷や粒子負荷により破損を被る可能性が極めて高く，このため破損時には容易に交換が可能であることが要求される。このような組立保守上の要求事項を満足するため，重量物であるブランケットモジュールから機械的に分離し，冷却も独立して行う第一壁を提案した。本提案の第一壁は重量の軽さ（約350kg）により容易な取り回しが可能であり，保守作業時間の短縮，放射性廃棄物の最小に押さえることができる等の利点を持っている。

プラズマ対向壁に金属繊金網を挟み込んだ薄肉二重壁構造を採用することで，リークの発生を未然に防止するフェイルセーフ機能を実現し，供用中の検査が可能な信頼性の高い設計とした。材料はオーステナイトステンレス鋼（SUS316）であり，0.3MW／m^2以上の表面熱負荷と核発熱に対する除熱性能と2MPaにおよぶ電磁力に対する強度を確保するため，二重壁をキルティング構造となるよう加工し，内部を低温低圧水（2MPa，100－150℃）で冷却した。

本報告は，分離第一壁の本体構造，冷却，支持等の構造及び製作設計並びに熱構造解析と小型モックアップ試験に関する試験結果をまとめたものである。

那珂研究所：〒311-01　茨城県那珂郡那珂町向山801-1
＋　核融合工学部
＊　株式会社　東芝

Contents

目　　次

1. Introduction

A first wall of tokamak fusion experimental reactors is a plasma facing component, and is exposed to severe damages caused by high surface heat flux and particle loads during normal and off-normal operations. Also, it is subjected to large electromagnetic loads induced by plasma disruptions. Because of these high potential risks, the first wall needs to be easily replaced in case of failure, while a blanket module is expected to survive anticipated design load conditions under the operation environments through its lifetime and classified into "semi-permanent components". For this reason, mechanically separated first wall consistent with maintenance scenario is indispensable for fusion experimental reactors. To realize this requirement, the first wall concept mechanically separated and separately cooled from the massive blanket module has been developed.

Water ingress into the vacuum vessel due to rupture of the coolant pressure boundary is the most crucial events of accident for the design of water-cooled in-vessel components. High temperature operation of the in-vessel components is preferable from both of the plasma impurity and reactor relevancy view points. Higher temperature operations of the water coolant increase the potential consequences in the case of water ingress into the vacuum vessel. Then, high reliability is also one of the most important design issues of the water-cooled first wall. In order to achieve high reliable components, a fail-safe structure is essential, which is consistent with in-service inspection to detect coolant leakage before break. A double-walled thin shell structure sandwiching metallic mesh is one of the solution of such a fail-safe structure. In this configuration, leak detection is possible by detecting water leakage through the mesh region. This concept has been originally developed aiming at application to the heat exchanger pipe of Fast Breeder Reactors (FBR) and fabrication technology and its applicability to FBR have been successfully developed.

From these points of view, a separated first wall, which has reliable double-walled thin shell structure with mesh inserted for fail-safe features, has been proposed for the first wall of fusion experimental reactors to improve its reliability, maintainability and inspectability. A quilting structure of austenitic stainless steel (SS316) cooled by low pressure water is employed to accommodate high surface heat flux of more than 0.3 MW/m^2 and associated nuclear heating. This structure is also effective to obtain electrical connection between adjacent blanket modules and also workable as bumper limiters, start-up limiters and ripple-loss protectors with adequate plasma facing armors or coatings. This paper outlines the structural design of separated first wall, fabrication procedure, the results of thermal and mechanical analyses, and the results of related R&D activities.

2. Design activities

2.1 Configuration

The first wall (FW) of fusion experimental reactors requires a thin-walled structure to reduce thermal stresses caused by high surface and volumetric heat loads. In this configuration, the most likely failure mode is a small coolant leakage and fatigue crack initiation has to be expected. Thermal stress cycles due to normal and off-normal operations are also responsible for crack growth. For this reason, a double-walled fail-safe structure has been employed for the basic configuration of the FW. Configuration of the FW panel designed in this study is shown in Fig. 2.1.1. The FW panel consists of a fail-safe quilting thin shell structure made of SS316. Both of outer and inner skins are composed of two walls of 2.0 mm thickness sandwiching metal mesh of 0.4 mm thickness as shown in Fig. 2.1.2. For separating inlet and outlet paths of the coolant, a center plate of 2.0 mm thickness is installed between the outer and inner skins. The total height of the FW panel is 40 mm including Beryllium (Be) limiter. The mesh region is filled with probe gas and used for continuous leak monitoring for in-service-inspection (ISI). With this double-walled configuration, failure of the inner wall is detectable by monitoring water leakage into probe gas region, and that of outer wall is also detectable by a probe gas leakage into vacuum. In addition to these functions, the mesh region is also expected to be effective to arrest crack propagation. Application of Cu-alloy is possible to accommodate higher heat flux up to 3 MW/m^2.

The first wall structure is divided toroidally and poloidally into many small-sized panels, typically 1 m wide x 2.0 m long. Typical weight of the FW panel is around 350 kg. This segmentation enables assembly/disassembly of the FW panel independently from the adjacent FW panels and massive blanket structures. This configuration is also effective for bridging adjacent blanket modules to provide one-turn electrical connection in the toroidal direction as shown in Fig. 2.1.3. The major advantageous features of this configuration are summarized as follows;

1) easy handling during assembly/disassembly due to light weight (~350 kg),
2) short shut-down-time for maintenance operation,
3) minimized amount of radwaste,
4) reduced thermal stresses of massive blanket structure,
5) possible higher temperature operation of FW than the blanket structure, particularly in case of baking operation.

2.2 Mechanical support

During the initial assembly and disassembly, the FW panels are installed and replaced by in-vessel manipulator through a horizontal port of the vacuum vessel. The FW panels are supported by a number of DS (Dispersion Strengthened) copper bolts, which have a diameter of 16 mm, and fixed to the blanket module as shown in Fig. 2.2.1.

Brazing-assisted bolts are employed to assure good thermal conductivity between the bolts and support disks, and between the bolts and SS316 stud bolts, and also to prevent loosening of the bolts. In order to allow thermal expansion of the FW panel, only one bolt for each panel is utilized for fixing the panel, while the other bolts are expected to suppress the out-of-plane deflection only. For this purpose, clearance holes are provided for their connections. Bolt pitch of 150 mm is decided to support electromagnetic pressures up to 2 MPa. These bolts are cooled indirectly by surrounding components such as the FW panel and the blanket module.

2.3 Surface alignment and protection

Adjustable function for surface alignment is provided by the support disc made of DS copper as shown in Fig. 2.2.1. The support disc is designed to have an internal tap for the connection with the stud bolt welded on to the blanket module and the required accuracy of surface alignment is assured by adjusting the height of the support disc. For the surface protection against particle loading, replaceable mushroom-shaped Be guard limiters are attached on the FW surface. Be limiters are fixed on the concave surface of the FW panel by bolting and filler metal. These Be limiters are designed as sacrificing elements and replaceable easily by in-vessel manipulator. The pitch of the Be limiters is tentatively 60 mm.

2.4 Cooling scheme and manifold routing

Surface heat flux and nuclear heating on to the FW panel are cooled by low pressure water (2 MPa), separately from the massive blanket module. Cooling scheme of the FW panel is shown in Fig. 2.4.1. Two inlet lines and two outlet lines, which have a diameter of 30 mm, are connected to the individual FW panel. Cooling paths of the FW panel are provided within the inside of the quilting structure and the cooling water flows along the poloidal direction of the FW panel. Flow velocity is tentatively specified to be 5 m/s in the FW panel. Pressure drop between the inlet and outlet is estimated to be less than 0.2 MPa with the total path length of 4 m. Inlet and outlet cooling pipes of each FW panel are connected to their mother manifolds located in the space between the vacuum vessel and the back plate of the blanket module. Fig. 2.4.2 shows manifold routing of separated FW. For the penetration of the cooling pipes, penetration holes are prepared between the adjacent blanket modules. For the connection of the cooling pipes and the mother manifolds, internal access welding technique by means of laser beam is applicable. Leak monitor lines of the FW panel are also connected to their mother lines.

2.5 Fabrication procedure

Fabrication procedures of the double-walled fail-safe structure and quilting panel have been examined based on current industrial basis. A candidate fabrication procedure is shown in Fig. 2.5.1. Fabrication procedures of the FW panel are composed of the following 4 steps; fabrication of concave surfaces by press forming, (2) diffusion

bonding of two inner plates and center plate by Hot Pressing (HP), (3) Hot Isostatic Pressing (HIP) bonding of mesh inserts and outer walls for the integration with inner walls, and (4) seal welding of panel ends and bolt connecting regions. The critical process in the fabrication procedure is the step of the HIP bonding, because it is required to maintain internal mesh space for fail-safe feature. Optimum HIP conditions were examined by a series of trial fabrications, and are decided as follows; HIP pressure of 4.9 MPa, the temperature of 1100°C, and the holding time of 2 hours. Diffusion bonding by HP is also a candidate bonding technique to fabricate the double-walled fail-safe structure. The seal welding methods of the panel ends and the bolt connecting regions for making double-boundary for the coolant are presented in Fig. 2.5.2 (a) and (b), respectively. Laser beam (LB) welding technique, which transmits laser beam by optical fibers, can be applicable for the seal welding.

2.6 Thermo-mechanical analysis

Thermal and mechanical behaviors of the double-walled FW panel have been analyzed by using 3-dimensional FEM model. Calculation conditions considered in a series of analyses are summarized in Table 1, which is consistent with the ITER/EDA design parameters. Material properties employed for the stress analysis of the FW panel are also summarized in Table 2.

Temperature and stress distributions of the double-walled FW panel under the surface heat flux of 0.3 MW/m^2 are shown in Fig. 2.6.1 and Fig. 2.6.2, respectively. In this analysis, the inner pressure and nuclear heating of the FW panel are also considered. The maximum temperature and Von Mises stress of the SS316 structure are found to be 240°C and 353 MPa, respectively. The maximum stress in SS316 structure was observed at the inner wall of the concave surface adjacent to Be limiter due to large heat flux concentration through Be limiter.

Maximum Von Mises stresses in SS316 structure are shown in Fig. 2.6.3 as a function of surface heat fluxes. This figure shows the double-walled structure can accommodate the surface heat fluxes of more than 0.3 MW/m^2 even if the maximum stress of SS316 is limited by 3Sm specified in the conventional stress criteria such as ASME. Also, it is shown that the reduction of thermal stress is possible by optimizing wall thickness. However, the application of conventional stress criteria is not suitable for this new FW configuration, because it can not make good use of a big advantage of the fail-safe structure. As lowest permissible level of residual strength can be retained by one of two walls, and also crack can be arrested in the mesh region, new compatible design criteria needs to be discussed for such a fail-safe structure, based on actual failure stress and failure loads of double-walled fail-safe structure obtained by experiments.

In the case that the Cu-alloy is applied to the FW panel, FEM mechanical analyses show that the FW panel can accommodate much higher surface heat flux up to 3 MW/m^2

together with the inner pressure and nuclear heating. Thus, the double-walled fail-safe structure can give a wide design window for the FW, which enables high temperature operation of around 300°C under high surface heat flux and nuclear heating.

2.7 Mechanical analysis under electromagnetic loading

Mechanical behaviors of the double-walled FW panel under electromagnetic load due to plasma disruption have been analyzed by using two types of 3-dimensional FEM models, Model-1 and Model-2. In Model-1, double-walled quilting structure which is supported by DS copper bolts was modeled into a single wall shell elements with equivalent stiffness and spring elements representing bolt stiffness. The effect of bolt pitch on the maximum displacement and stress of the panel was analyzed under the loading condition of 2.0 MPa. The maximum displacement and maximum Von Mises stresses of quilting panel obtained by analysis are shown in Fig. 2.7.1 and Fig. 2.7.2 as a function of bolt pitches. The figures show that the designed bolt pitch of 150 mm can reduce the maximum displacement and stress of FW panel to 0.1 mm and 90 MPa . In Model-2, the same FEM model employed for thermo-mechanical analyses was adopted to evaluate the stress distribution in the quilting structure, The detailed deformation and stress distribution of quilting panel under out-of-plane load of 2 MPa are shown in Fig. 2.7.3 and Fig. 2.7.4, respectively. The maximum displacement of quilting panel was calculated to be 1 mm. The maximum stress in the panel was also calculated to be 65.5 MPa. The stress level in the panel has much margin to the allowable limit of 1.5 Sm.

3. R&D activities

3.1 Double-walled structure

Trial fabrication of the double-walled fail-safe structure sandwiching the metal mesh has been performed by using HIP bonding technique and the thermal characteristics of the double-walled structure were examined by a series of experiments. In this trial, SS304 was employed for the structural material of the inner/outer walls and the metal mesh. The size of this panel structure is 300 mm square. In order to examine a suitable weaving type and a wire diameter of the metal mesh for assuring adequate leak detection space, several types of wire cloths and wire diameters were examined in the bonding tests.

Typical microscopic structure of the leak detection layer (mesh region) after the completion of the HIP bonding is shown in Fig. 3.1.1. As shown in the figure, interface between the woven wires and the inner/outer walls are metallurgically bonded, while sufficient space for leak detection is maintained under the optimum HIP conditions. Ratio of bonding area in the mesh region obtained by a series of measurements were 38 ~ 41% of total area.

Effective thermal conductivity of the double-wall (in the direction across the mesh) was also measured by using conventional laser flushing method. Test results are

together with the inner pressure and nuclear heating. Thus, the double-walled fail-safe structure can give a wide design window for the FW, which enables high temperature operation of around 300°C under high surface heat flux and nuclear heating.

2.7 Mechanical analysis under electromagnetic loading

Mechanical behaviors of the double-walled FW panel under electromagnetic load due to plasma disruption have been analyzed by using two types of 3-dimensional FEM models, Model-1 and Model-2. In Model-1, double-walled quilting structure which is supported by DS copper bolts was modeled into a single wall shell elements with equivalent stiffness and spring elements representing bolt stiffness. The effect of bolt pitch on the maximum displacement and stress of the panel was analyzed under the loading condition of 2.0 MPa. The maximum displacement and maximum Von Mises stresses of quilting panel obtained by analysis are shown in Fig. 2.7.1 and Fig. 2.7.2 as a function of bolt pitches. The figures show that the designed bolt pitch of 150 mm can reduce the maximum displacement and stress of FW panel to 0.1 mm and 90 MPa . In Model-2, the same FEM model employed for thermo-mechanical analyses was adopted to evaluate the stress distribution in the quilting structure, The detailed deformation and stress distribution of quilting panel under out-of-plane load of 2 MPa are shown in Fig. 2.7.3 and Fig. 2.7.4, respectively. The maximum displacement of quilting panel was calculated to be 1 mm. The maximum stress in the panel was also calculated to be 65.5 MPa. The stress level in the panel has much margin to the allowable limit of 1.5 Sm.

3. R&D activities

3.1 Double-walled structure

Trial fabrication of the double-walled fail-safe structure sandwiching the metal mesh has been performed by using HIP bonding technique and the thermal characteristics of the double-walled structure were examined by a series of experiments. In this trial, SS304 was employed for the structural material of the inner/outer walls and the metal mesh. The size of this panel structure is 300 mm square. In order to examine a suitable weaving type and a wire diameter of the metal mesh for assuring adequate leak detection space, several types of wire cloths and wire diameters were examined in the bonding tests.

Typical microscopic structure of the leak detection layer (mesh region) after the completion of the HIP bonding is shown in Fig. 3.1.1. As shown in the figure, interface between the woven wires and the inner/outer walls are metallurgically bonded, while sufficient space for leak detection is maintained under the optimum HIP conditions. Ratio of bonding area in the mesh region obtained by a series of measurements were 38 ~ 41% of total area.

Effective thermal conductivity of the double-wall (in the direction across the mesh) was also measured by using conventional laser flushing method. Test results are

summarized in Table 3. Effective thermal conductivities including the mesh region were in the range of 13.3 ~ 13.8 W/m-K at 20°C in atmosphere. These values correspond to 80 ~ 83 % of those of the base metal of 4.0 mm thickness. Conductance of the leak detection layer (mesh region) was also measured and found to be in the range of 1.1 ~ 1.7 x 10^{-6} m^3/s, which seems enough for in-service leak monitoring.

Leak detectability was examined with small holes put on one side of the double walled structure, sized 0.36, 0.18, 0.14 mm in diameter respectively. Leak rate of N_2 gas was controlled as 0.1, 0.5,1.0 SCCM (atm cm^3/min) and measurement was conducted 2 times for each condition. Test setups are shown in Figs. 3.1.2 ~ 6, and the results are shown in Figs. 3.1.7 ~ 10. The results for the case of a hole of 0.14 mm in diameter was not described here because the hole was put just on the mesh wire and didn't reach another side. The rate of pressure rise depends on the conductance which is decided by the distance from the leakage location and the size of the hole. The conductance of the panel was found to be 1.7 x 10^{-6} m^3/s (30 cm away from the leakage location) as mentioned above, so that the total conductances including the conductances of the holes as orifices were estimated as 1.5 x 10^{-6} m^3/s (0.36 mm in diameter) and 1.1 x 10^{-6} m^3/s (0.18 mm in diameter) respectively. Linearity could be found between conductance and pressure rise rate. Subsequently, relationship between flaw opening size and the leak rate could be derived in further investigation. Leakage can be detected in any case.

3.2 Quilting panel

Trial fabrication of the double-walled quilting panel structure was performed with the process as mentioned in Section 2.5. This panel was designed for the surface heat flux of 0.4 MW/m^2 and operation coolant pressure of 4.9 MPa. Figs. 3.2.1 ~ 4 show the fabricated structure, and Figs. 3.2.5 ~ 8 show the cross section of the panel. In Fig. 3.2.6, slight deformation of center plate was confirmed at outlet tube. It is considered that thermal or mechanical forces acting on double-wall induce the deformation of center plate through the outlet tube. This can be avoided by modifying the outlet tube as sliding type one between double wall and center plate. Destructive examination of the fabricated panel was conducted, and microstructures at seven points were inspected. Fig. 3.2.9 shows the seven points employed for inspection and their microstructures are presented in Figs. 3.2.10 ~ 23. It can be seen that leak detection region is maintained both at straight and curving regions.

The conductance of exhaust gas through the layer of meshes between walls was measured. Fig. 3.2.24 and Fig. 3.2.25 show the test piece shows and the test equipment, respectively. Leak rate of N_2 gas was controlled to be 0.05 ~ 1.0 SCCM (atm cm^3/min)

and measurement was conducted 2 times for each condition. The results are shown in Fig. 3.2.26 with the results of double walled flat panel described in chapter 3.1. Conductance of quilting panel was 2.4 x 10^{-6} ~ 3.3 x 10^{-6} m^3/s, which is almost twice of that of double walled flat panel, because there are two flow paths in quilting panel.

Pressure proof test, pressure loss test and destruction test were conducted with the test piece shown in Fig. 3.2.27 and equipment in Fig. 3.2.28. The internal pressure of 7.4 MPa, which was 1.5 times of operation pressure 4.9 MPa, was applied for 10 minutes in pressure proof test. The test was repeated 3 times and the results are shown in Table. 4 and Figs. 3.2.29 and Fig. 3.2.30. The first trial induced some plastic deformation at point 1, but 2nd and 3rd trial induced almost no plastic deformation. No failure was observed in any case. Coolant pressure drop was measured and the results are shown in Table. 5 and Fig. 3.2.31. Flow velocity was varied in the range of 2, 3, 4, and 4.5 m/s. From the results of the test, pressure loss of test piece including water supplying line was 16 ~ 20 % of the inlet pressure. Calculation described in Appendix A shows pressure drop at quilting panel is 87 % of this pressure loss, and 80 % of this drop is caused by return point from inlet to outlet path. Destruction test was conducted by applying over pressure up to 14.9 MPa, and the results are shown in Table. 6 and Figs. 3.2.32 ~ 37. Figs. 3.2.34 ~ 37 show fracture was observed at point 1 region, where quilting is coarse because of inlet/outlet tubes, and this point was confirmed as the weakest point in this panel.

4. Summary

A concept of the first wall panel mechanically separated and separately cooled from the massive blanket module has been developed as a promising concept for the FW of tokamak fusion experimental reactors. Replaceable FW panel has many advantageous features, such as a) easy handling during assembly/disassembly due to light weight (~350 kg), b) short shut-down-time for maintenance operation, c) minimized amount of radwaste, d) reduced thermal stresses of the massive blanket module separated from the high heat flux component, and e) possible higher temperature operation of the FW than the blanket module, especially for baking operation. In addition to these attractive features, a reliable double-walled quilting structure of SS316 is also employed for FW panels with fail-safe features. Results of the thermo-mechanical analyses have shown the double-walled FW panel made of SS316 can accommodate high surface heat flux of more than 0.3 MW/m^2 and nuclear heating, and application of Cu-alloy can increase operation range up to 3 MW/m^2.

Trial fabrications of the double-walled fail-safe panel made of SS304 have been conducted successfully and optimum HIP conditions and the optimum combination of the wire diameter and weaving type were examined. Measurements of the effective thermal conductivity of double-walled structure and exhaust conductance of the mesh

and measurement was conducted 2 times for each condition. The results are shown in Fig. 3.2.26 with the results of double walled flat panel described in chapter 3.1. Conductance of quilting panel was 2.4 x 10^{-6} ~ 3.3 x 10^{-6} m^3/s, which is almost twice of that of double walled flat panel, because there are two flow paths in quilting panel.

Pressure proof test, pressure loss test and destruction test were conducted with the test piece shown in Fig. 3.2.27 and equipment in Fig. 3.2.28. The internal pressure of 7.4 MPa, which was 1.5 times of operation pressure 4.9 MPa, was applied for 10 minutes in pressure proof test. The test was repeated 3 times and the results are shown in Table. 4 and Figs. 3.2.29 and Fig. 3.2.30. The first trial induced some plastic deformation at point 1, but 2nd and 3rd trial induced almost no plastic deformation. No failure was observed in any case. Coolant pressure drop was measured and the results are shown in Table. 5 and Fig. 3.2.31. Flow velocity was varied in the range of 2, 3, 4, and 4.5 m/s. From the results of the test, pressure loss of test piece including water supplying line was 16 ~ 20 % of the inlet pressure. Calculation described in Appendix A shows pressure drop at quilting panel is 87 % of this pressure loss, and 80 % of this drop is caused by return point from inlet to outlet path. Destruction test was conducted by applying over pressure up to 14.9 MPa, and the results are shown in Table. 6 and Figs. 3.2.32 ~ 37. Figs. 3.2.34 ~ 37 show fracture was observed at point 1 region, where quilting is coarse because of inlet/outlet tubes, and this point was confirmed as the weakest point in this panel.

4. Summary

A concept of the first wall panel mechanically separated and separately cooled from the massive blanket module has been developed as a promising concept for the FW of tokamak fusion experimental reactors. Replaceable FW panel has many advantageous features, such as a) easy handling during assembly/disassembly due to light weight (~350 kg), b) short shut-down-time for maintenance operation, c) minimized amount of radwaste, d) reduced thermal stresses of the massive blanket module separated from the high heat flux component, and e) possible higher temperature operation of the FW than the blanket module, especially for baking operation. In addition to these attractive features, a reliable double-walled quilting structure of SS316 is also employed for FW panels with fail-safe features. Results of the thermo-mechanical analyses have shown the double-walled FW panel made of SS316 can accommodate high surface heat flux of more than 0.3 MW/m^2 and nuclear heating, and application of Cu-alloy can increase operation range up to 3 MW/m^2.

Trial fabrications of the double-walled fail-safe panel made of SS304 have been conducted successfully and optimum HIP conditions and the optimum combination of the wire diameter and weaving type were examined. Measurements of the effective thermal conductivity of double-walled structure and exhaust conductance of the mesh

region showed the double-walled structure has a thermal conductivity of 13. 3 ~ 13.8 W/m-K including mesh region and exhaust conductance of 1.1 ~ 1.7 x 10^{-6} m^3/s, respectively. Both of which are satisfactory from thermal and leak-detection view points. Trial fabrications of the double-walled quilting panel have been also conducted successfully and useful information about inlet/outlet tube structure have been obtained. Exhaust conductance of quilting panel measured was 2.4 x 10^{-6} ~ 3.3 x 10^{-6} m^3/s. Pressure test have shown the panel have enough strength for operation pressure of 4.9 MPa and failure of this panel was around 14.9 MPa, three times higher than the design pressure. The coolant pressure loss obtained in this test were 0.04 ~ 0.23 MPa for coolant velocities of 2~4.5 m/s and 80 % of pressure loss is caused by the return point.

Acknowledgment

The authors would like to express their sincere appreciation to Drs. M. Ohta, S. Matsuda and S. Shimamoto for their continuous encouragements on this work. The contribution of Toshiba Co. on the trial fabrication are gratefully acknowledged.

region showed the double-walled structure has a thermal conductivity of 13. 3 ~ 13.8 W/m-K including mesh region and exhaust conductance of 1.1 ~ 1.7 x 10^{-6} m^3/s, respectively. Both of which are satisfactory from thermal and leak-detection view points. Trial fabrications of the double-walled quilting panel have been also conducted successfully and useful information about inlet/outlet tube structure have been obtained. Exhaust conductance of quilting panel measured was 2.4 x 10^{-6} ~ 3.3 x 10^{-6} m^3/s. Pressure test have shown the panel have enough strength for operation pressure of 4.9 MPa and failure of this panel was around 14.9 MPa, three times higher than the design pressure. The coolant pressure loss obtained in this test were 0.04 ~ 0.23 MPa for coolant velocities of 2~4.5 m/s and 80 % of pressure loss is caused by the return point.

Acknowledgment

The authors would like to express their sincere appreciation to Drs. M. Ohta, S. Matsuda and S. Shimamoto for their continuous encouragements on this work. The contribution of Toshiba Co. on the trial fabrication are gratefully acknowledged.

Table 1 Conditions of Thermo-mechanical analysis

Temperature of inlet path:	100°C
Temperature of outlet path:	150°C
Coolant pressure:	
Inlet path:	2.0 MPa
Outlet path:	1.8 MPa
Nuclear heating:	
Be limiter:	10 MW/m^3
SS316 plate:	18 MW/m^3
SS316 mesh:	18 MW/m^3
Surface heat flux of Be and SS316 structure	0, 0.3, 0.5 MW/m^2
Heat transfer coefficient	3.0 x 10^4 W/m^2-K
Thermal conductivity	
Be limiter:	114W/m-K
SS316 plate:	18 W/m-K
SS316 mesh:	4.5W/m-K

Table 2 Material properties employed for the stress analysis of FW panel

	Inner and outer wall (SS316)	Metal mesh (SS316)	Be limiter
Young's Modulus E (GPa)	174	43	297
Poisson's Ratio υ	0.3	0.3	0.08
Shear Modulus G (GPa)	67	17	138
Thermal expansion Coefficient α (1/K)	1.73 x 10^{-5}	1.73 x 10^{-5}	1.35 x 10^{-5}
Thermal Conductivity λ (W/m-K)	18	4.5	114
Reference Temperature (°C)	200	200	200

Table 3 Characteristics of double-walled fail-safe panel of SS304 fabricated by HIP method with HIP conditions of 1100°C x 2 hours and HIP pressure of 4.9 MPa.

Sample No.				Thickness of layer	leak detection	Ratio of bonding	Effective thermal conductivity
	Weave Type	Wire Dia. (mm)	Mesh number	Before hipping	After hipping	Area	(in atmosphere at 20°C)
1	Twilled weave	0.24	60/inch	0.48 mm (0.24 x 2)	0.35 ~ 0.36	0.414	13.56 W/m-K
2	Twilled weave	0.24	60/inch	0.48 mm (0.24 x 2)	0.35 ~ 0.36	0.379	13.81 W/m-K
3	Twilled weave	0.28	60/inch	0.56 mm (0.28 x 2)	0.43 ~ 0.44	0.385	13.44 W/m-K
4	Twilled weave	0.28	60/inch	0.56 mm (0.28 x 2)	0.43 ~ 0.44	0.382	13.31 W/m-K

Table 4 Displacement at pressure test

Test No.	Pressure (MPa)	Displacement (mm)				
		Point①	Point②	Point③	Point④	Point⑤
1	0.0	0.00	0.00	0.00	0.00	0.00
	1.0	0.03	0.00	0.00	0.02	0.00
	2.0	0.06	0.00	0.01	0.02	0.02
	3.0	0.08	0.00	0.02	0.03	0.02
	4.0	0.10	0.00	0.02	0.03	0.03
	5.0	0.12	0.00	0.02	0.04	0.04
	5.9	0.18	0.01	0.03	0.05	0.05
	2) 7.4	0.46	0.03	0.06	0.08	0.10
	6.0	0.43	0.02	0.06	0.07	0.10
	4.9	0.41	0.02	0.06	0.06	0.09
	3.9	0.38	0.01	0.05	0.06	0.08
	2.9	0.37	0.01	0.05	0.05	0.07
	2.0	0.34	0.01	0.05	0.05	0.07
	1.0	0.31	0.00	0.05	0.04	0.06
	0.0	0.29	0.00	0.04	0.03	0.05
1) 2	0.0	0.00	0.00	0.00	0.00	0.00
	1.0	0.02	0.00	0.01	0.00	0.00
	2.0	0.04	0.00	0.01	0.01	0.02
	3.0	0.06	0.00	0.01	0.01	0.02
	4.0	0.09	0.00	0.02	0.02	0.03
	4.9	0.10	0.01	0.02	0.03	0.04
	6.0	0.13	0.02	0.03	0.04	0.05
	2) 7.4	0.19	0.02	0.03	0.06	0.06
	5.9	0.16	0.01	0.03	0.05	0.06
	5.0	0.14	0.01	0.02	0.04	0.04
	3.9	0.12	0.01	0.02	0.03	0.04
	3.0	0.10	0.00	0.02	0.03	0.03
	2.0	0.08	0.00	0.01	0.02	0.02
	1.0	0.05	0.00	0.01	0.01	0.02
	0.0	0.02	0.00	0.00	0.00	0.00

Note 1) No.2 was tested after reset

Note 2) Hold 7.4 MPa (75 kgf / cm^2 G) for 10 minutes

Test No.	Pressure (MPa)	Displacement (mm)				
		Point①	Point②	Point③	Point④	Point⑤
3	0.0	0.00	0.00	0.00	0.00	0.00
	3) 7.3	0.16	0.02	0.03	0.05	0.06
	0.0	0.00	0.00	0.01	0.00	0.00

Note 3) Hold 7.3 MPa (75 kgf / cm^2 G) for 10 minutes

Table 5 Results of coolant pressure loss test

TestNo.	Flow rate Q (ℓ /min)	Velocity V* ' (m/s)	Inlet pressure P_0 (MPa)	outlet pressure P_1 (MPa)	Pressure loss $P_0 - P_1$ (MPa)
1	20.88	4.43	1.10	0.89	0.21
	14.46	3.07	0.54	0.44	0.10
	9.62	2.04	0.25	0.21	0.04
	14.53	3.08	0.55	0.45	0.10
	19.04	4.04	0.92	0.74	0.18
	21.02	4.46	1.10	0.89	0.21
2	19.33	4.10	0.93	0.75	0.18
	14.45	3.07	0.54	0.44	0.10
	9.56	2.03	0.25	0.21	0.04
	14.44	3.07	0.54	0.44	0.10
	19.36	4.11	0.94	0.76	0.18
	21.0	4.46	1.10	0.88	0.22
3	9.53	2.02	0.25	0.21	0.04
	14.48	3.07	0.55	0.45	0.10
	19.14	4.06	0.93	0.75	0.18
	21.55	4.58	1.16	0.93	0.23
	19.38	4.11	0.95	0.76	0.19
	14.46	3.07	0.54	0.44	0.10
	9.46	2.01	0.24	0.20	0.04

Note Flow Velocity is calculated by V=Q/A
(A= cross section of flow path, ø 10mm : Path diameter of flow mater)

Table 6 Water pressure and displacement at destruction test

Test No.	pressure (MPa)	Displacement(mm)				
		Point①	Point②	Point③	Point④	Point⑤
1	0.0	0.00	0.00	0.00	0.00	0.00
	2.5	0.04	0.01	0.01	0.01	0.01
	5.0	0.11	0.02	0.02	0.03	0.04
	7.4	0.16	0.03	0.03	0.04	0.06
	8.8	0.34	0.05	0.06	0.08	0.10
	9.6	0.63	0.08	0.11	0.12	0.15
	9.7	0.85	0.11	0.14	0.15	0.17
	10.6	1.11	0.12	0.15	0.19	0.20
	11.2	1.45	0.14	0.20	0.22	0.24
	12.4	2.09	0.20	0.27	0.32	0.33
	14.0	3.31	0.32	0.37	0.52	0.54
	14.9	3.95	0.39	0.47	0.68	0.65
	9.8	3.86	0.38	0.48	0.66	0.64
	0.0	3.56	0.34	0.43	0.56	0.53

(Test in the presence of a witness)

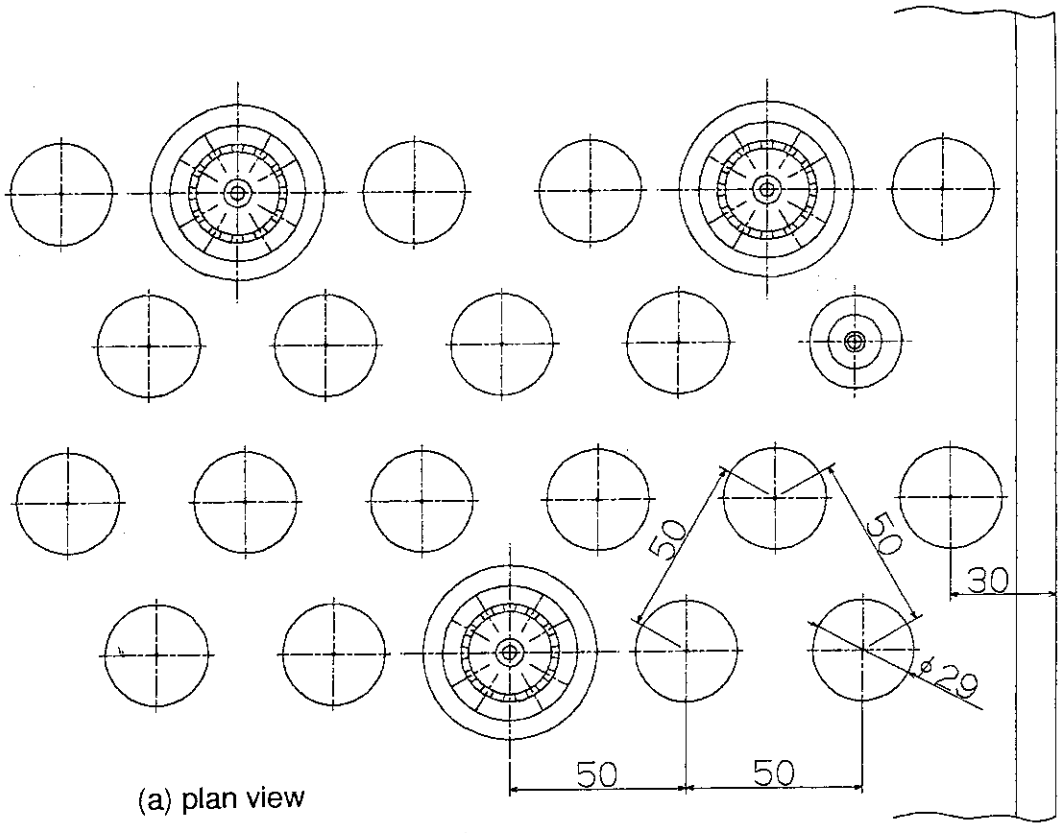

(a) plan view

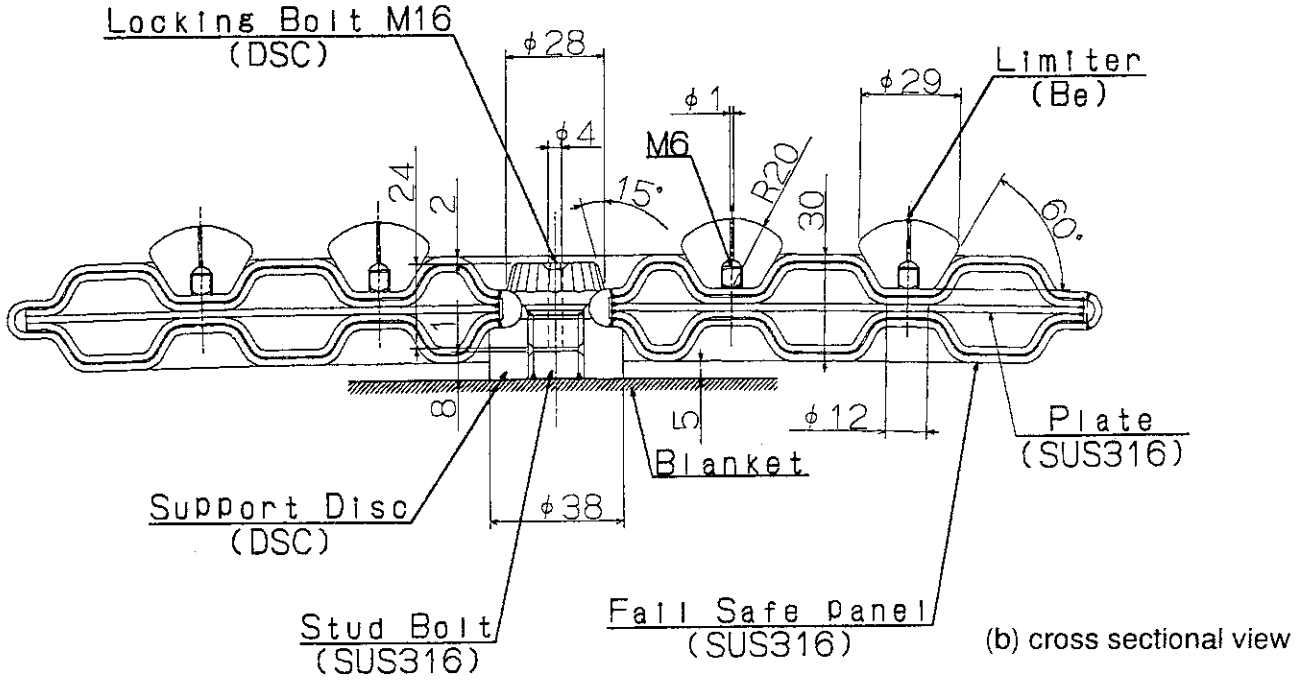

(b) cross sectional view

Fig. 2.1.1 Configuration of mechanically separated first wall

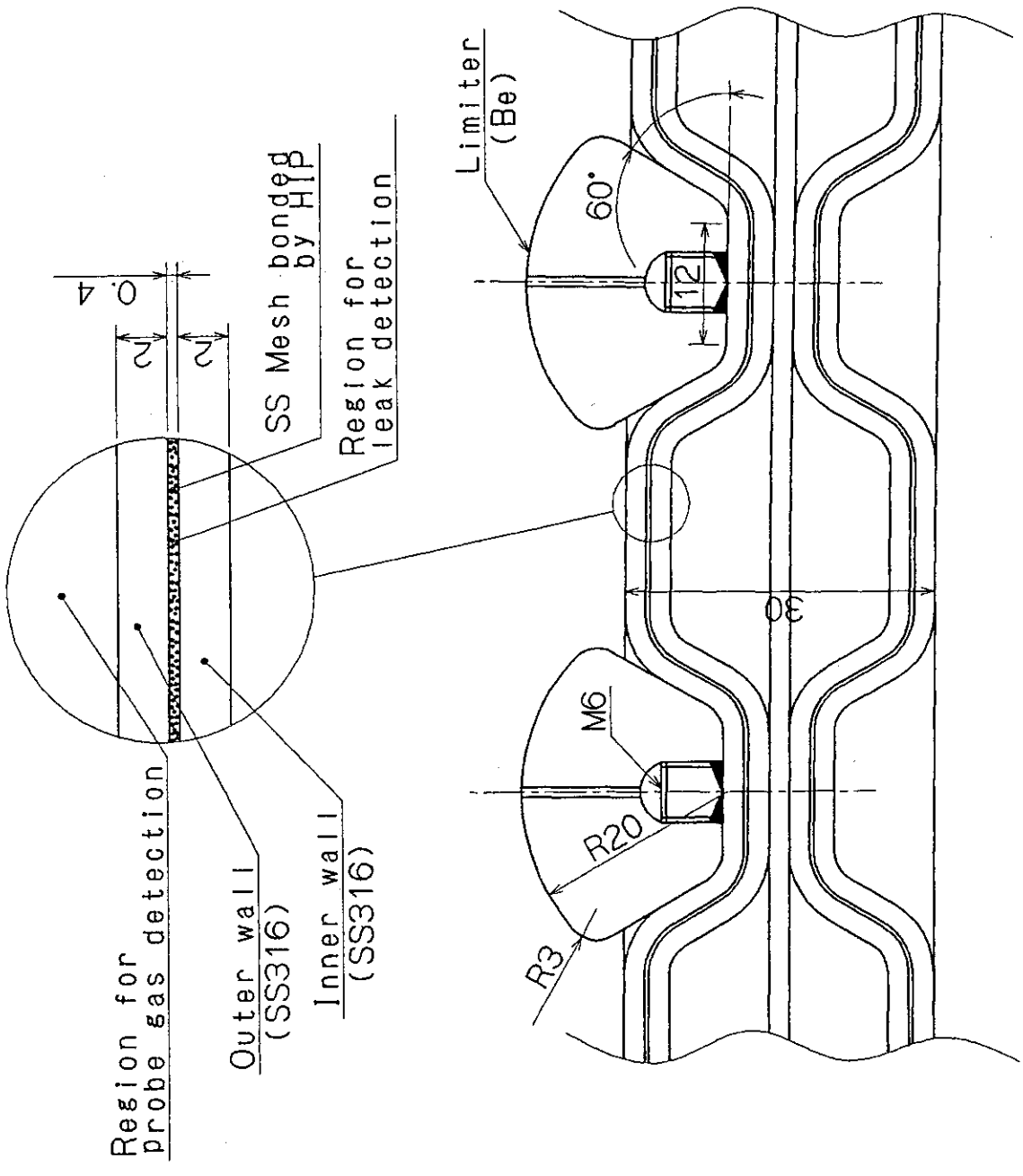

Fig.2.1.2 Double-walled fail-safe structure of Separated FW

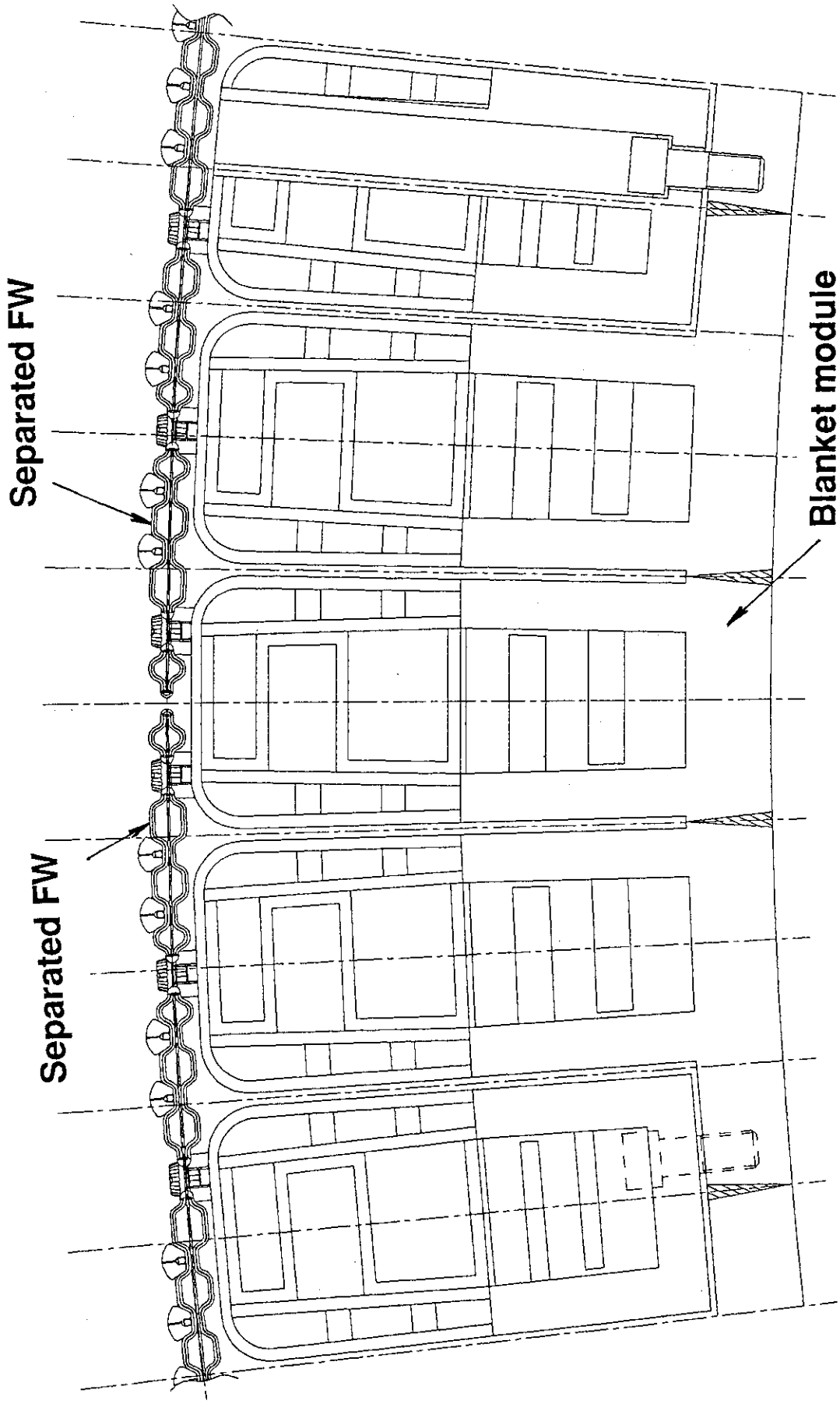

Fig.2.1.3 Separated FW connected to blanket module

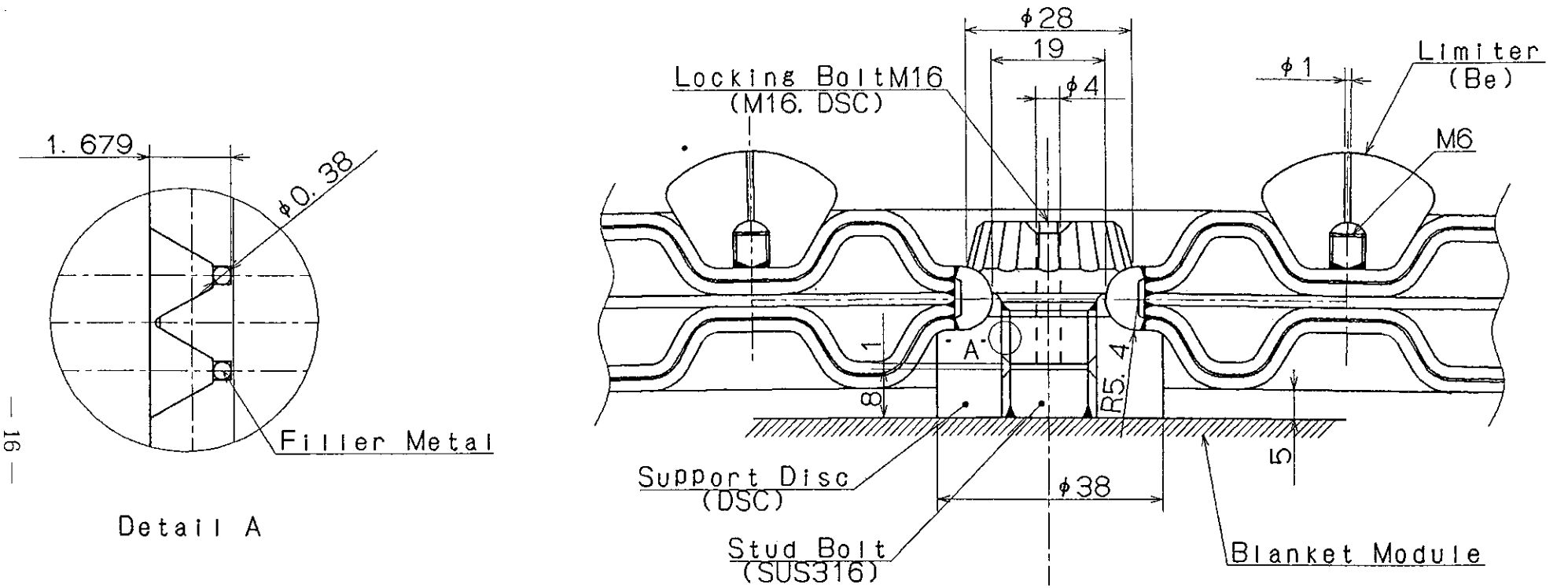

Fig.2.2.1 Mechanical support, surface alignment and
Surface protection of Separated FW

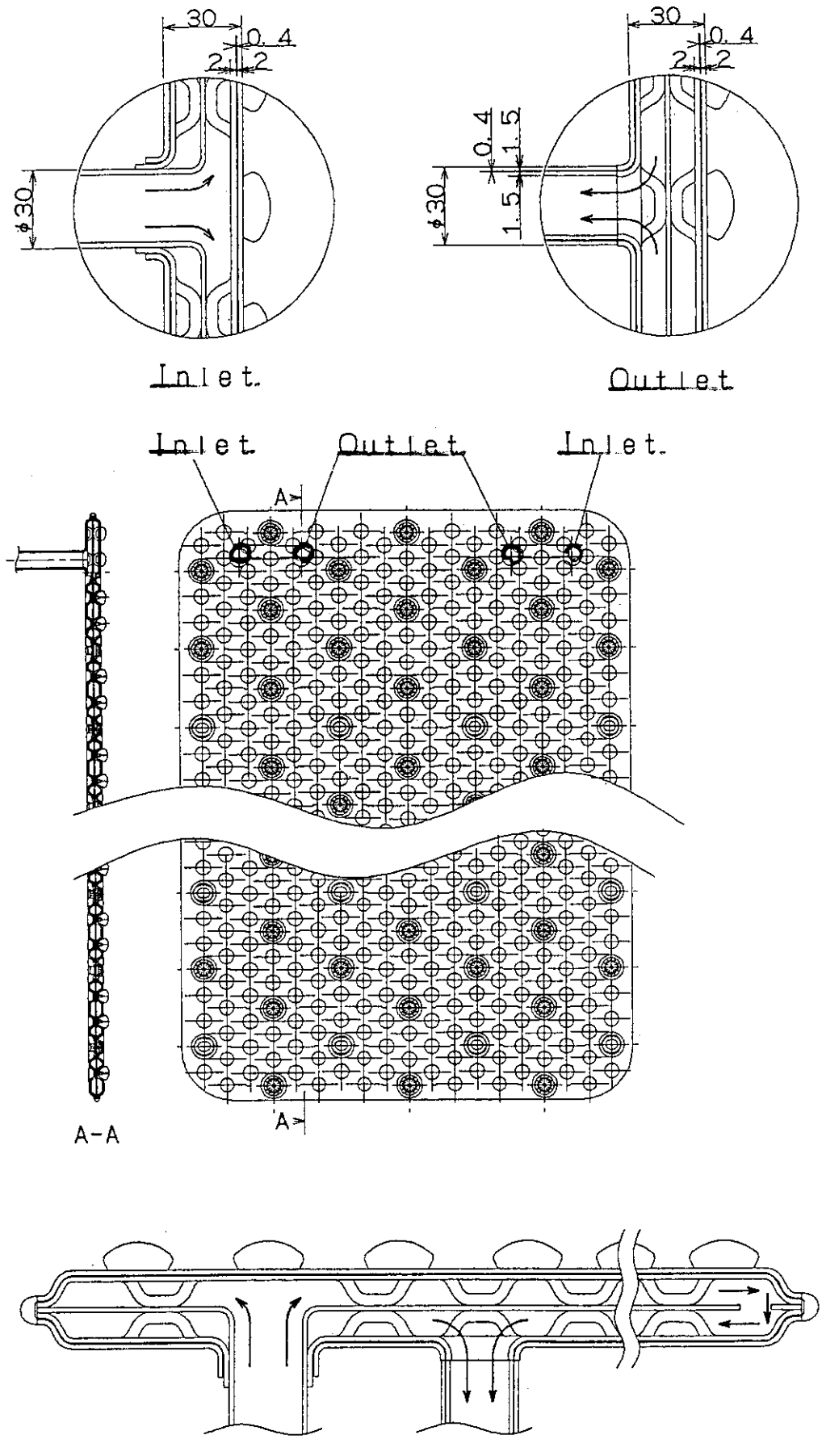

Fig.2.4.1 Cooling scheme of Separated FW

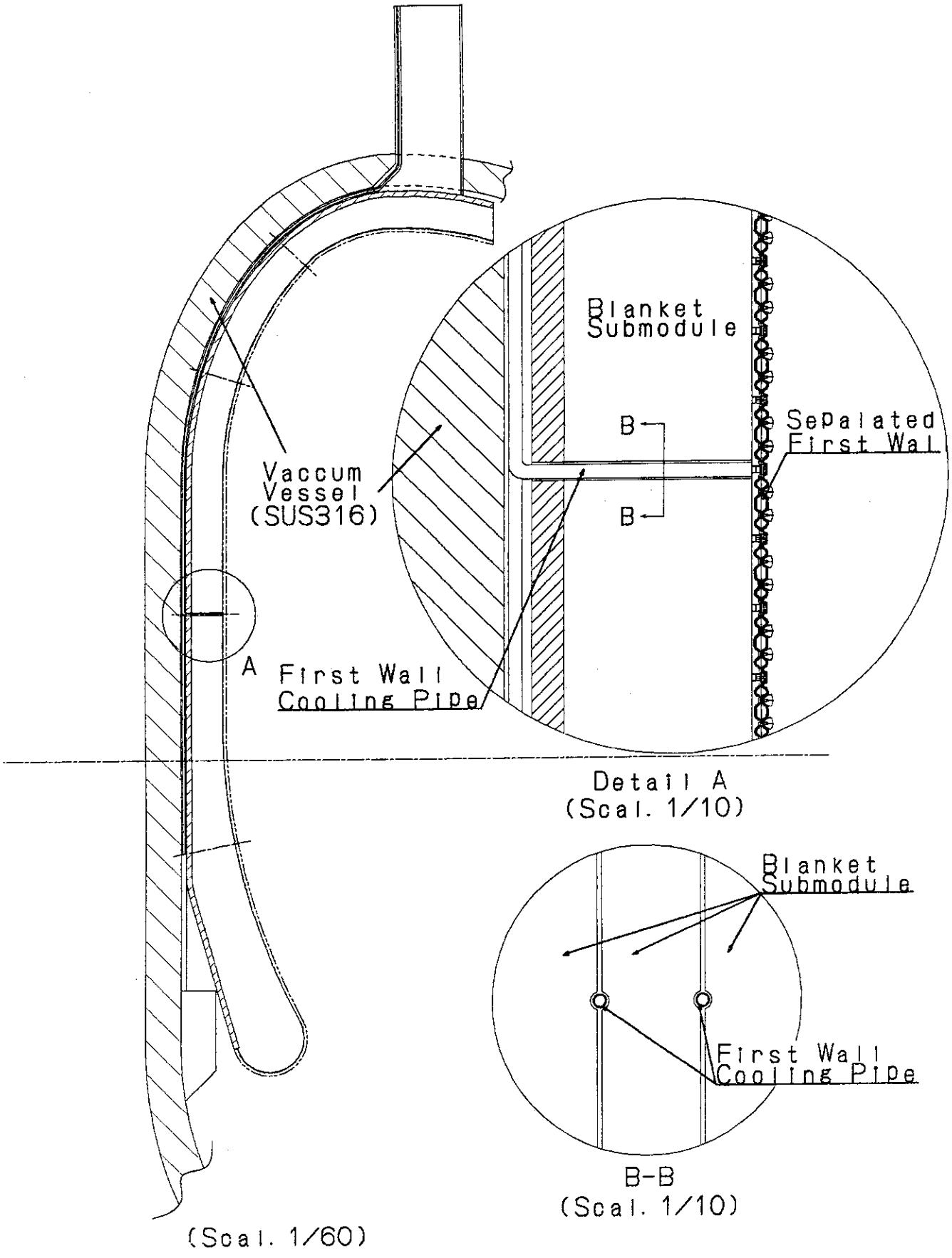

Fig.2.4.2 Manifold routing of Separated FW

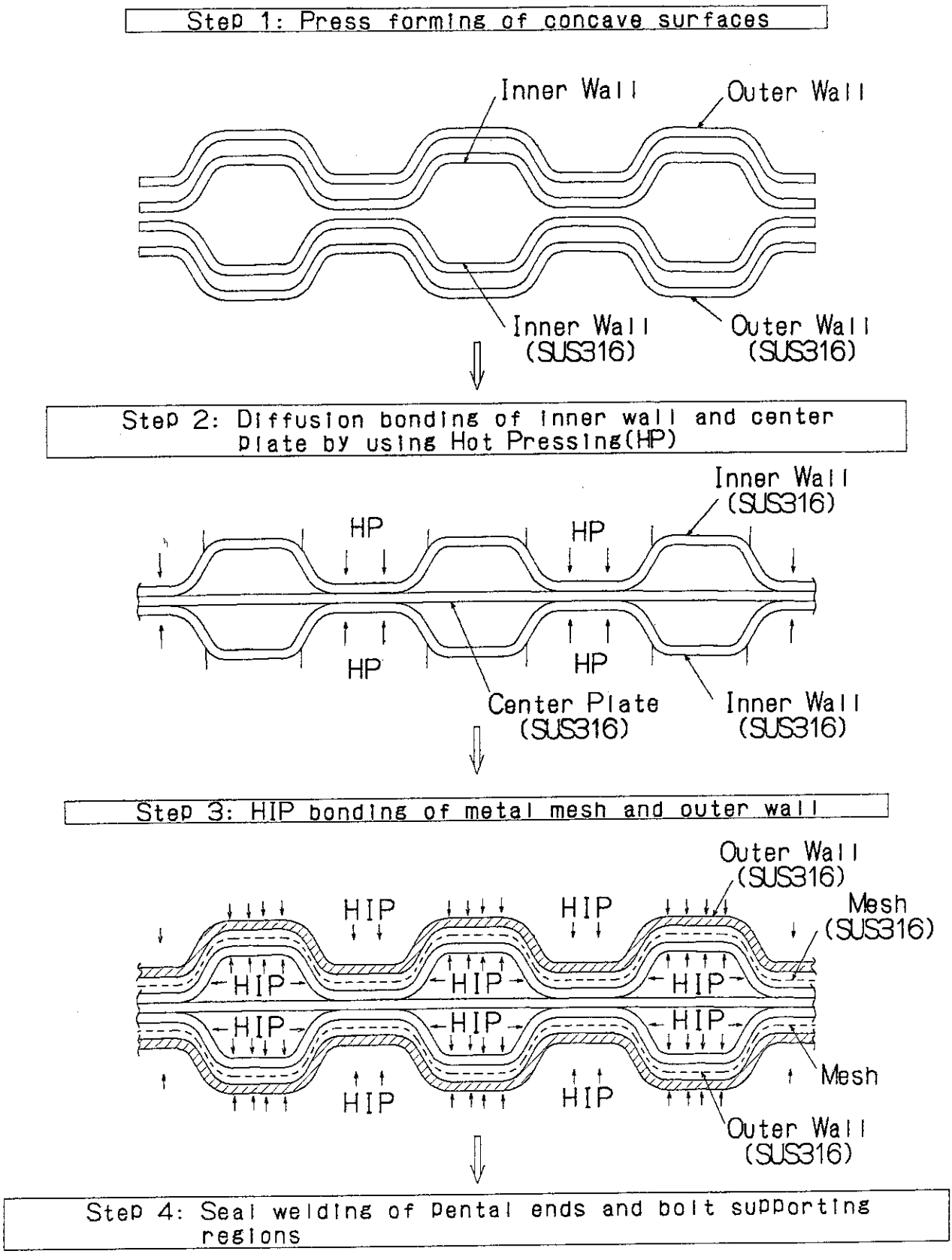

Fig. 2.5.1 Candidate fabrication procedure of double-walled FW

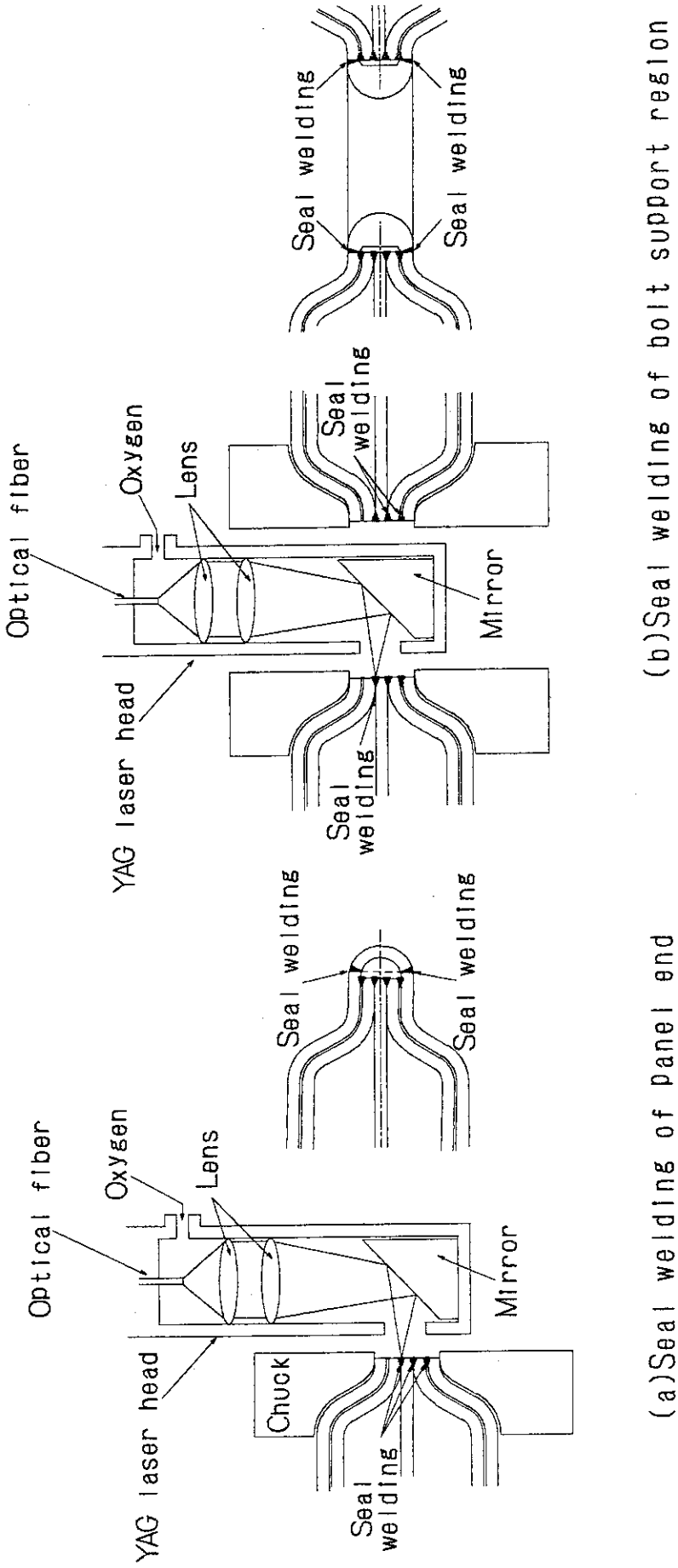

(a)Seal welding of panel end (b)Seal welding of bolt support region

Fig. 2.5.2 Seal welding method of panel end and bolt connecting region by laser beam welding

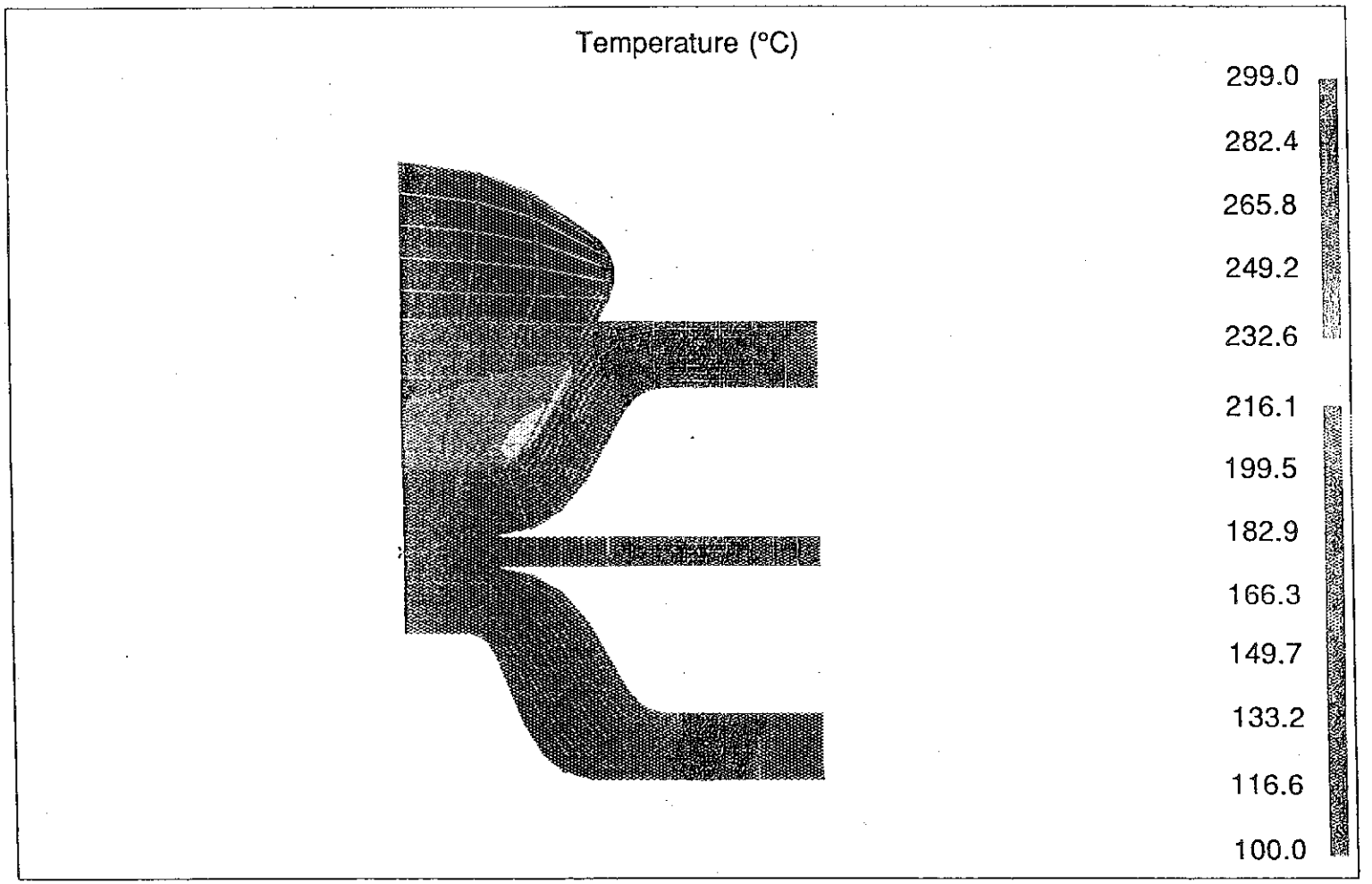

Fig. 2.6.1 Temperature distribution of FW panel under surface heat flux of 0.3 MW/m^2 and nuclear heating.

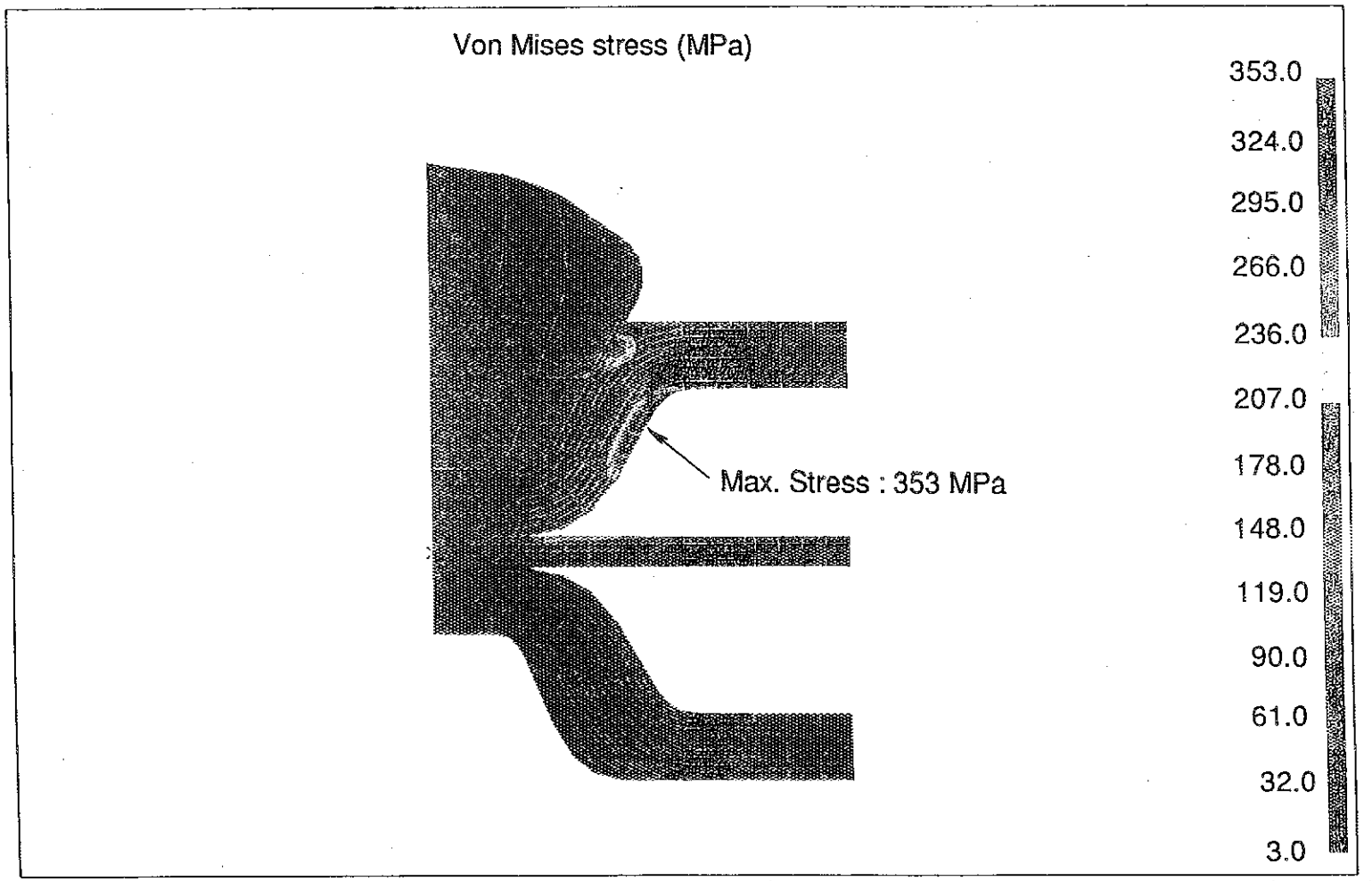

Fig. 2.6.2 Distribution of Von Mises stress in FW panel due to surface heat flux of 0.3 MW/m^2 , nuclear heating, and coolant pressure.

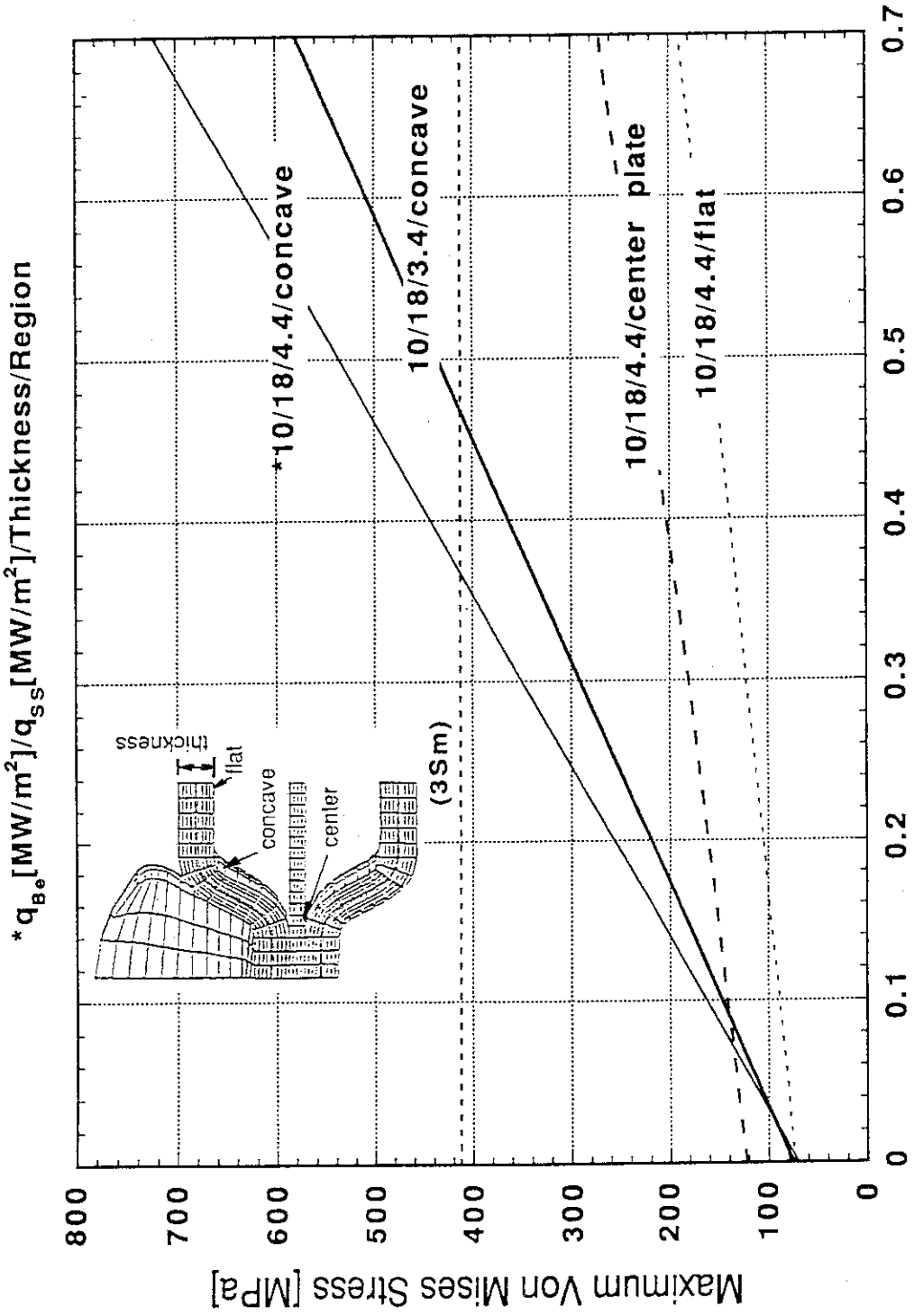

Fig.2.6.3 Maximum Von Mises stress in SUS316 separated FW panel as a function of surface load (Coolant pressure : 2MPa)

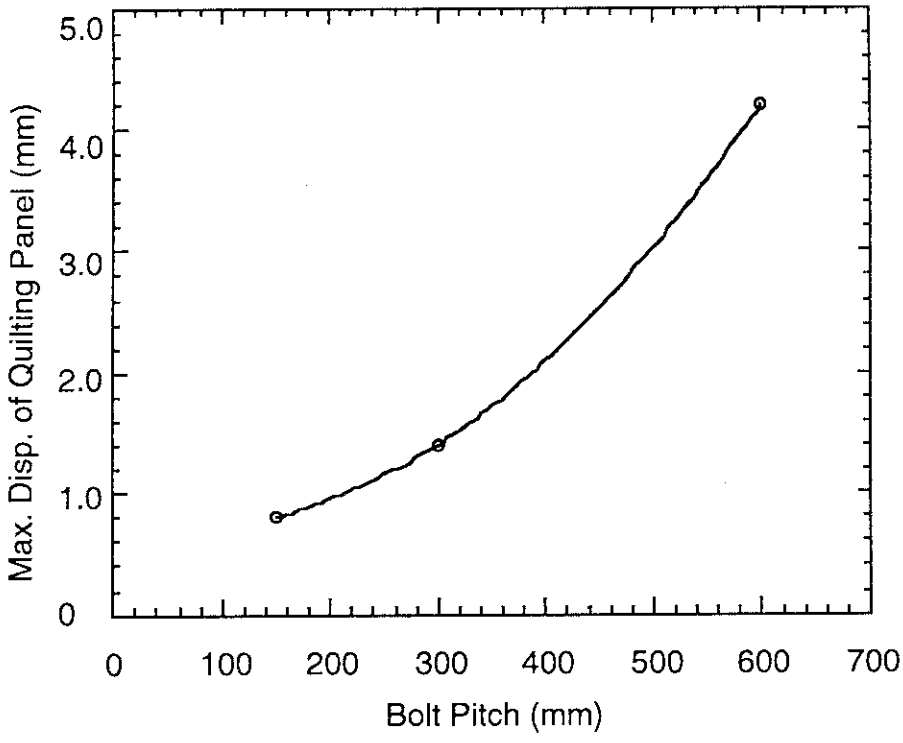

Fig. 2.7.1 Maximum displacement of quilting panel due to electromagnetic load of 2 MPa in the out-of-plane direction. Maximum displacements are shown as a function of supporting bolt pitches

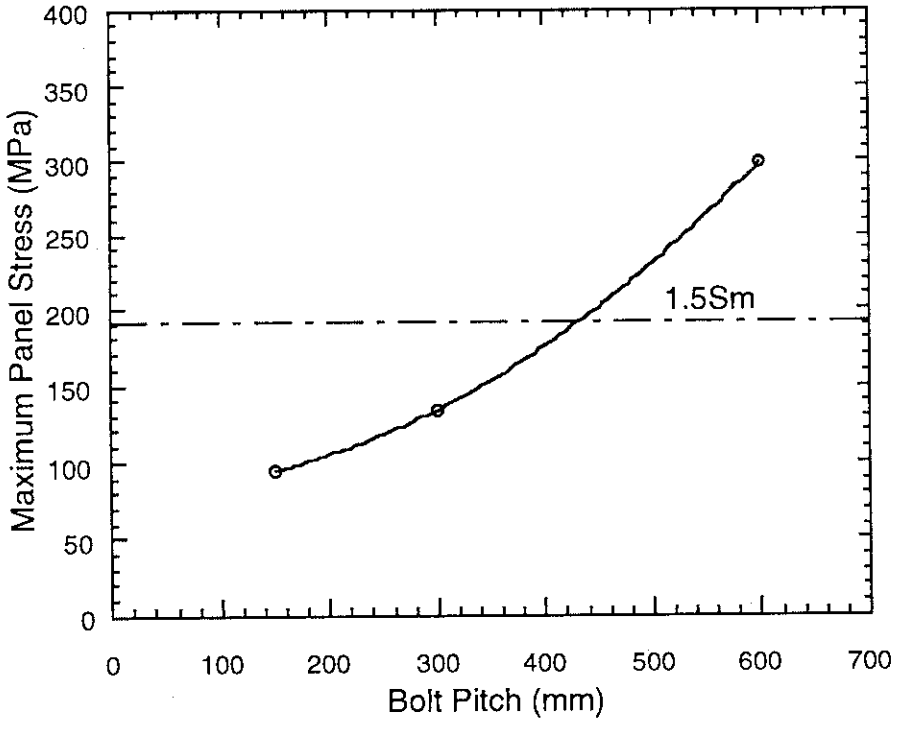

Fig. 2.7.2 Maximum stresses of quilting panel due to electromagnetic load of 2 MPa in the out-of-plane direction. Maximum Von Mises stresses are shown as a function of supporting bolt pitches

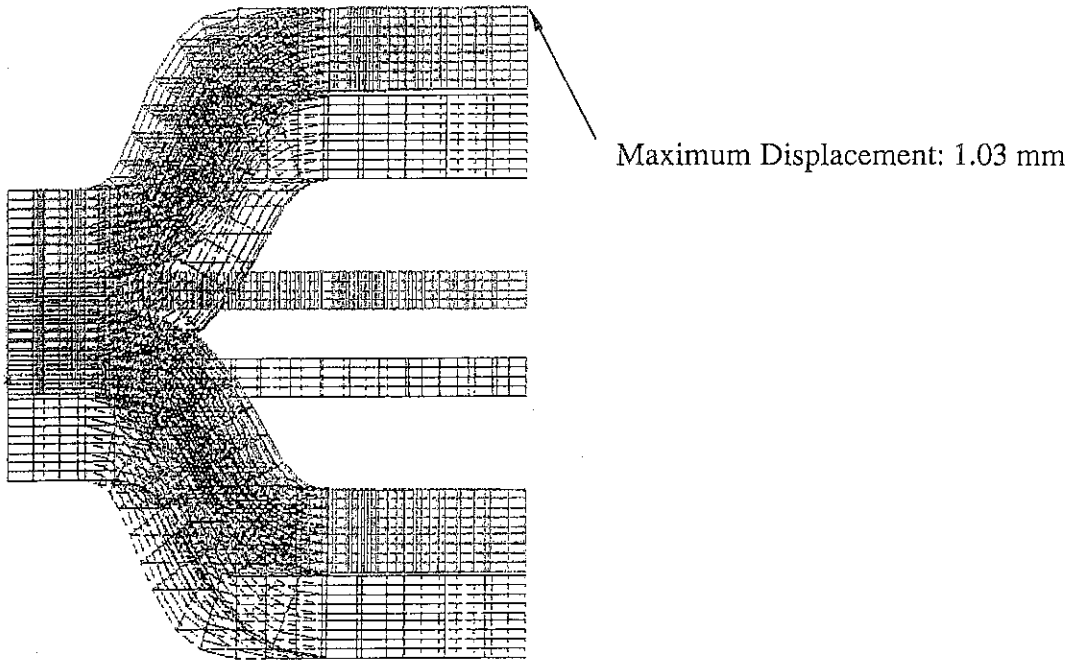

Fig. 2.7.3 Displacement of quilting panel due to electromagnetic load of 2 MPa in the out-of-plane direction (Bolt pitch: 150 mm)

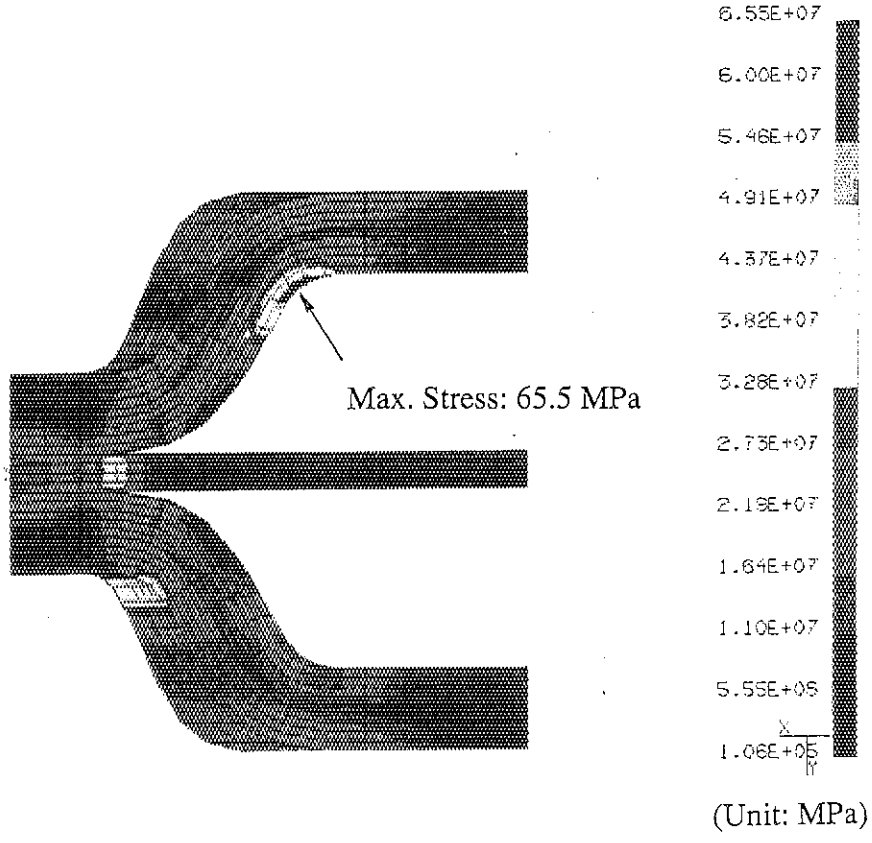

Fig. 2.7.4 Distribution of Von Mises stresses in the quilting panel due to electromagnetic load of 2 MPa in the out-of-plane direction
(Bolt pitch: 150 mm, Pitch of Be Limiter: 50mm)

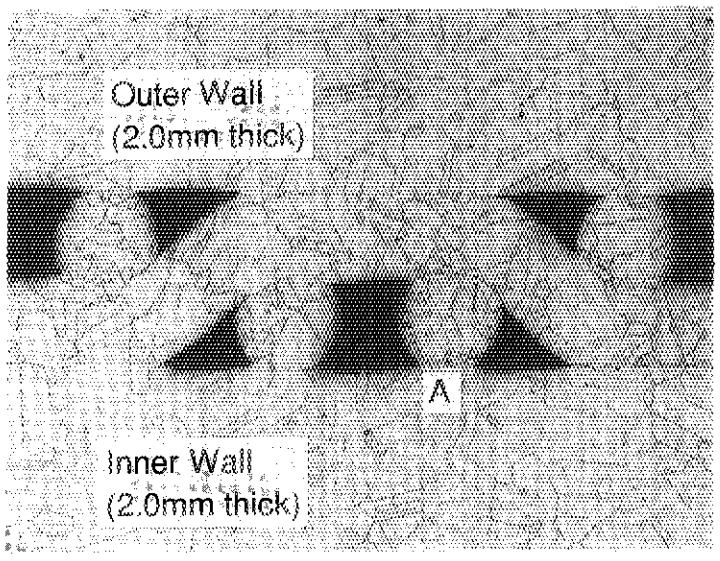

(a) Microscopic structure of leak detection layer (x 50)
Thickness of leak detection layer : 0.44 mm

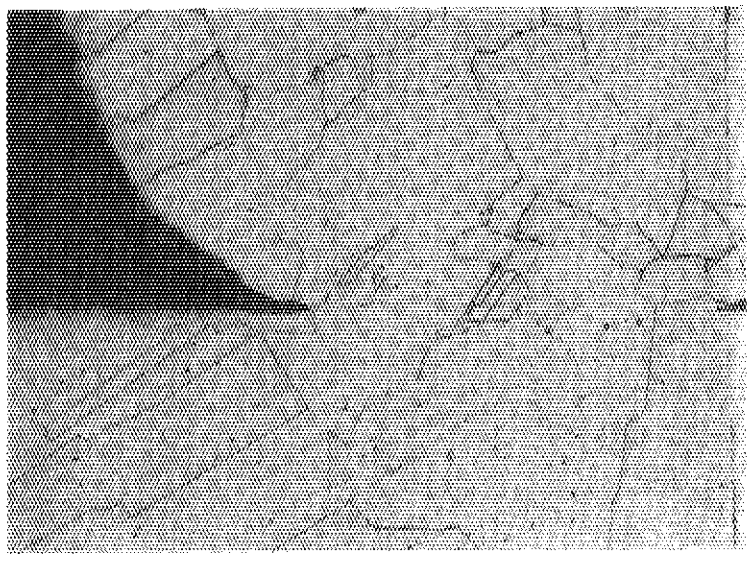

(b) Detailed structure of point A (x 400)

Fig. 3.1.1 Microscopic structure of leak detection layer of double-walled fail-safe panel made of SS304 after HIP bonding with HIP conditions of 1100℃ x 2 hours and HIP pressure of 4.9 MPa

Wire diameter : 0.28 mm
Mesh type : Twilled weave type
Mesh numbers : 60/inch

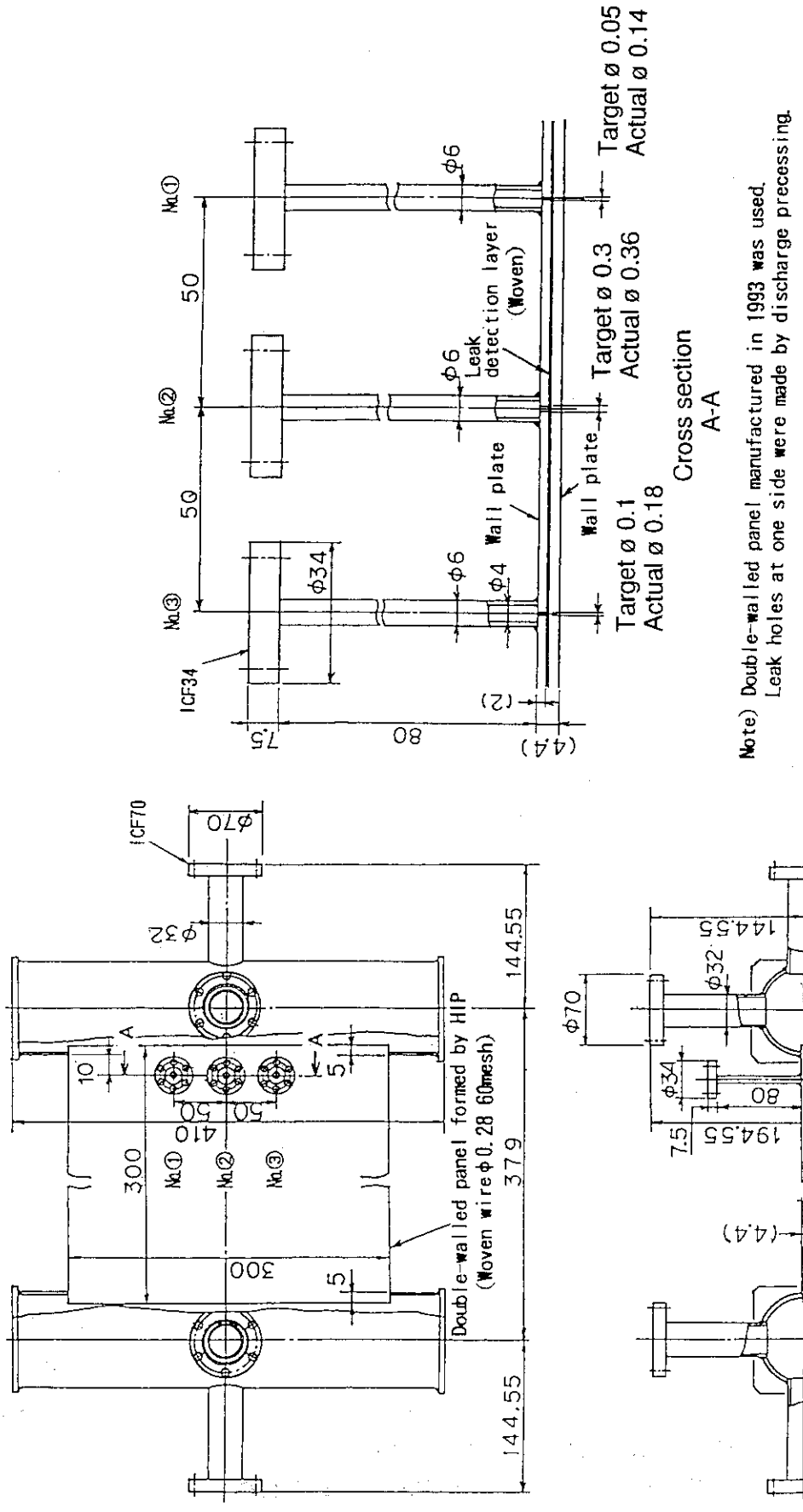

Fig. 3.1.2 Double-walled panel for leakage detection test

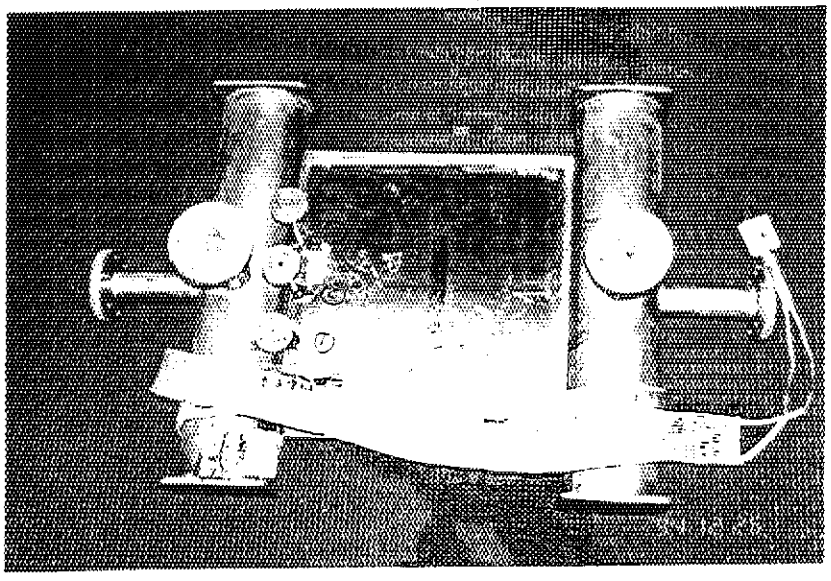

Fig. 3.1.3 Double-walled panel for leakage detection test

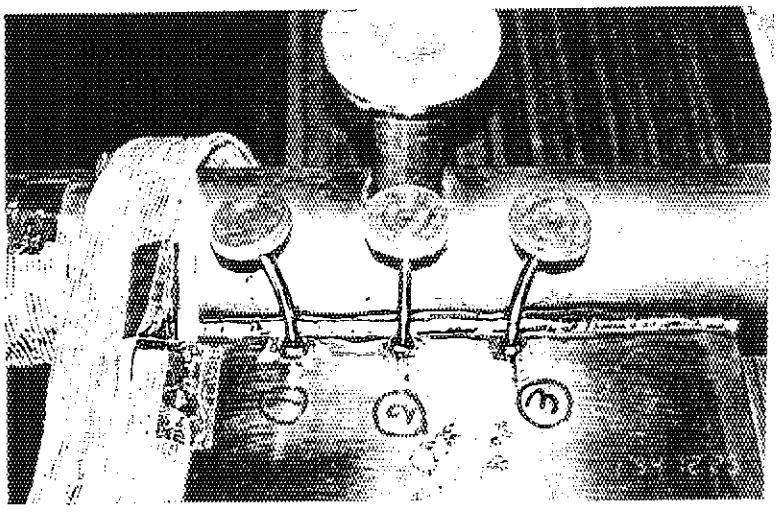

Fig. 3.1.4 Leakage holes on a double-walled panel (ICF34)

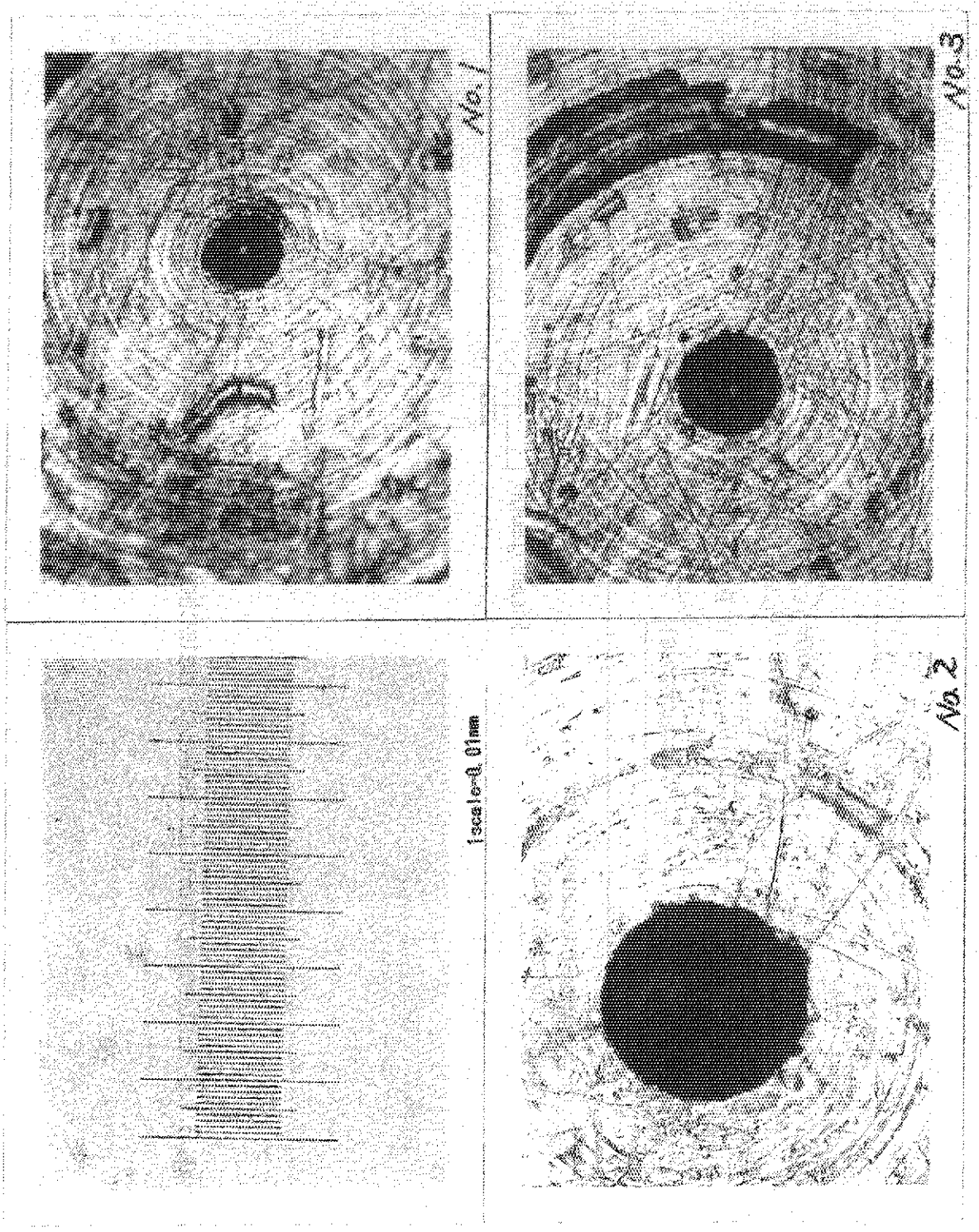

Fig. 3.1.5

Scale	No. 1 Leak hole
No. 2 Leak hole	No. 3 Leak hole

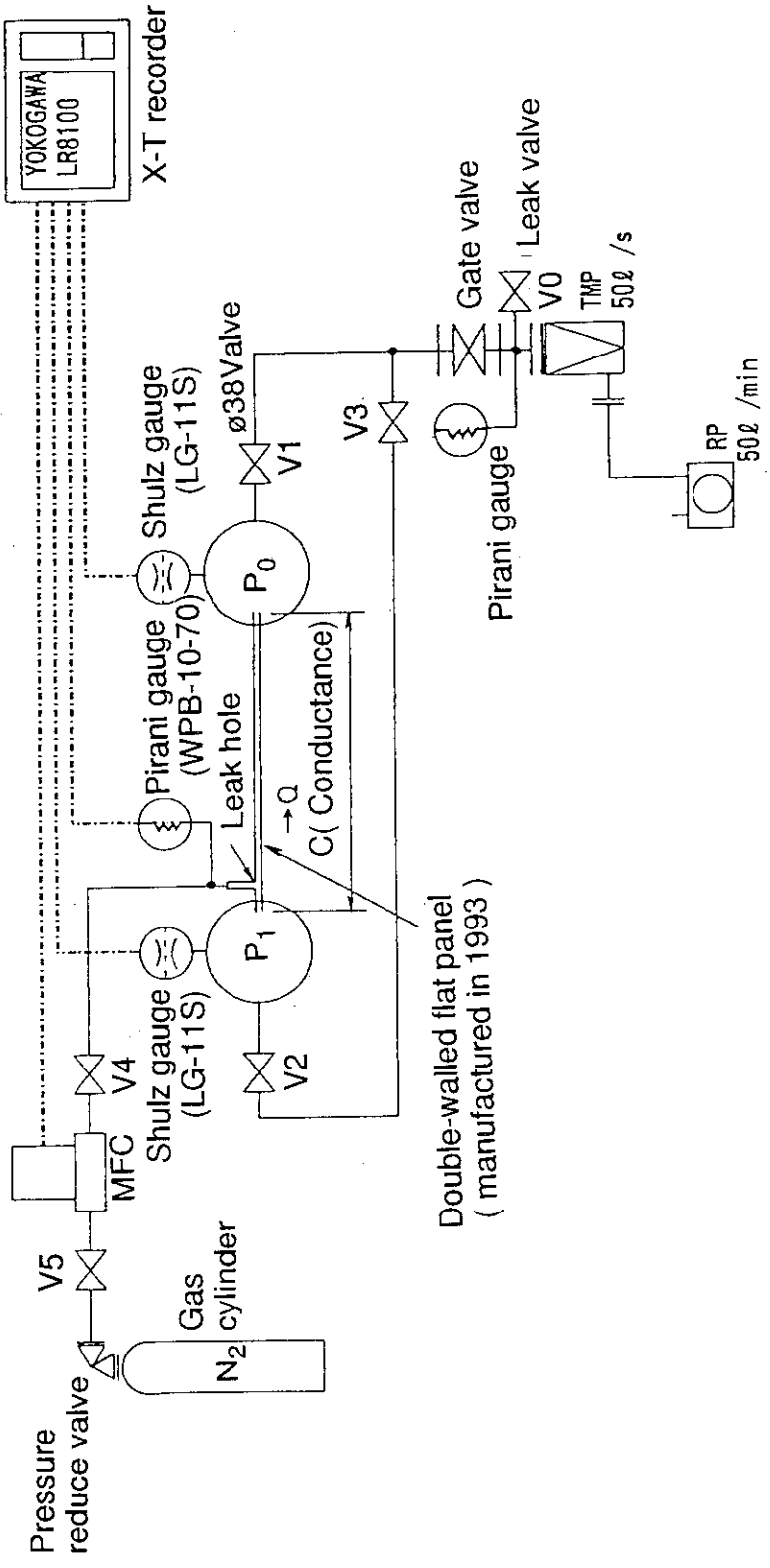

Fig. 3.1.6 Test equipment for leakage detection of double-walled panel

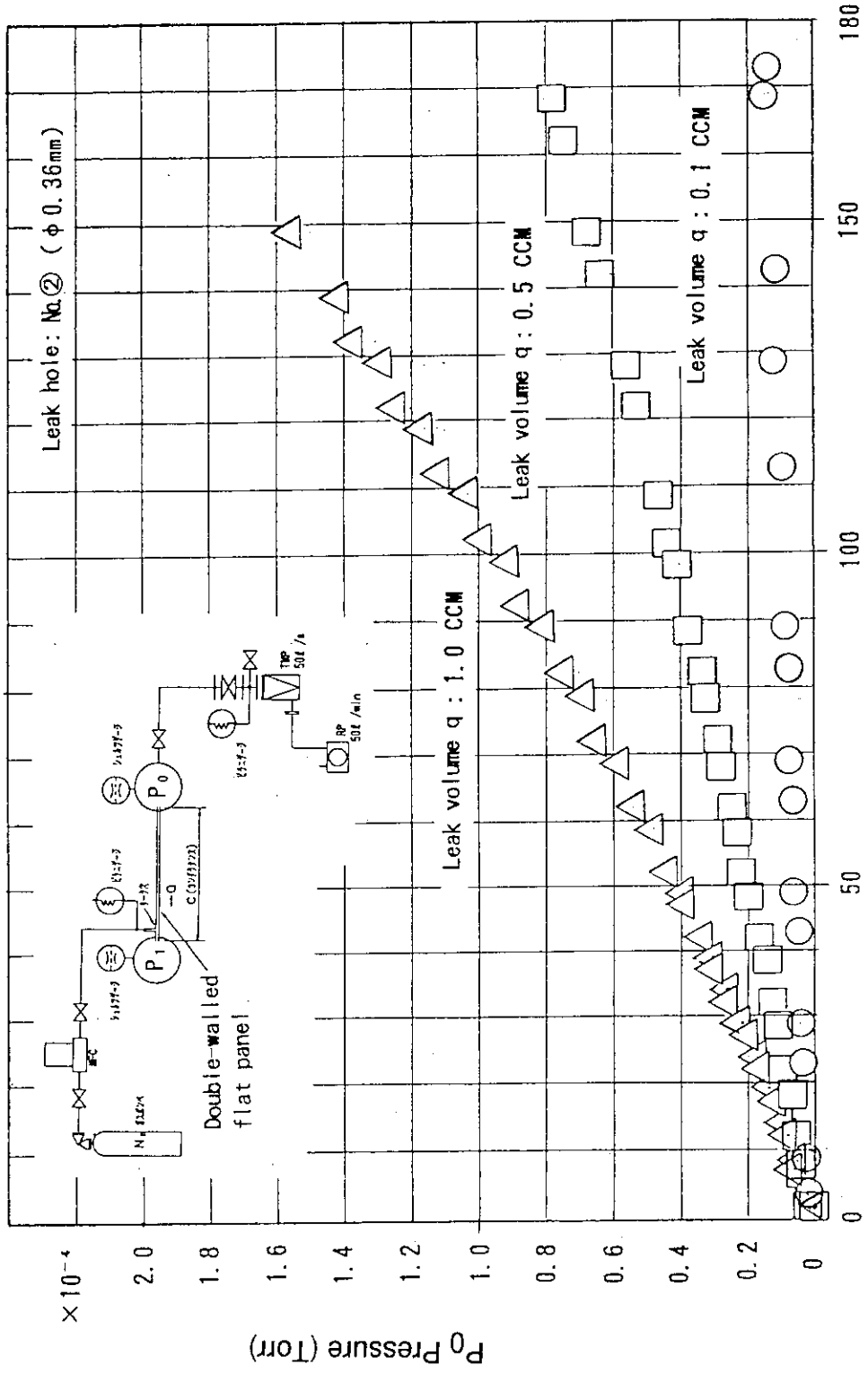

Fig. 3.1.7 Increment of pressure P_0 after leak (leak hole : φ 0.36 mm)

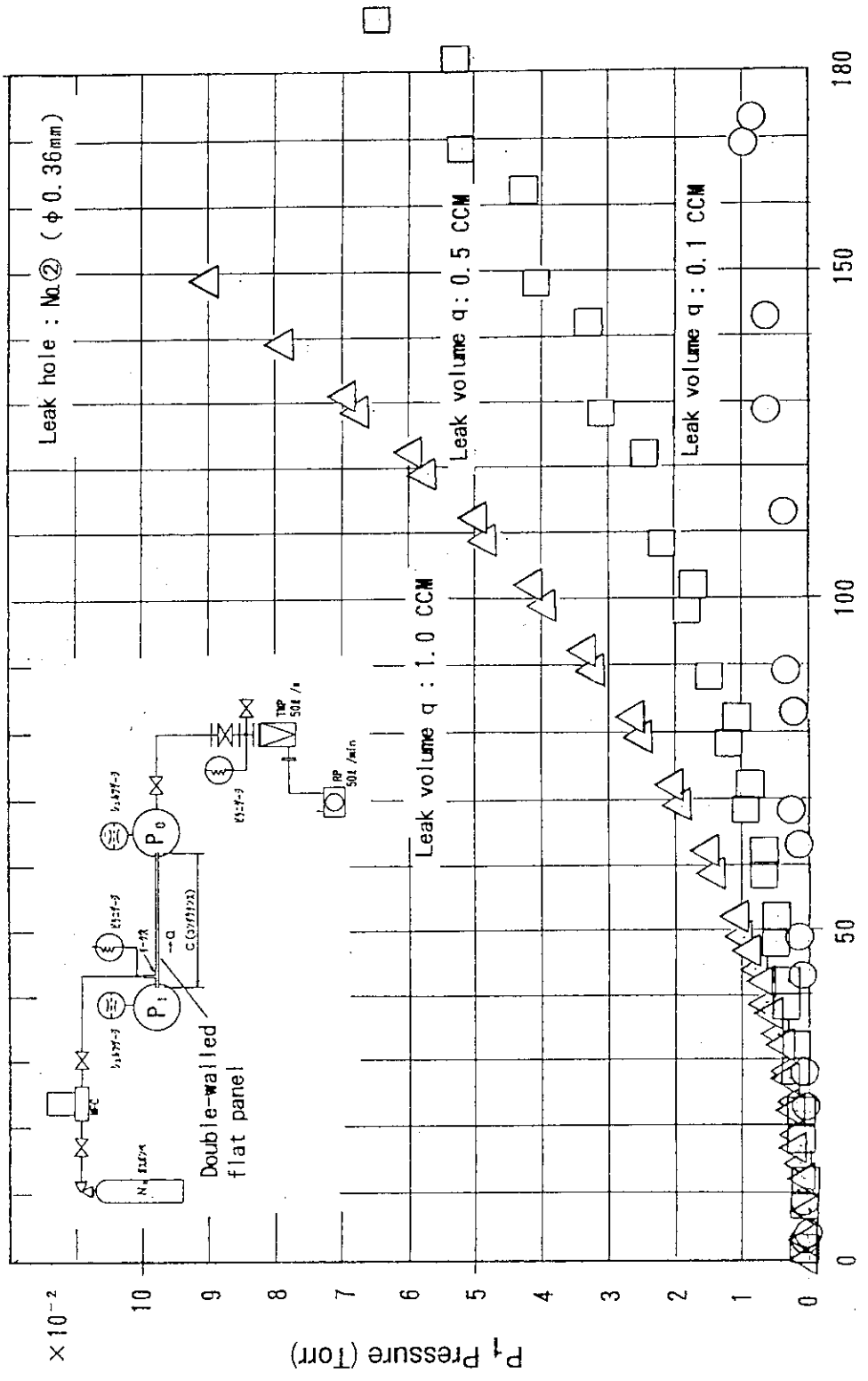

Fig. 3.1.8 Increment of pressure P_1 after leak (leak hole : φ 0.36 mm)

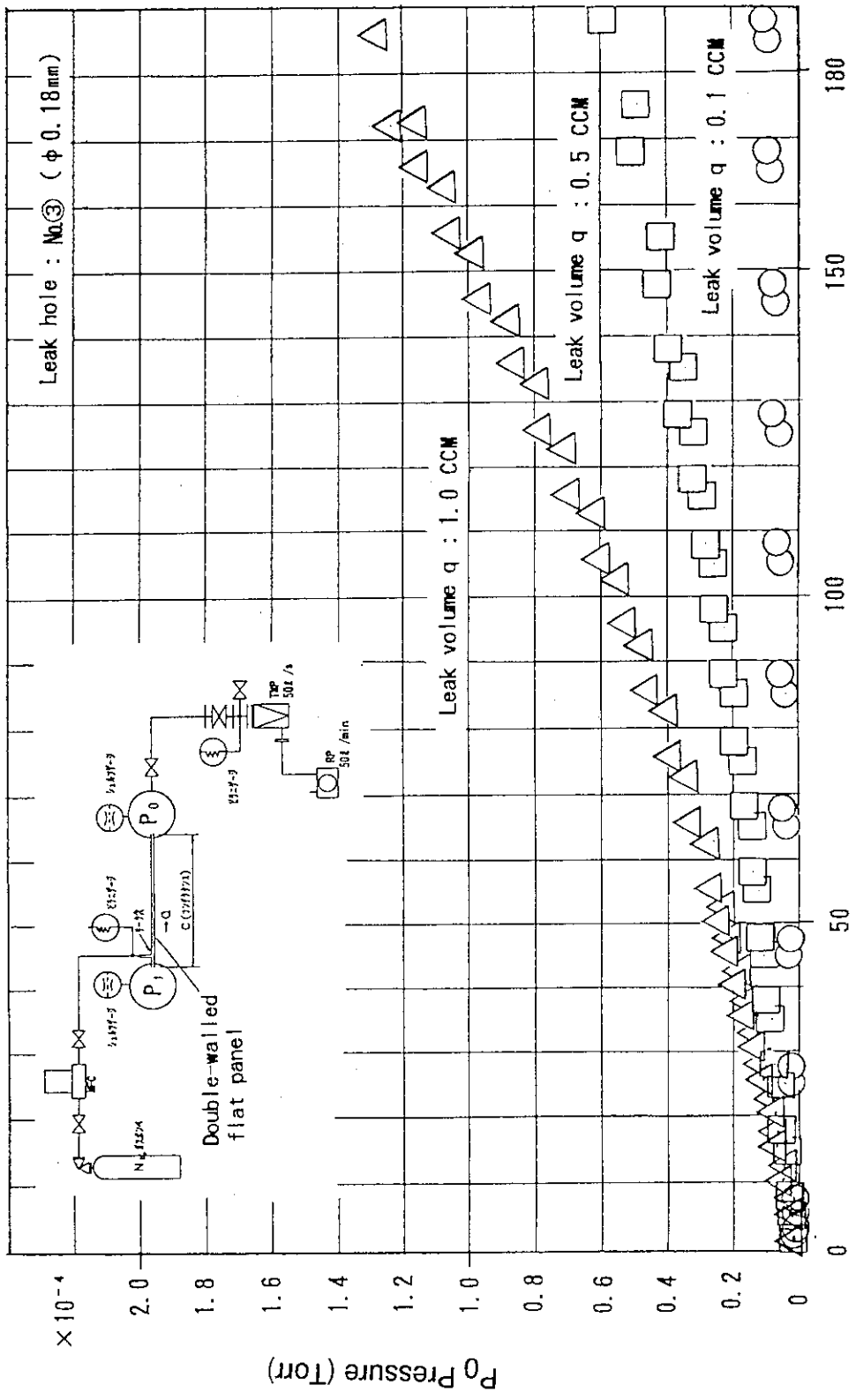

Fig. 3.1.9 Increment of pressure P_0 after leak (leak hole : φ 0.18 mm)

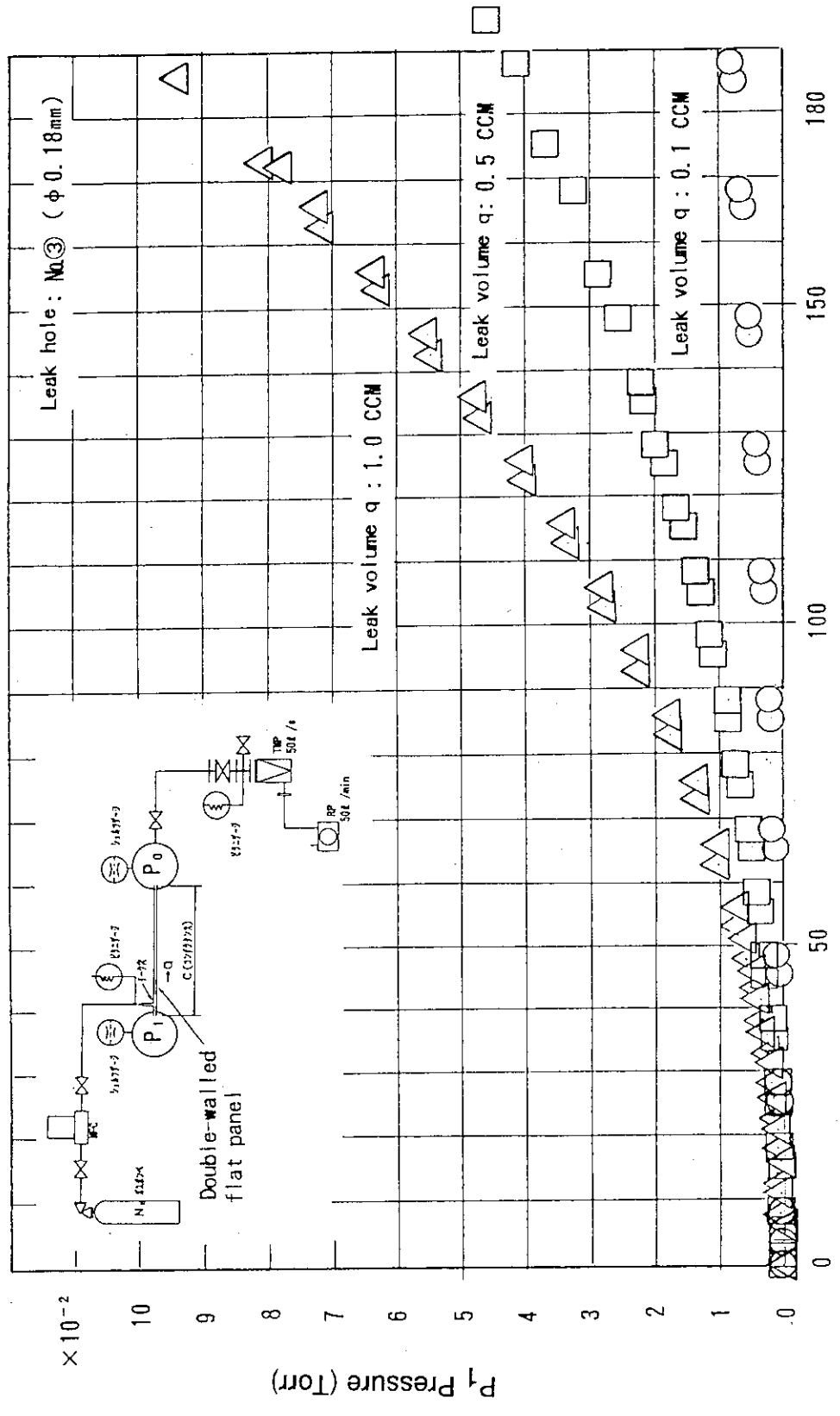

Fig. 3.1.10 Increment of pressure P_1 after leak (leak hole : φ 0.18 mm)

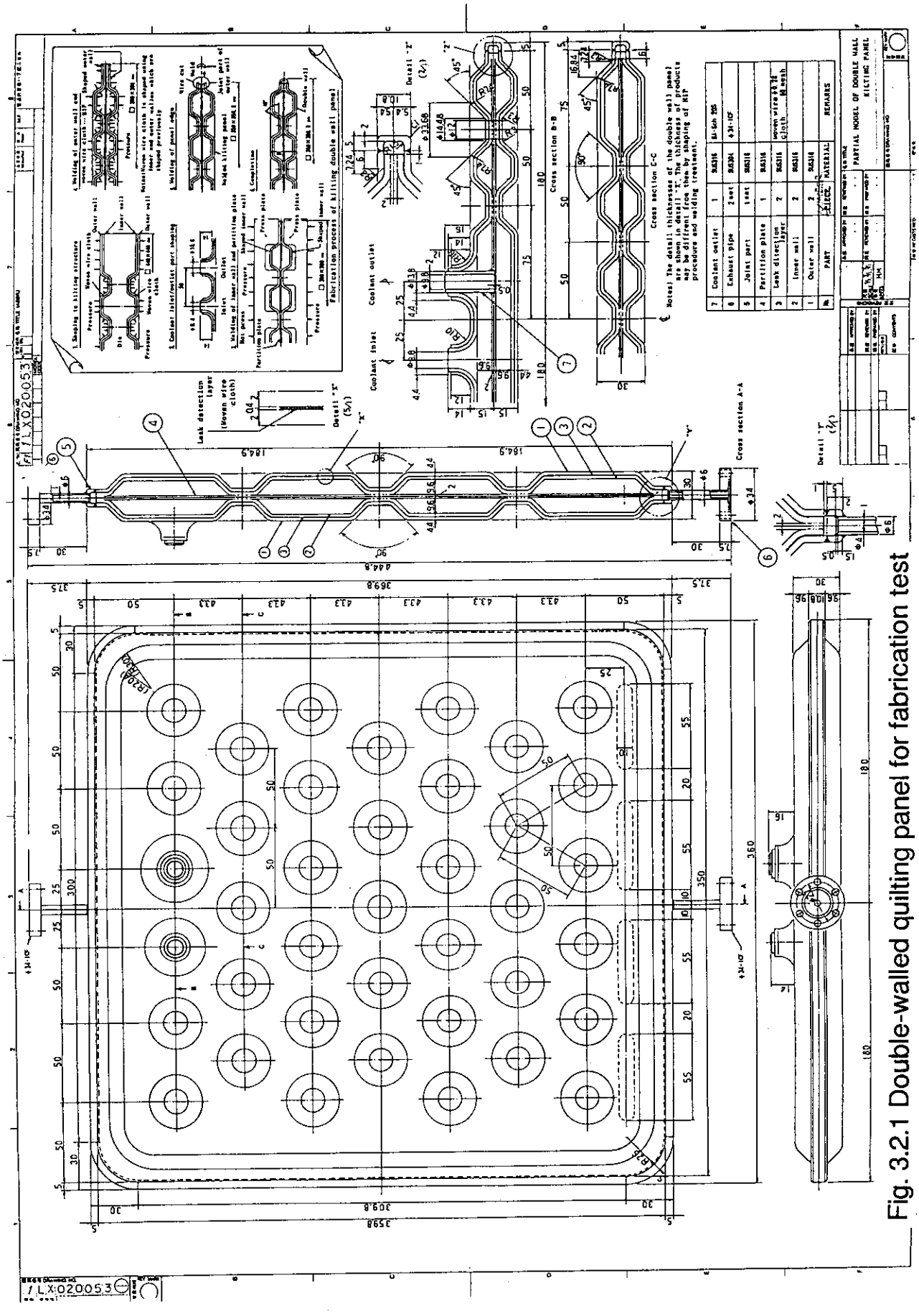

Fig. 3.2.1 Double-walled quilting panel for fabrication test

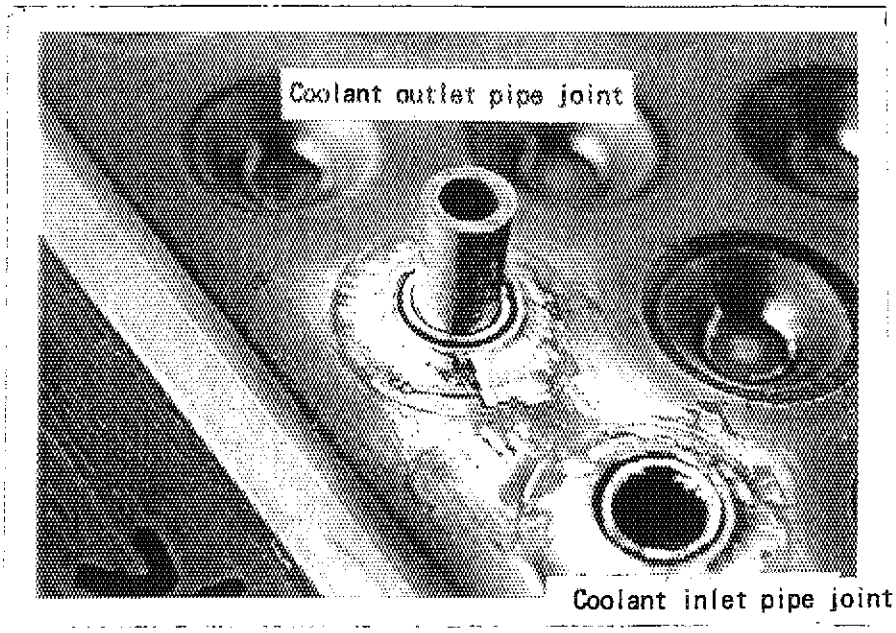

Fig. 3.2.2
Coolant inlet/outlet pipe (assembly)

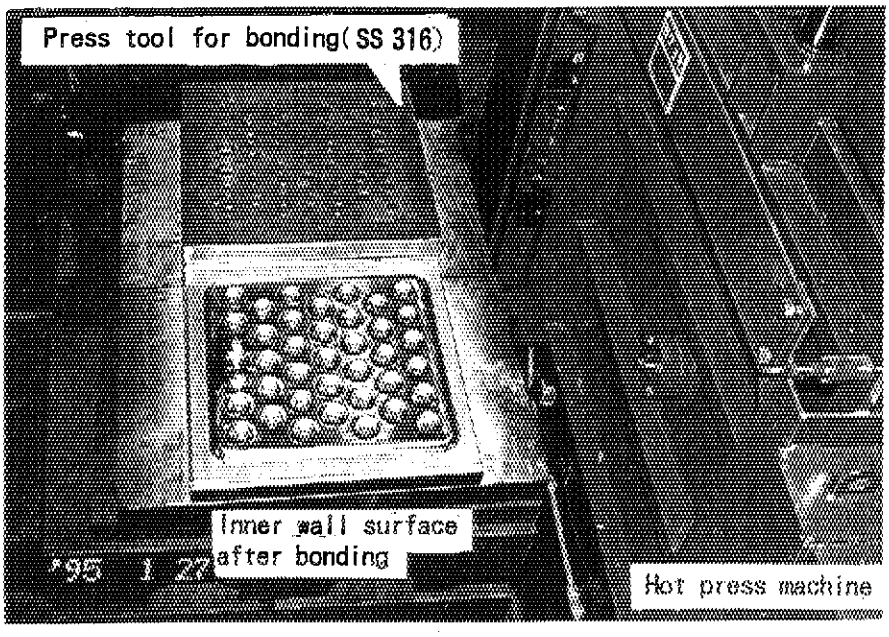

Fig. 3.2.3
Bonded inner wall and center wall

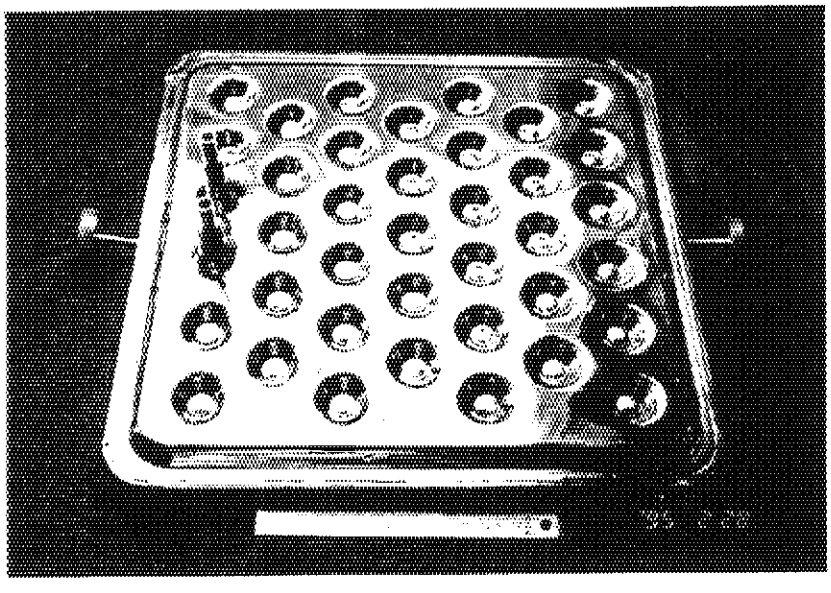

Fig. 3.2.4
Double walled quilting panel (for hydraulic test)

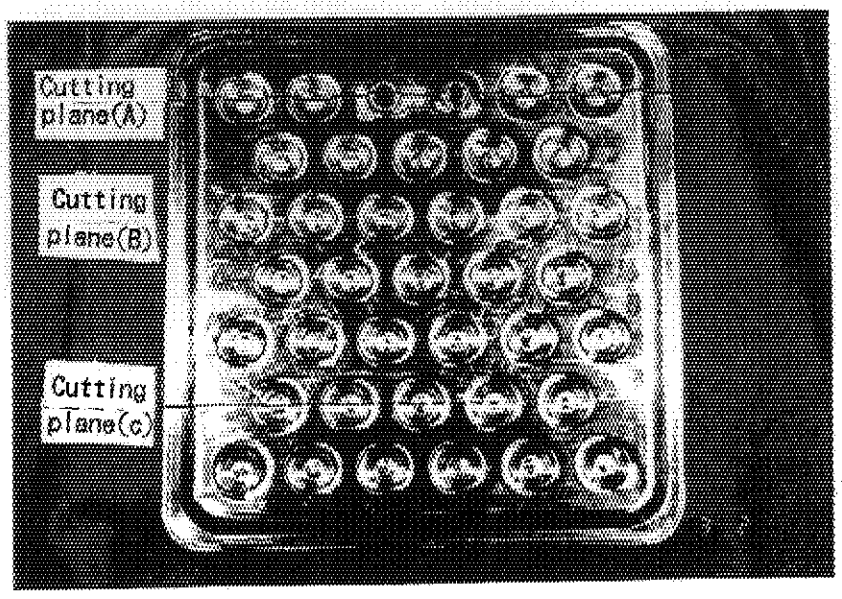

Fig. 3.2.5
Double walled quilting panel
(for cross section observation)

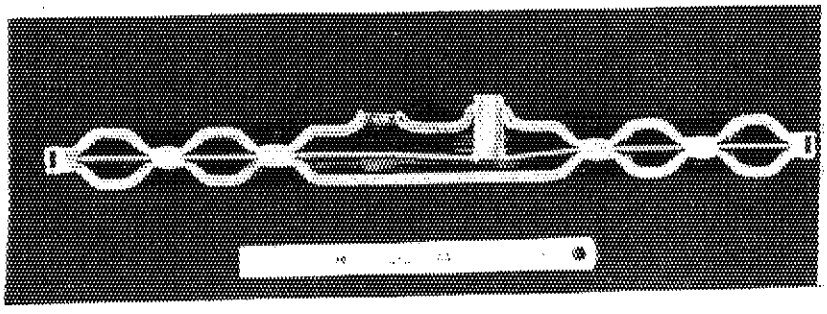

Fig. 3.2.6 Cross section (A)

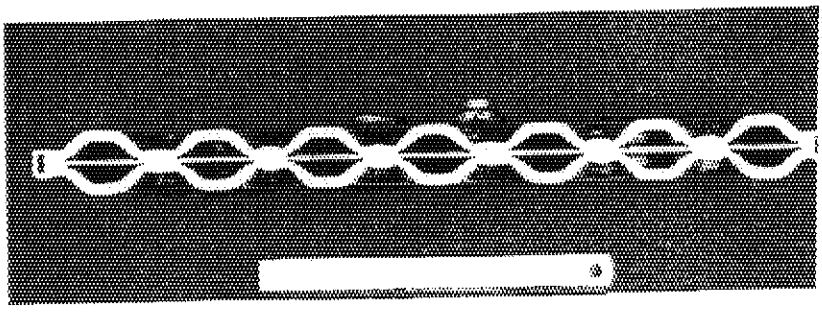

Fig. 3.2.7 Cross section (B)

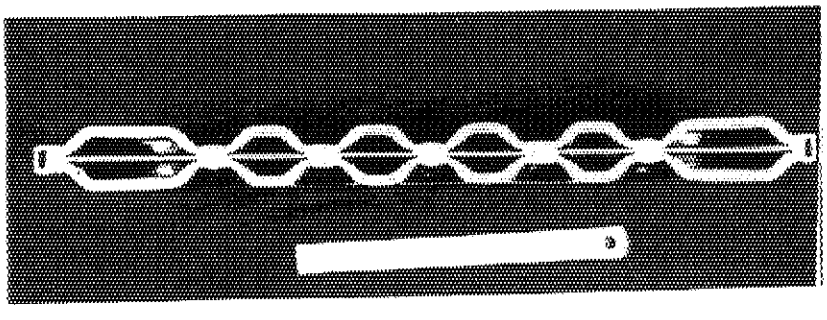

Fig. 3.2.8 Cross section (C)

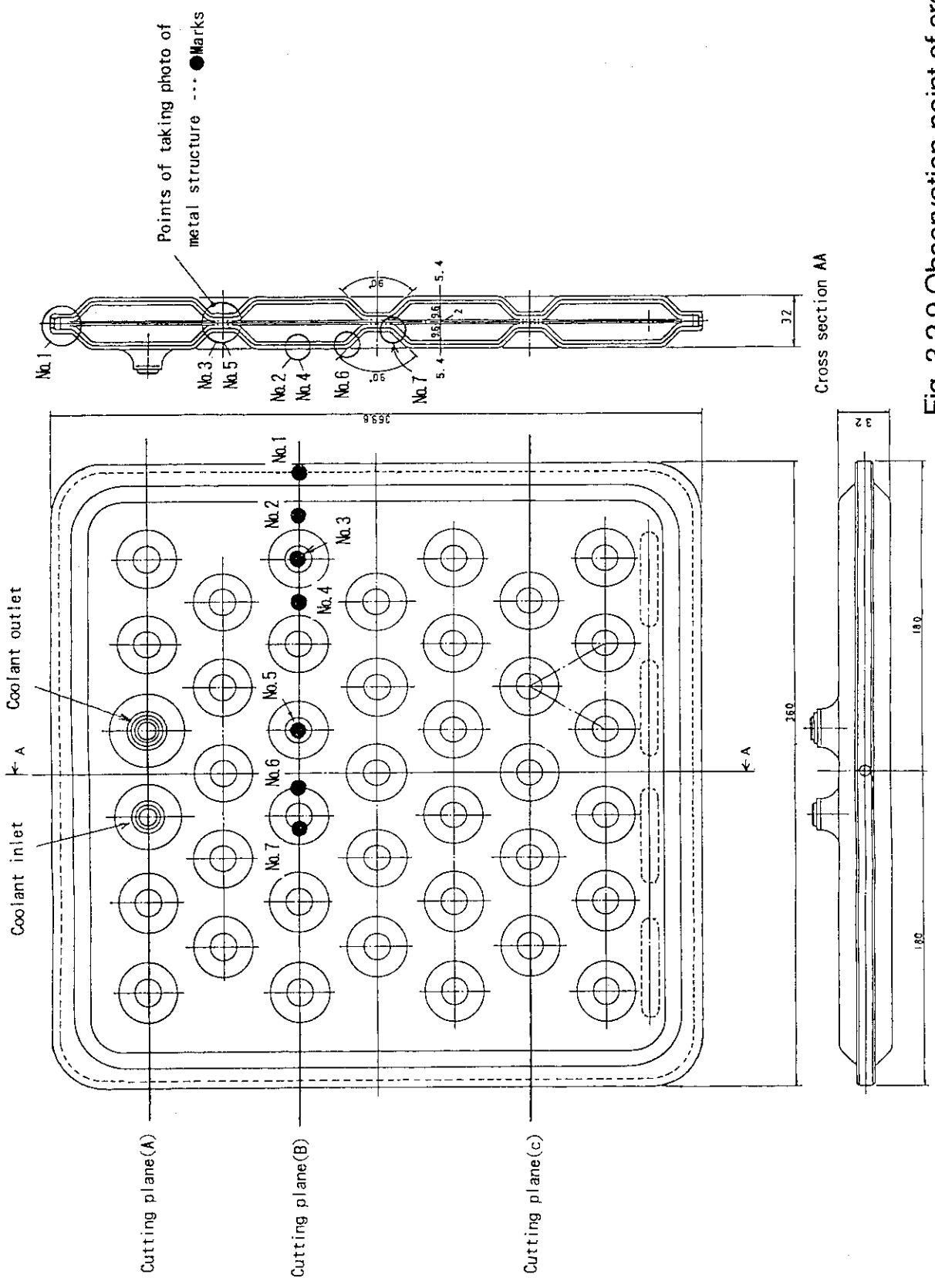

Fig. 3.2.9 Observation point of cross section

Fig. 3.2.10 View point No.1 ×10

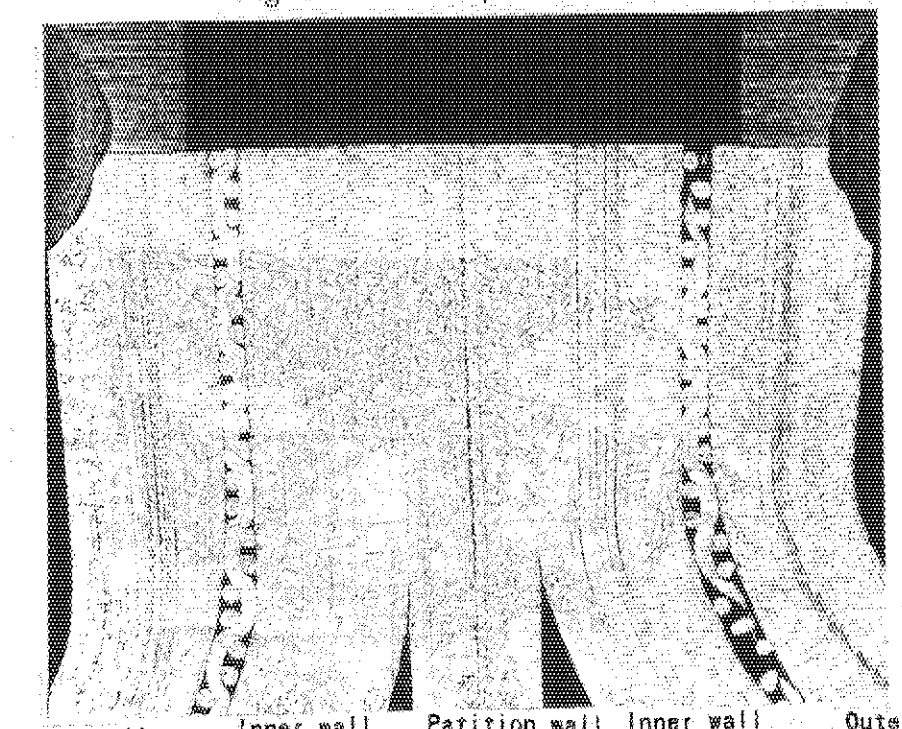

Fig. 3.2.11 View point No.2 ×10

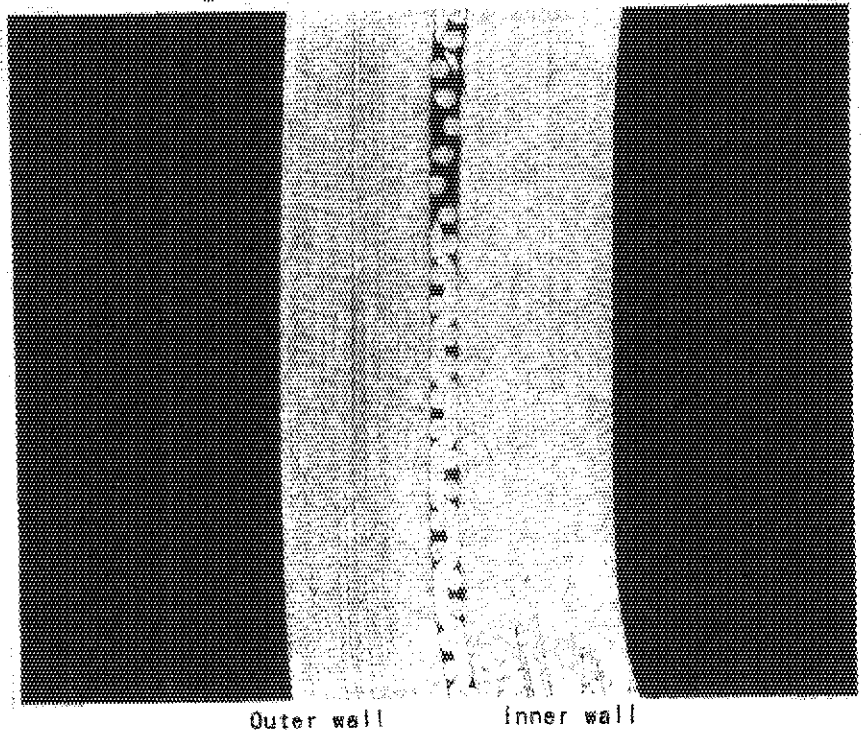

Fig. 3.2.12 View point No.3 ×10

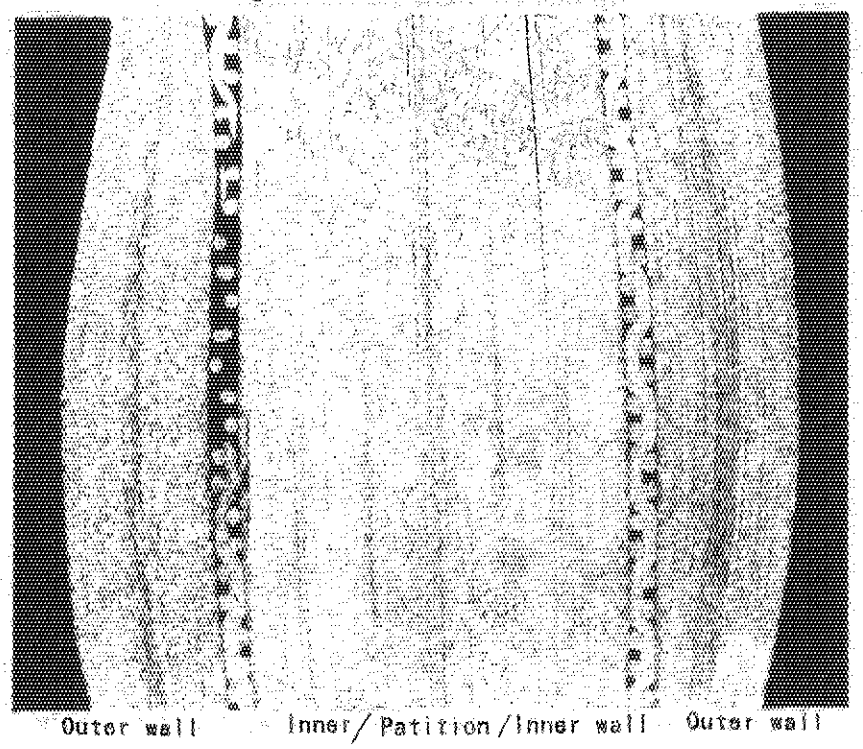

Fig. 3.2.13 View point No.4 ×10

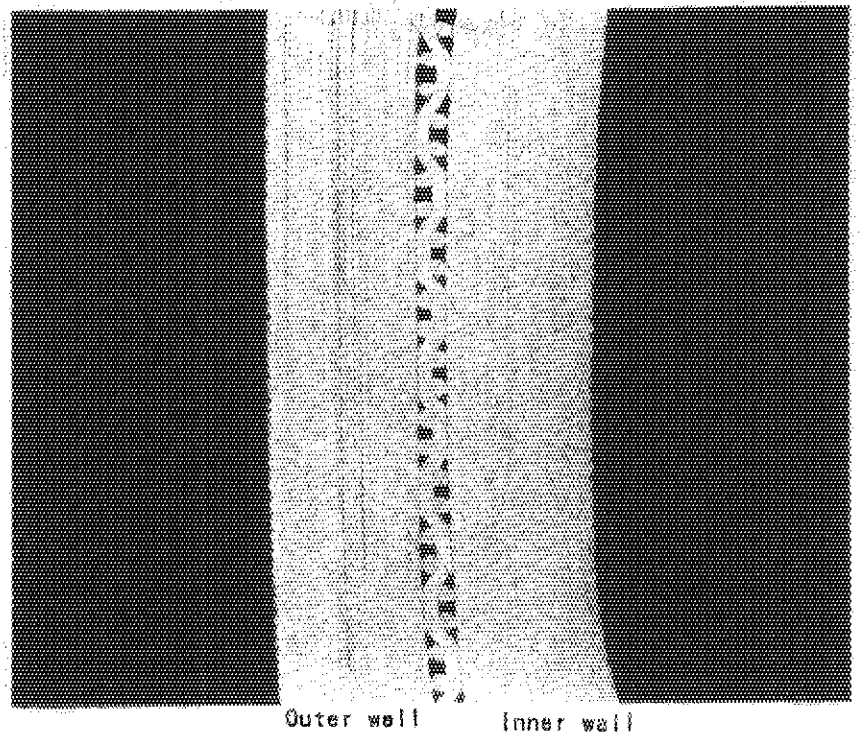

Fig. 3.2.14 View point No.5

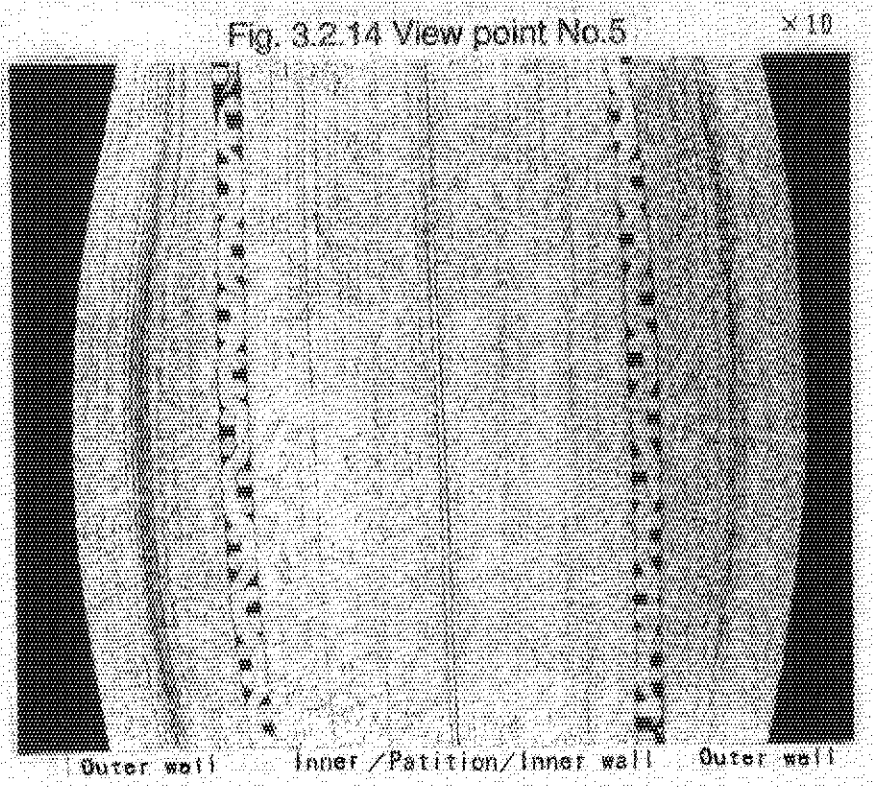

Fig. 3.2.15 View point No.6

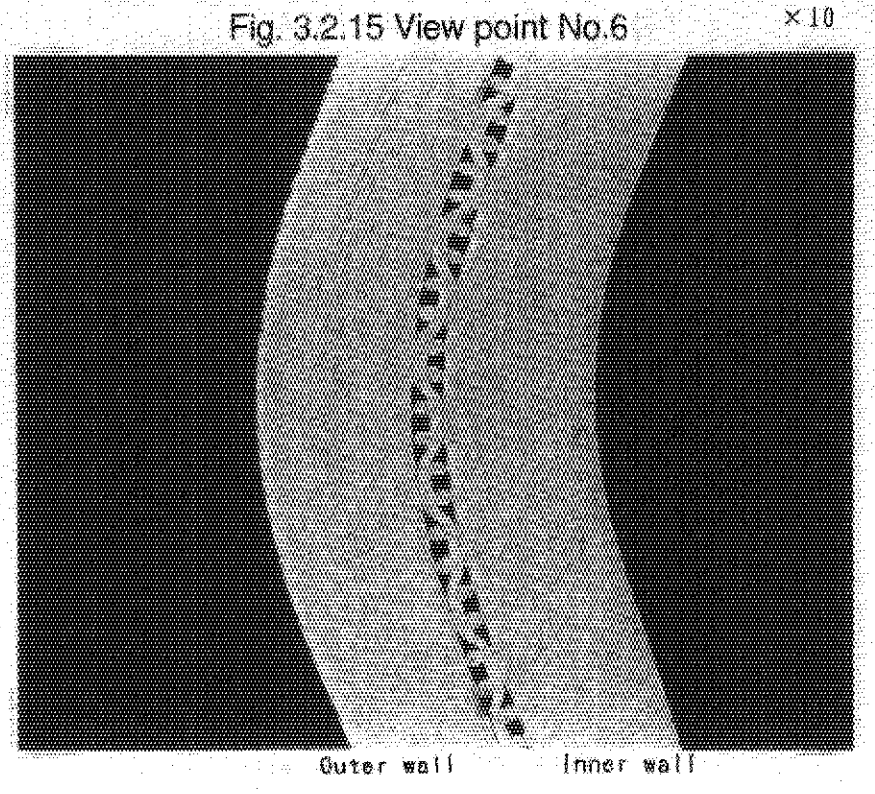

Fig. 3.2.16 View point No.7 ×10

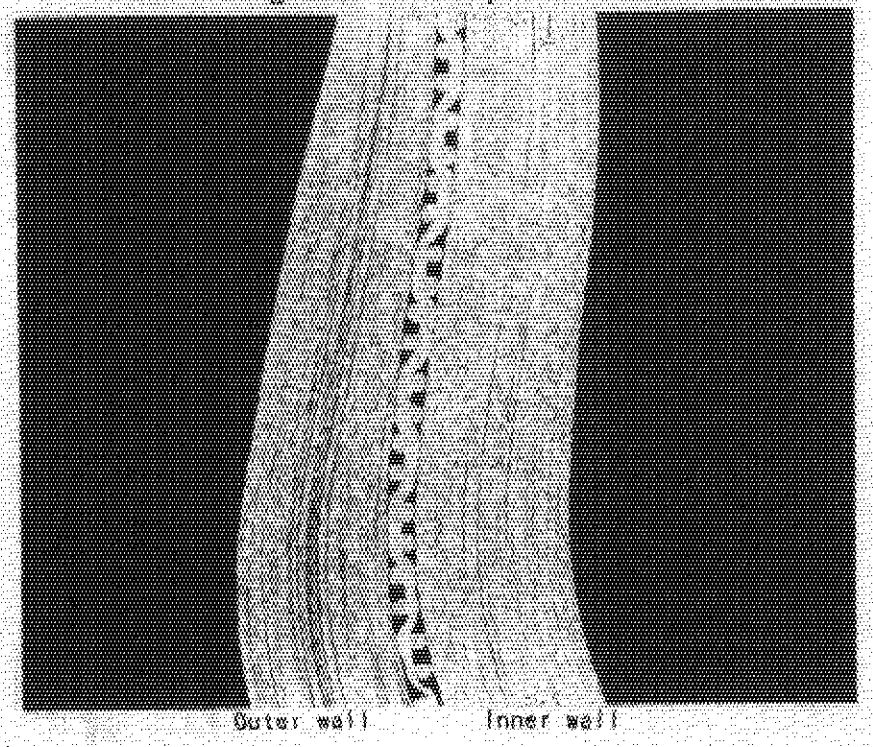

Scale

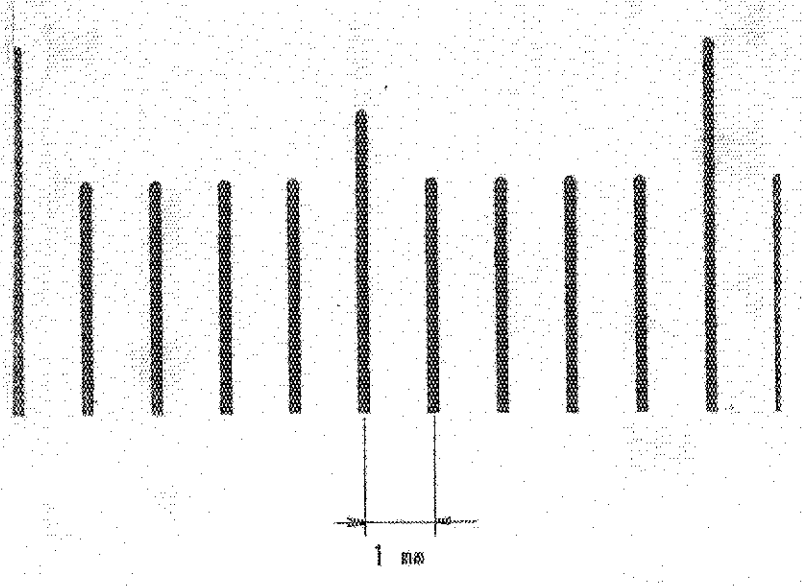

Fig. 3.2.17 Microstructure at view point No.1

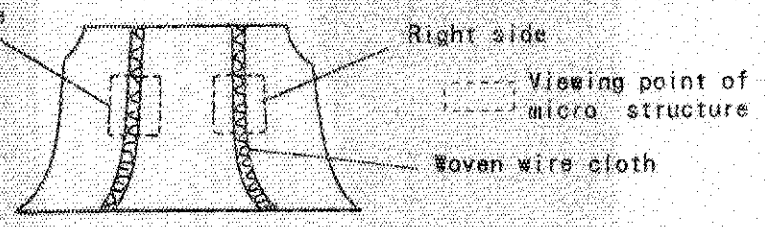

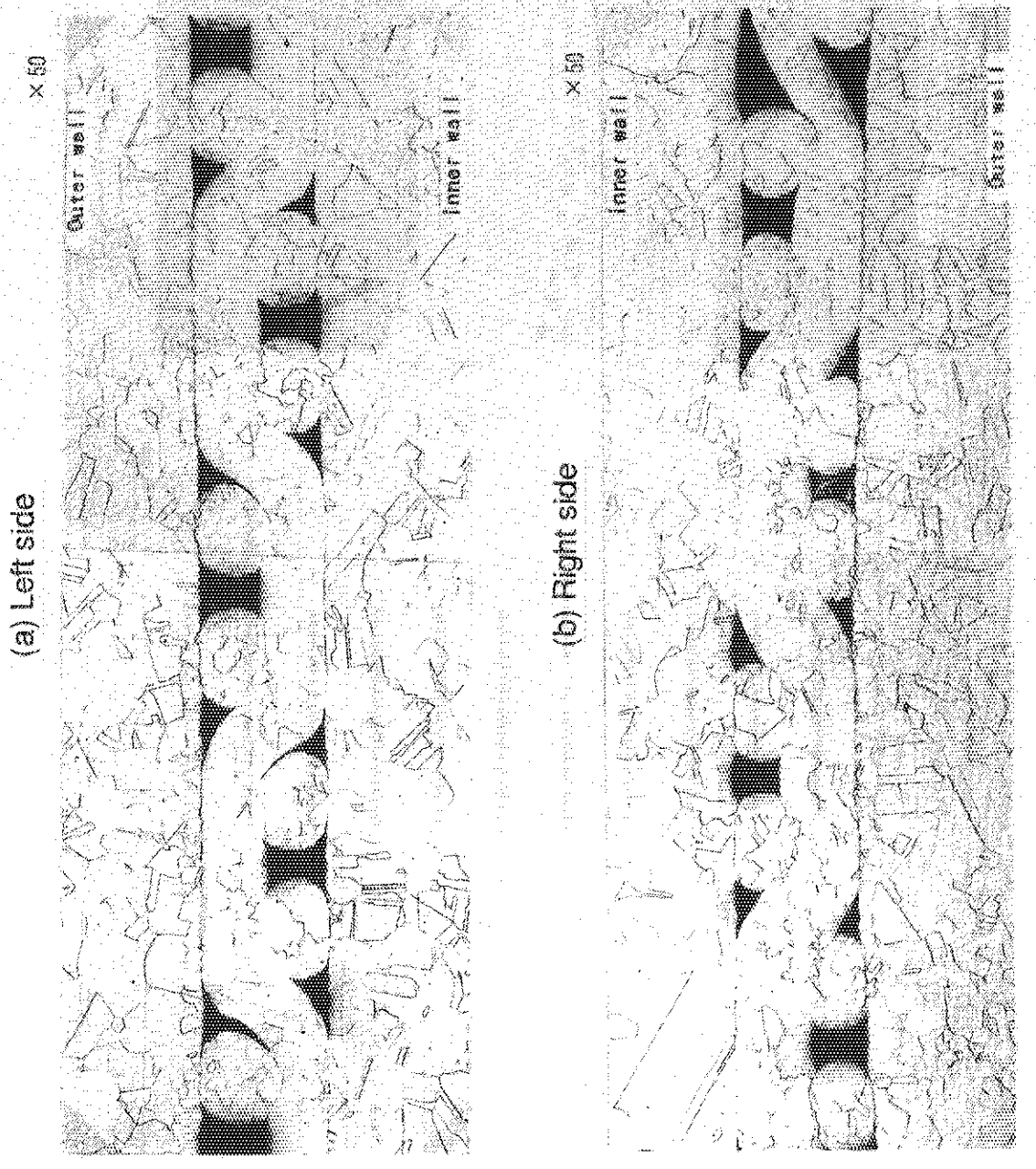

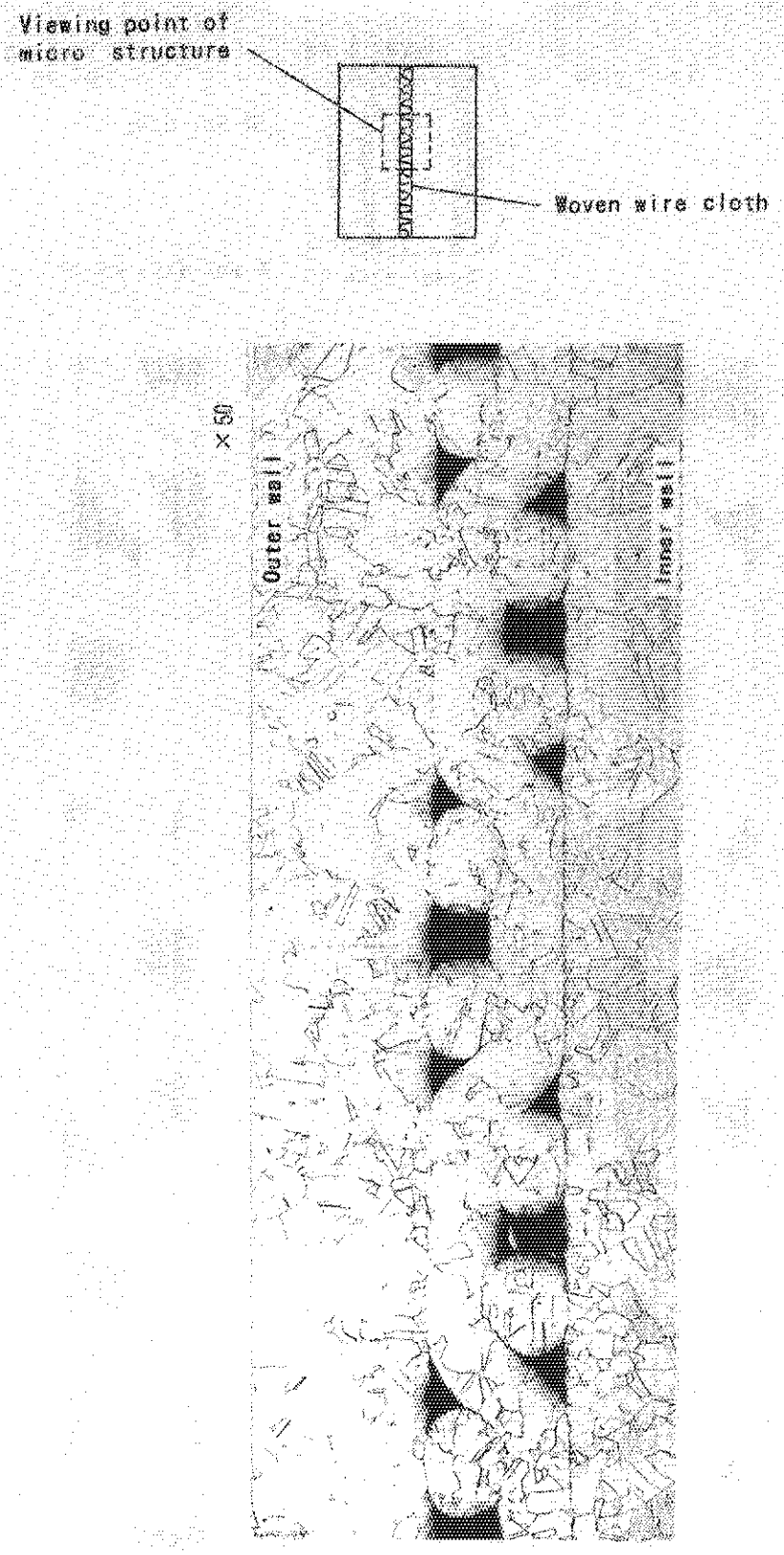

Fig. 3.2.18 Microstructure at view point No.2

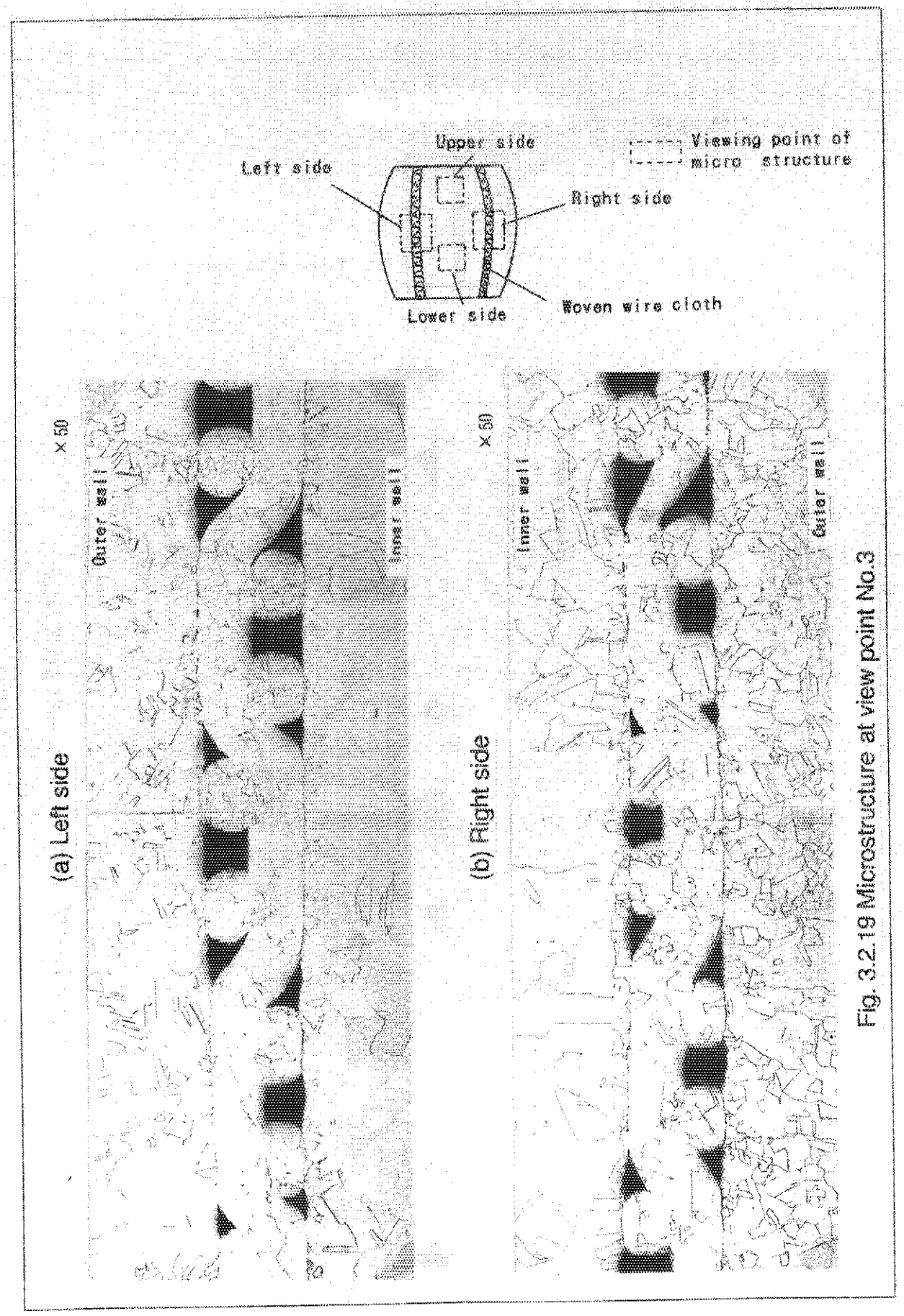

Fig. 3.2.19 Microstructure at view point No.3

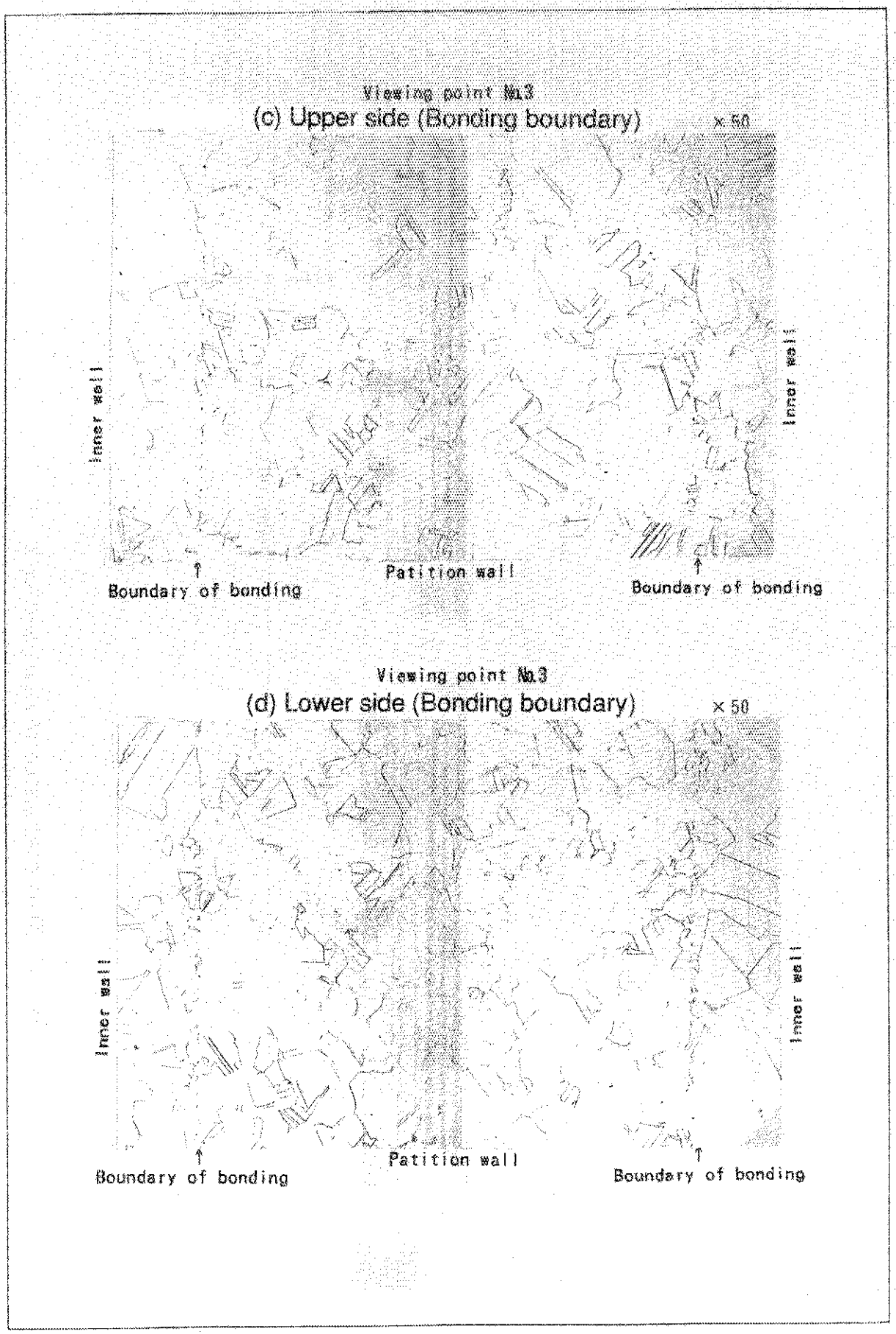
Viewing point №3
(c) Upper side (Bonding boundary)
×50
Inner wall
Inner wall
Boundary of bonding
Patition wall
Boundary of bonding
Viewing point №3
(d) Lower side (Bonding boundary)
×50
Inner wall
Inner wall
Boundary of bonding
Patition wall
Boundary of bonding

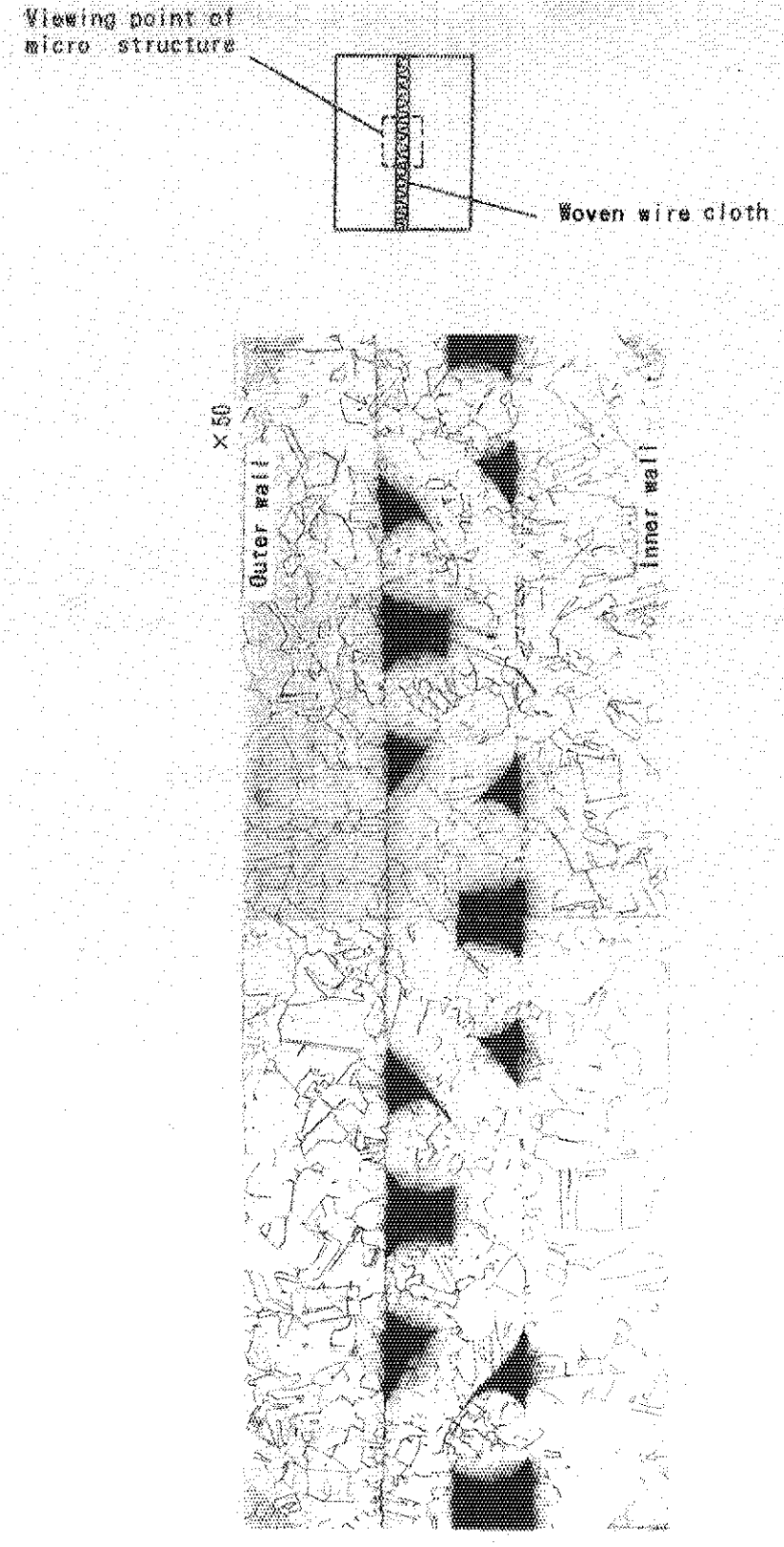

Fig. 3.2.20 Microstructure at view point No.4

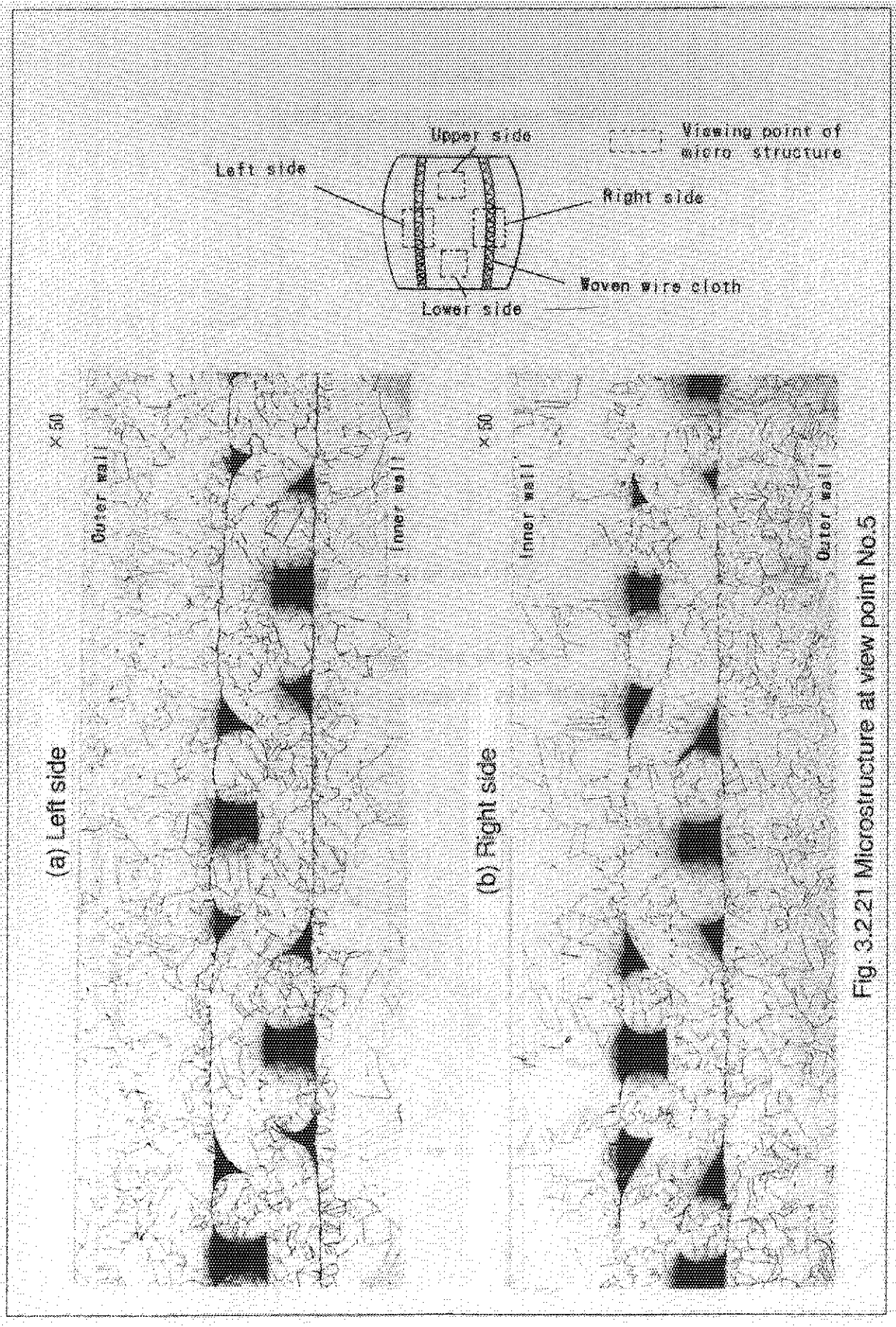

Fig. 3.2.21 Microstructure at view point No.5

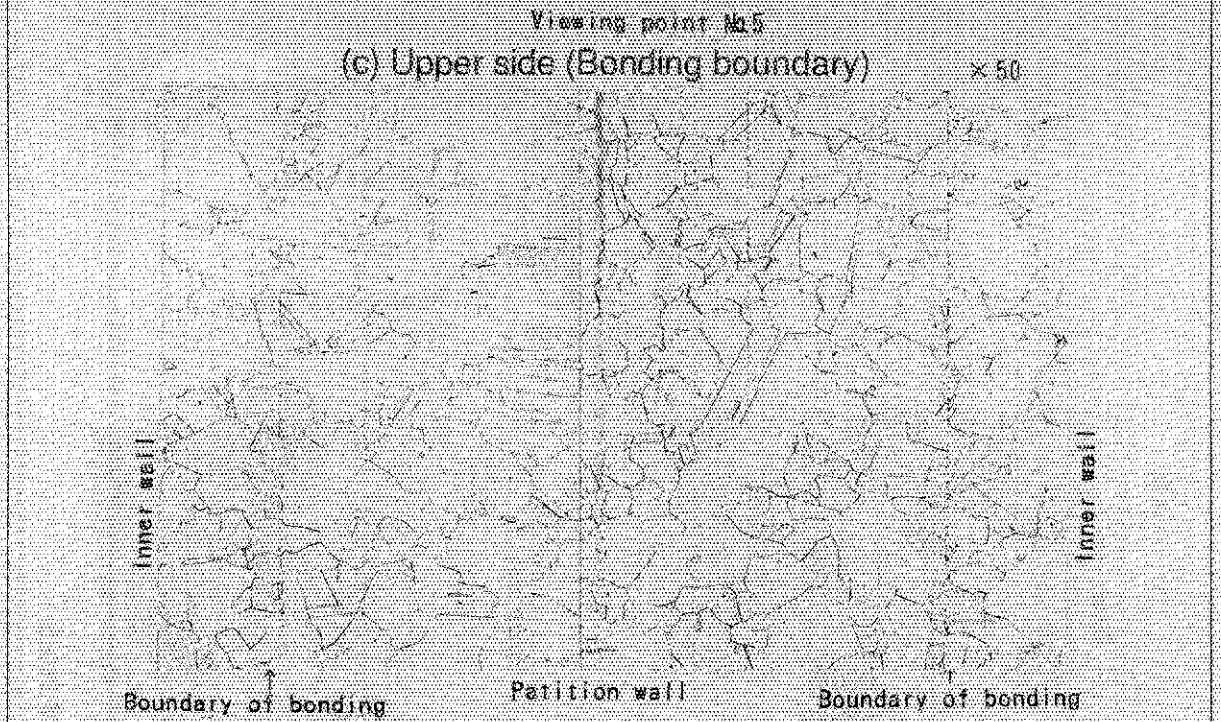
Viewing point №5
(c) Upper side (Bonding boundary)
×50
Inner wall
Inner wall
Boundary of bonding
Patition wall
Boundary of bonding

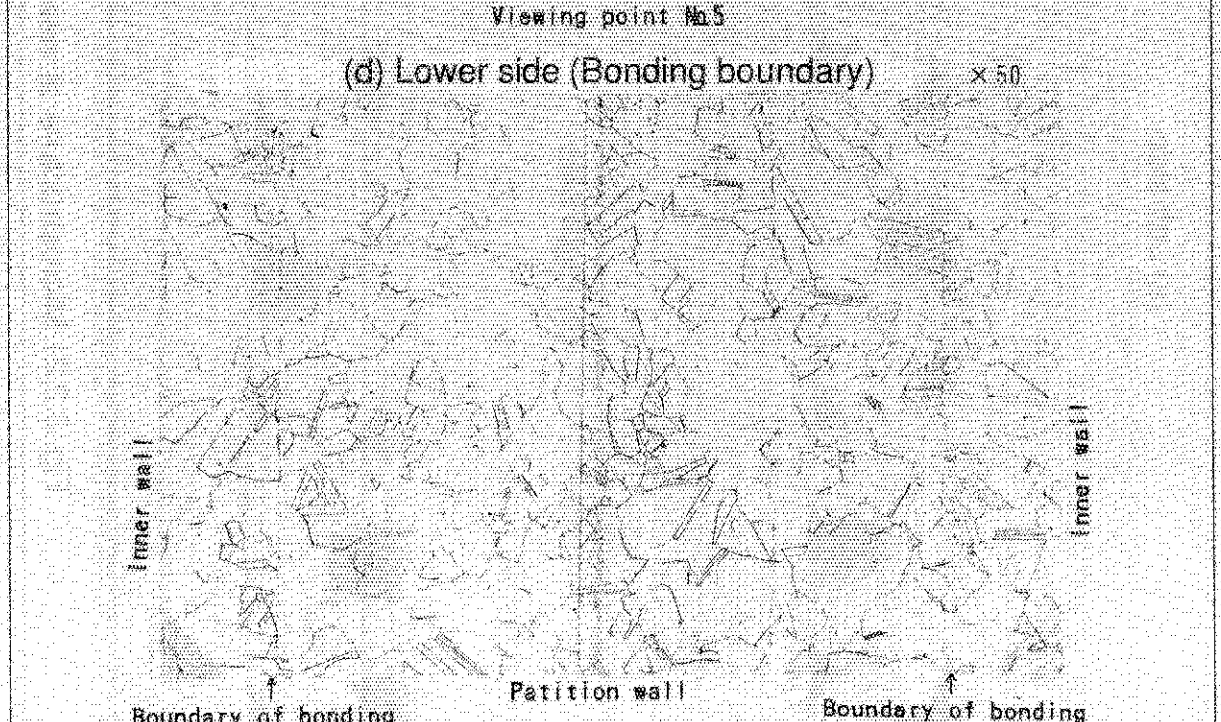
Viewing point №5
(d) Lower side (Bonding boundary)
×50
Inner wall
Inner wall
Boundary of bonding
Patition wall
Boundary of bonding

Fig. 3.2.22 Microstructure at view point No.6

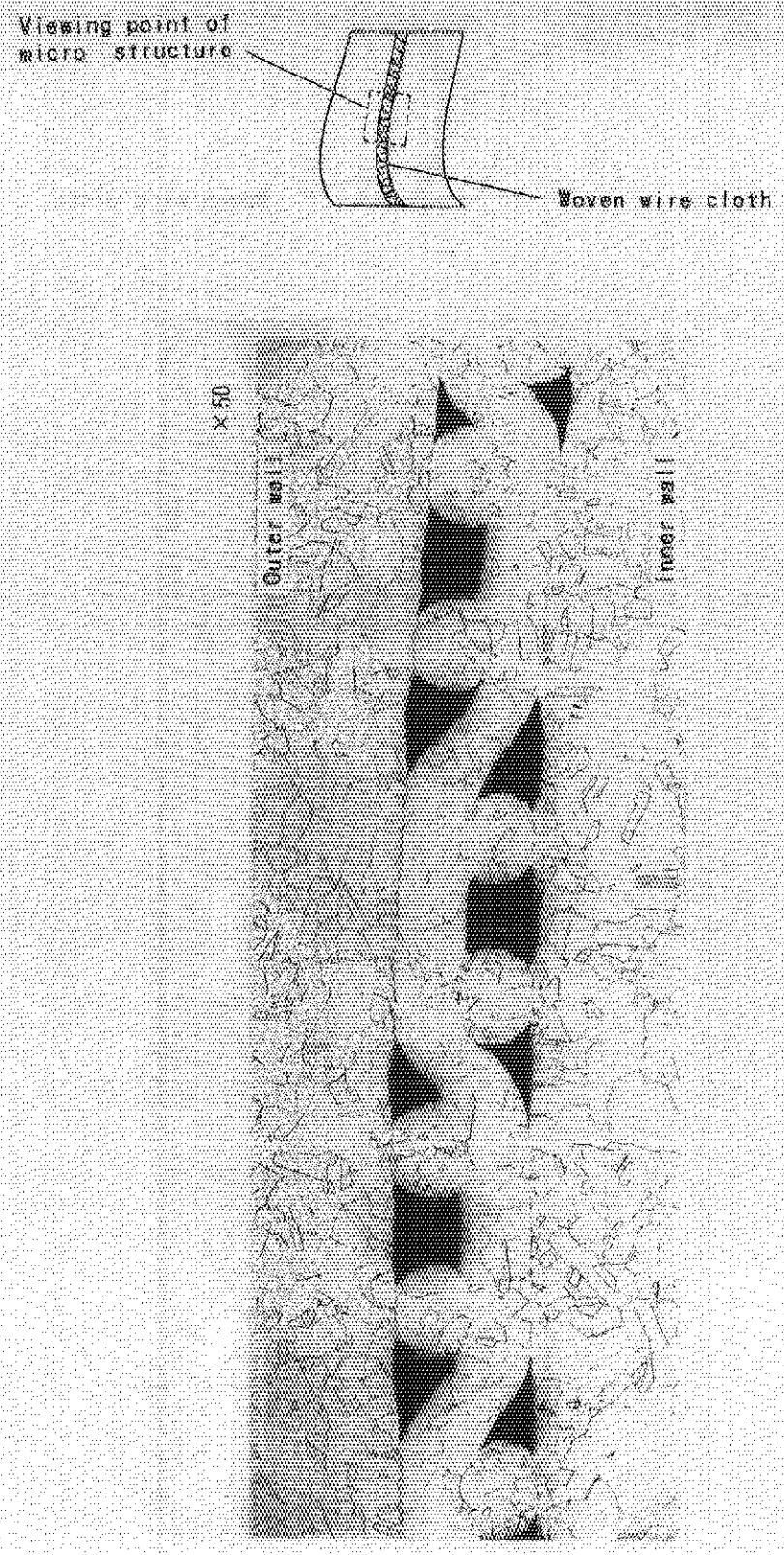

Fig. 3.2.23 Microstructure at view point No.7

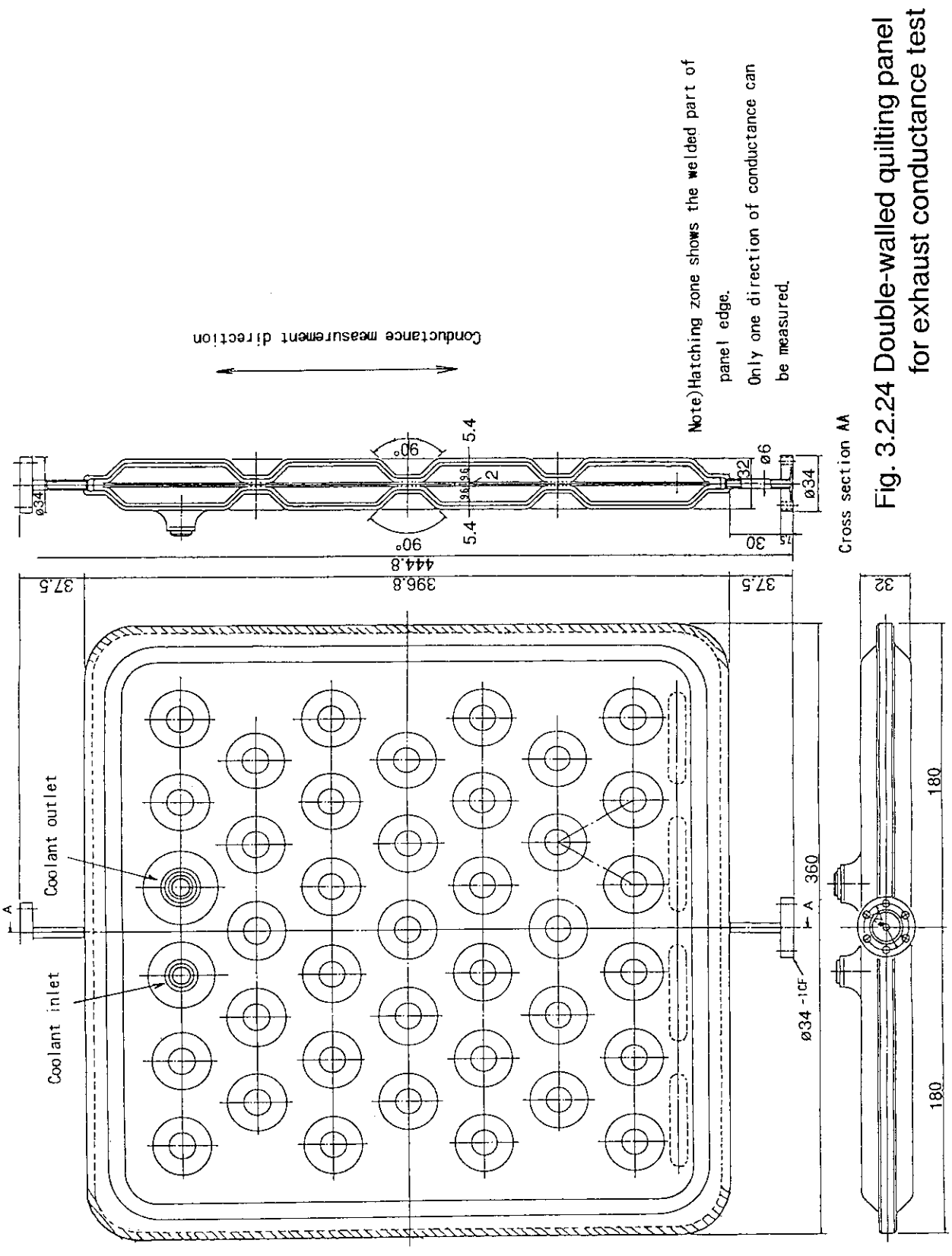

Fig. 3.2.24 Double-walled quilting panel for exhaust conductance test

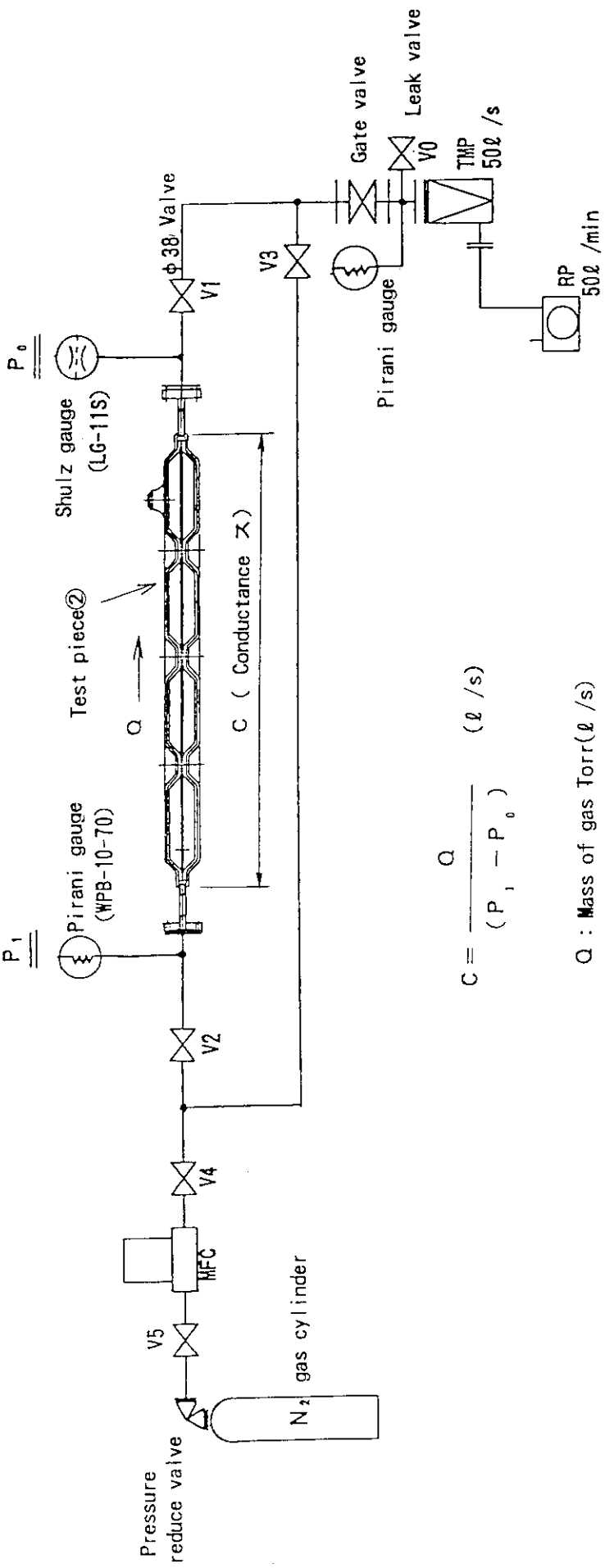

$$C = \frac{Q}{(P_1 - P_0)} \quad (\ell/s)$$

Q : Mass of gas Torr(ℓ /s)

P_0 、 P_1 : Pressure of both side(Torr)

Fig. 3.2.25 Test equipment for exhaust conductance of double-walled quilting panel

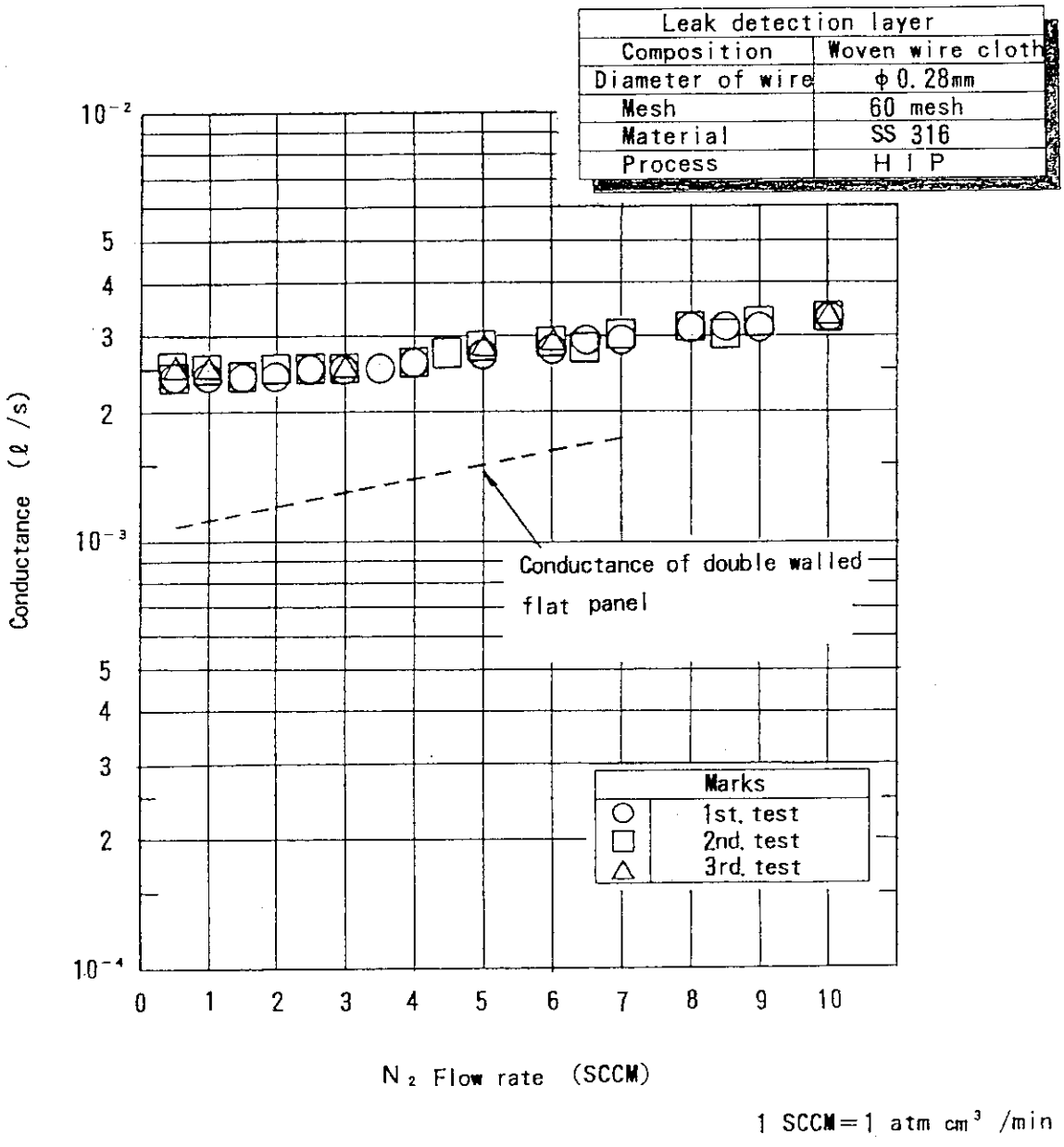

Fig. 3.2.26 Results of exhaust conductance test

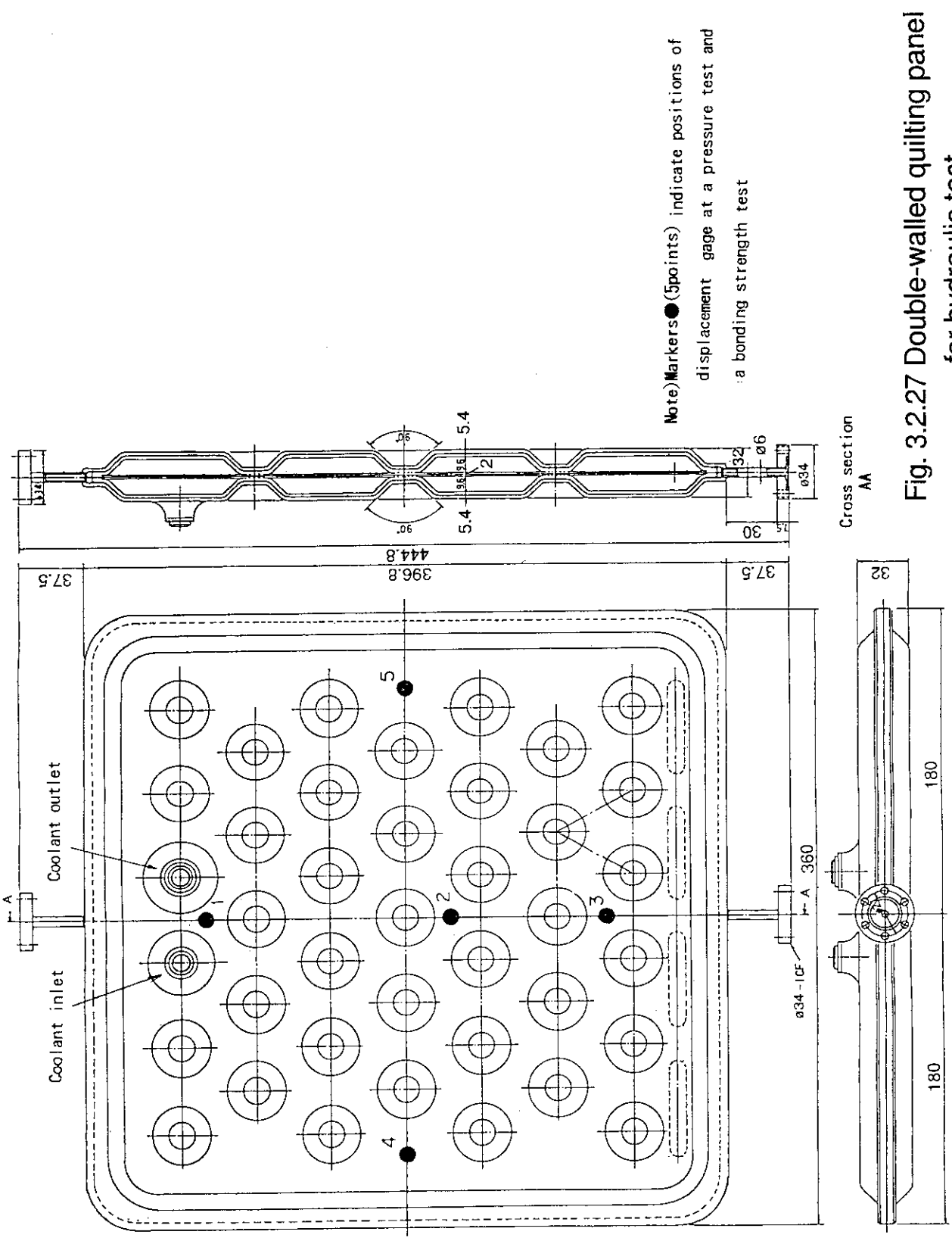

Fig. 3.2.27 Double-walled quilting panel for hydraulic test

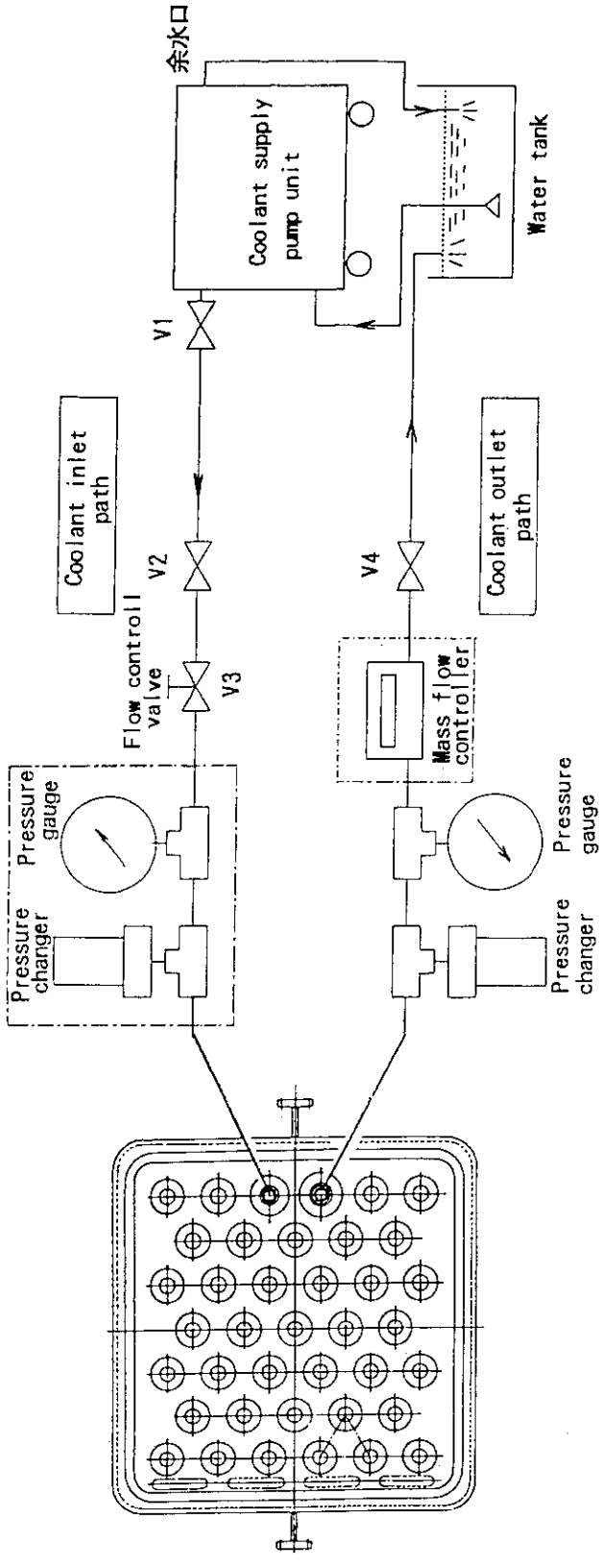

Note)This figure shows the system at pressure loss test. For a pressure test or a bonding strength test, the parts(surrounded by [ ]) are taken off (V4 close)

Fig. 3.2.28 Test equipment for hydraulic test of double-walled quilting panel

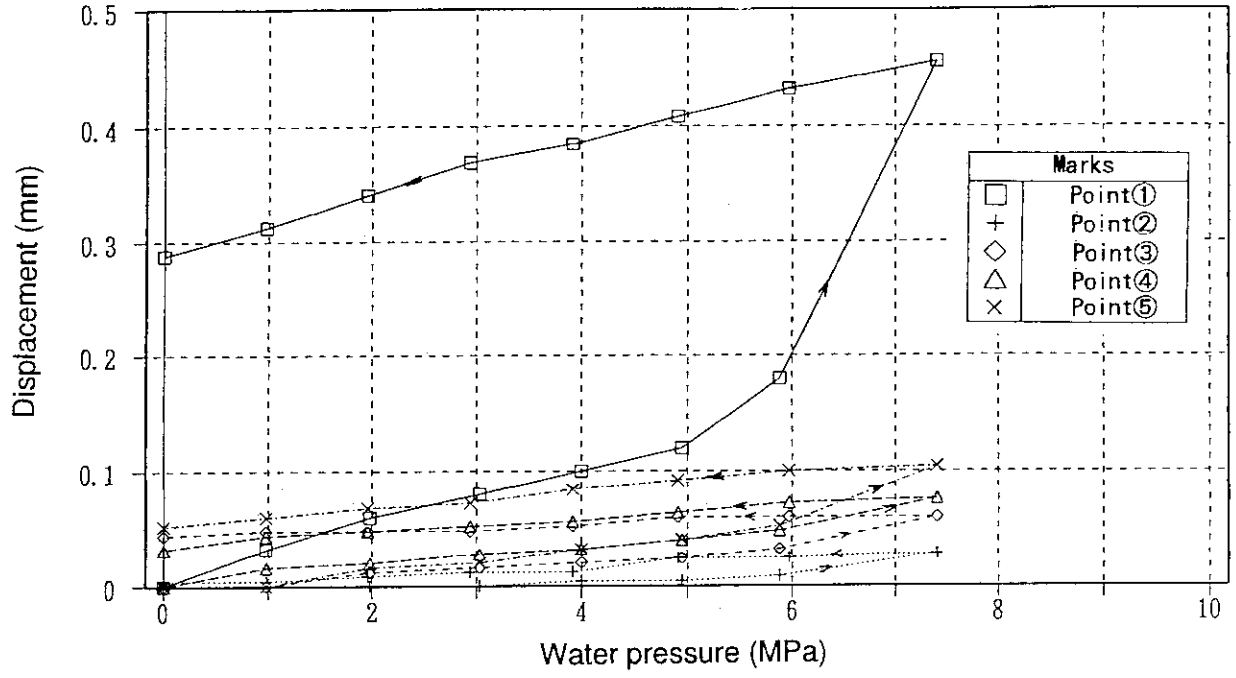

Fig. 3.2.29 Displacement at pressure proof test (1st)

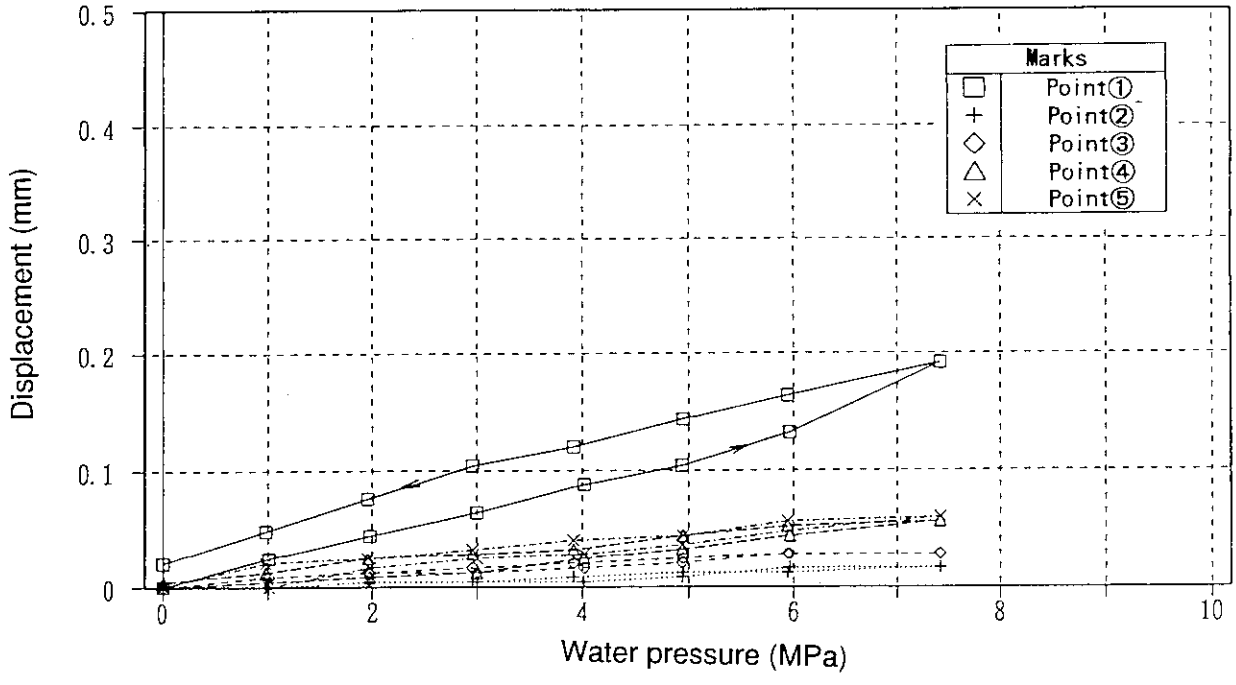

Fig. 3.2.30 Displacement at pressure proof test (2nd)

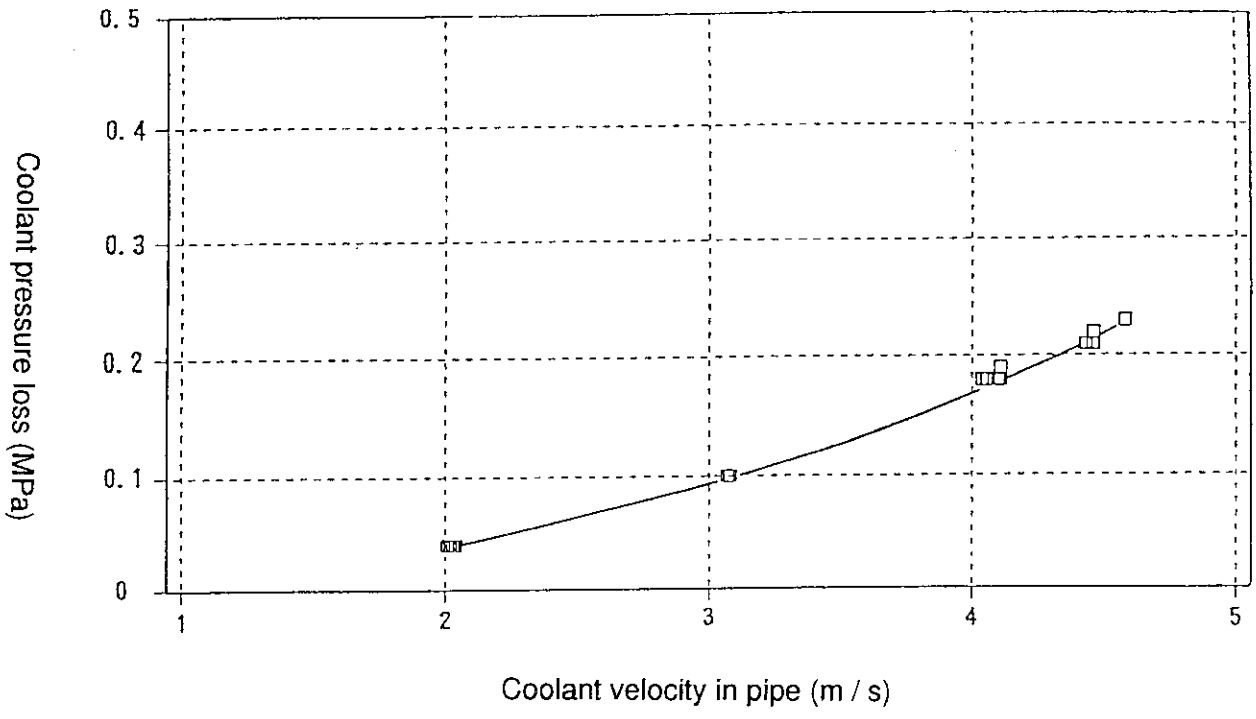

Fig. 3.2.31 Coolant pressure loss of double-walled quilting panel

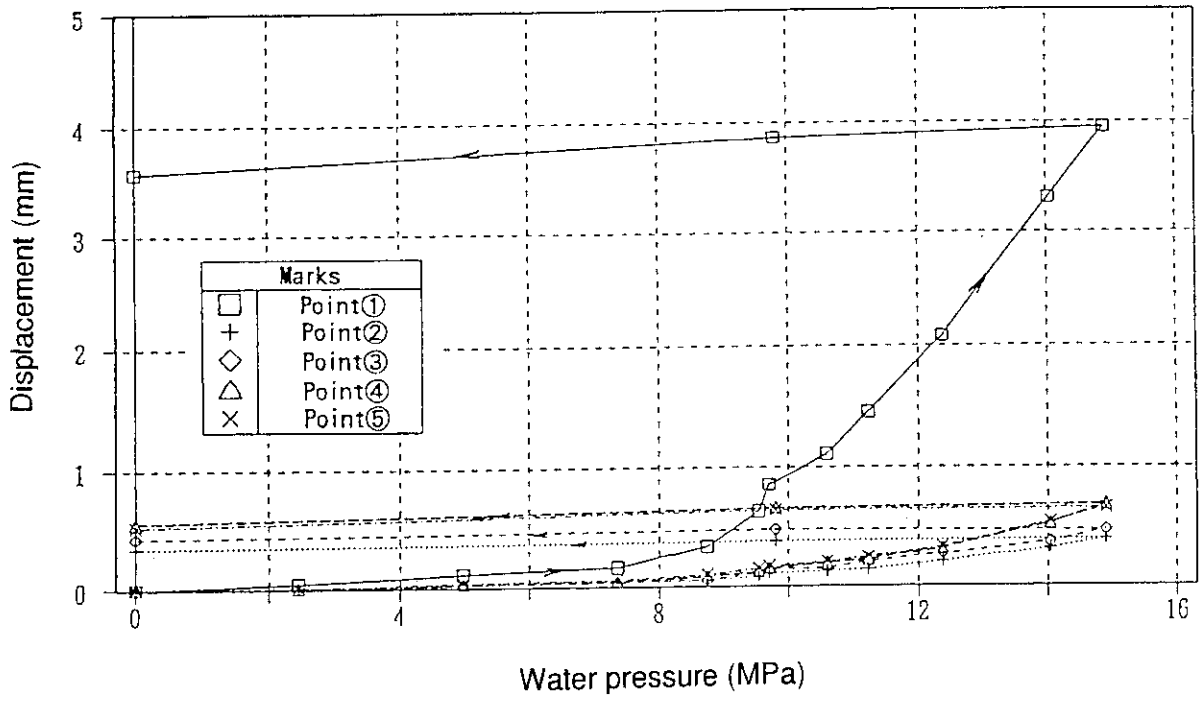

Fig. 3.2.32 Displacement at destruction test

Fig. 3.2.33
Destruction test

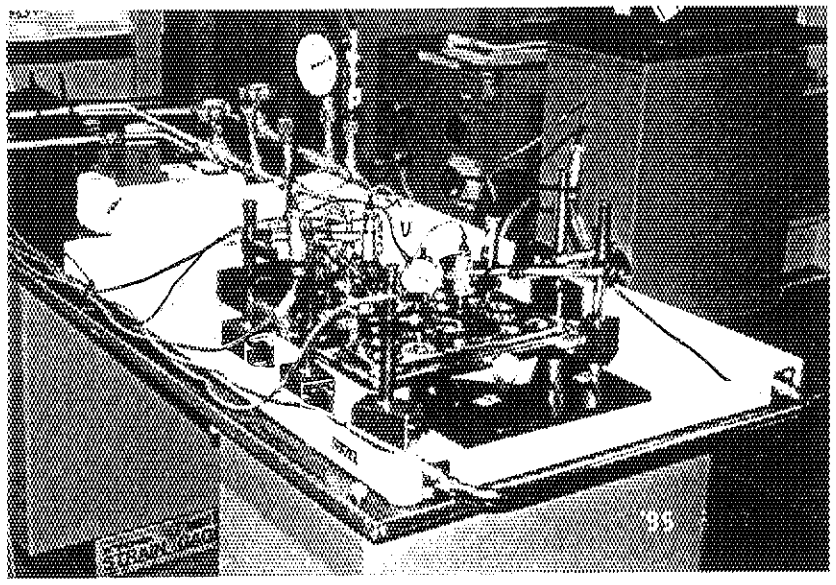

Fig. 3.2.34
Test piece
after destruction test (front)

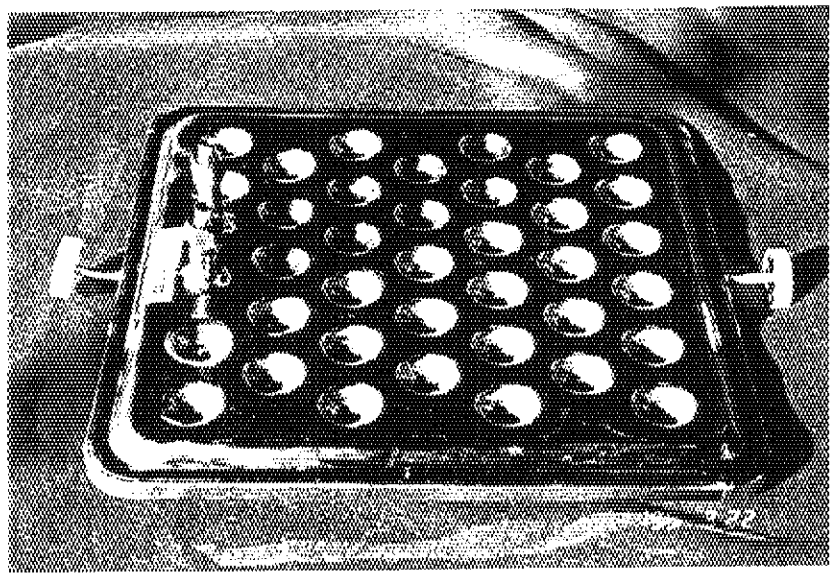

Fig. 3.2.35
Test piece
after destruction test (back)

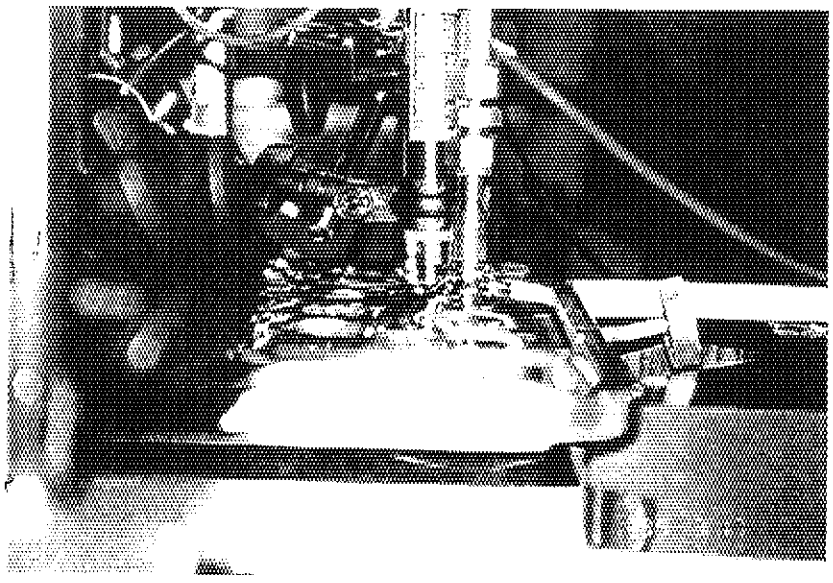

Fig. 3.2.36
Coolant inlet/outlet region
after destruction test (front)

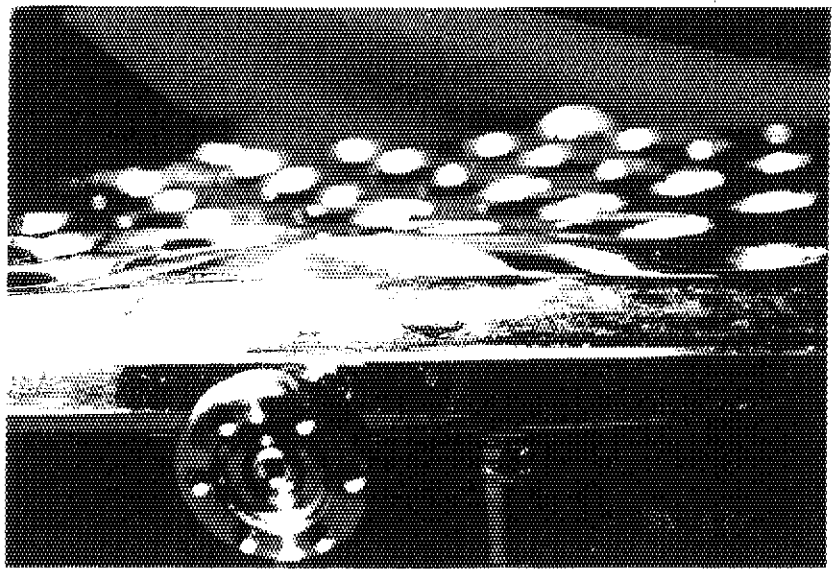

Fig. 3.2.37
Coolant inlet/outlet region
after destruction test (back)

Appendix A.

Pressure loss

The system is modeled as follows.

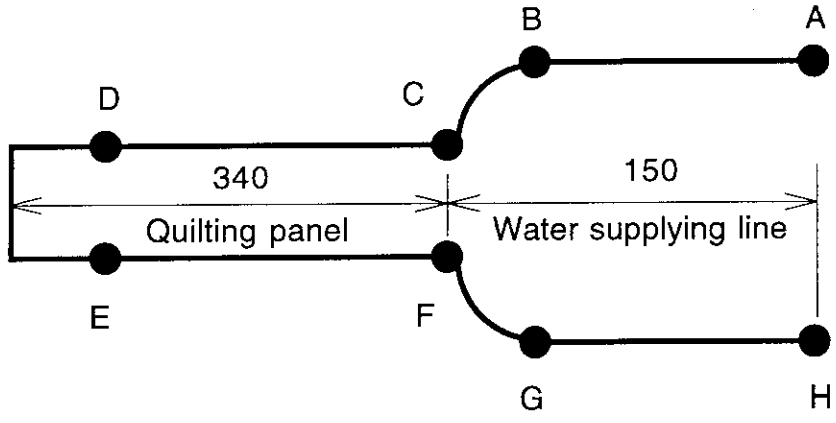

$$\Delta P = \sum \zeta_i \bullet \gamma \frac{v^2}{2g} + \Delta P_f$$

ζ : Loss coefficient

γ : Density (996.6 kg/m^3 : 300K)

v : Water velocity [m/sec]

λ : Friction factor (0.03)

ν : Kinematic viscosity (0.857×10^{-6} m^2/s)

1) Water supplying line : Straight pipe (A-B, G-H)

$$\zeta_1 = \frac{\lambda l}{d} = 0.56$$

Length l = 0.15 m

Diameter d = 0.008 m

2) Water supplying line : Bent pipe 90 deg. (B-C, F-G)

v [m/s]	Re	ζ_2
2	1.87 x 10^4	0.28
3	2.80 x 10^4	0.27
4	3.73 x 10^4	0.25

where

$$\zeta_2 = 0.0024 \bullet \alpha \bullet \theta \bullet Re^{-0.17} \left(\frac{R}{a}\right)^{0.84}$$

$$\alpha = 0.95 + 17.2\left(\frac{R}{a}\right)^{-1.96} = 1.28 \text{ (at } \theta = 90)$$

$$a = \frac{d}{2}, \quad R = 0.03 \text{ m (radius of curvature)}$$

3) Water inlet : Enlargement (C)

$$\zeta_3 = (1-\frac{A_1}{A_2})^2 = 0.93$$

Inlet area $A_1 = 5.03 \times 10^{-5}$ m^2

Inlet area $A_2 = 1.40 \times 10^{-3}$ m^2

4) Water outlet : Contraction (F)

$$\zeta_4 = 0.42$$

Inlet area $A_1 = 1.40 \times 10^{-3}$ m^2

Inlet area $A_2 = 5.03 \times 10^{-5}$ m^2

$$\frac{A_1}{A_2} = 0.036$$

5) Quilting panel : Straight pipe (C-D, E-F)

$$\zeta_5 = \frac{\lambda l}{d} = 0.67$$

Flow area	$A = 1.40 \times 10^{-3}$ m^2
Equivalent diameter	$d = 1.53 \times 10^{-2}$ m
Length	$l = 0.34$ m

6) Quilting panel : Tube banks (C-D, E-F)

v [m/s]	C_D	ΔP_f [MPa]
2	5.51×10^{-2}	0.0026
3	5.17×10^{-2}	0.0056
4	4.94×10^{-2}	0.0095

where

$$C_D = \frac{1}{4} \bullet \frac{\Delta P_f}{\gamma v^2/2} \bullet \frac{1}{N_T - 1}$$

$$= Re^{-0.16}\left[0.25 + \frac{0.1175}{(S_T/d_0 - 1)^{1.08}}\right]$$

Number of quilting line	$N_T = 7$
Distance between quilting	$S_T = 0.05$ m
Diameter of quilting	$d_0 = 0.012$ m

$$Re = \frac{d_0 v}{\nu}$$

7) Return point : Orifice (D-E)

$$\zeta_7 = \zeta_0/(\frac{d_1}{d_2}) = 12.5$$

Throttle area $A_1 = 2.11 \times 10^{-3}$ m^2

Equivalent diameter $d_1 = 1.91 \times 10^{-2}$ m

Outlet area $A_2 = 5.27 \times 10^{-3}$ m^2

Equivalent diameter $d_2 = 3.22 \times 10^{-2}$ m

$\frac{d_1}{d_2} = 0.59 \rightarrow \zeta_0 = 1.52$

8) Return point : Elbow (D-E)

$\zeta_8 = 4.01$

The pressure loss is summarized as follows;

v [m/s]	Water supplying line [MPa]	Panel [MPa]	Pressure loss ΔP [MPa]
2	0.006	0.041	0.047
3	0.014	0.092	0.106
4	0.024	0.162	0.186

These results match very well to experimental results shown in Table. 5 and Fig. 3.2.31.

Reference:

JSME Data Book, "Hydraulic Losses in Pipes and Ducts", 1979
JSME Mechanical Engineers' Handbook, "A5: Fluid Mechanics", 1986, p105